OCRWM	DESIGN CALCULATION OR ANALYSIS COVER SHEET	1. QA: QA 2. Page 1 of 114

3. System	4. Document Identifier
Emplacement Drifts	800-K0C-SSE0-00100-000-00A

5. Title

Ground Control for Emplacement Drifts for LA

6. Group

Design and Engineering/Geotechnical Group

7. Document Status Designation

☒ Preliminary ☐ Final ☐ Cancelled

8. Notes/Comments

1. This version supersedes the calculation issued previously under DI: 800-K0C-TEG0-00100-000-00A. The computer input and output files from previous version are not superseded and are available under an output DTN: MO0310MWDGCCED.001.
2. In addition to several small editorial changes, the major change in this document is related to the discussion of initial ground support methods in emplacement drifts, and contained in Sections 6.3.3 and 7. Changes are marked by vertical bars in the left border.
3. An AP-2.14Q review is not required because other organizations or disciplines will not be affected by this revision.
4. Carlos Carranza-Torres, Branko Damjanac, and Marc Ruest of Itasca Consulting Group, Inc. provided technical support for numerical analyses presented in Sections 5 and 6 of the superseded calculation.

Attachments	Total Number of Pages
None	N/A

RECORD OF REVISIONS

9. No.	10. Reason For Revision	11. Total # of Pgs.	12. Last Pg. #	13. Originator (Print/Sign/Date)	14. Checker (Print/Sign/Date)	15. QER (Print/Sign/Date)	16. Approved/Accepted (Print/Sign)	17. Date
00A	See Block 8	114	114	Yiming Sun 7/9/04	Jay Cho 7/9/04	Daniel J. Tunney 7/9/2004	Fei Duan	7/9/04

CONTENTS

Page

ACRONYMS AND ABBREVIATIONS 9

1. INTRODUCTION 11
   1.1 PURPOSE AND SCOPE 11
   1.2 QUALITY ASSURANCE 11

2. USE OF SOFTWARE 12
   2.1 FLAC COMPUTER SOFTWARE 12
   2.2 FLAC3D COMPUTER SOFTWARE 12
   2.3 SPREADSHEET SOFTWARE 13

3. INPUTS 14
   3.1 DATA AND PARAMETERS 14
      3.1.1 Time Histories of Rock Temperatures 14
      3.1.2 Rock Thermal Properties 14
      3.1.3 Rock Mass Coefficient of Thermal Expansion 15
      3.1.4 Rock Mass Mechanical Properties 15
         3.1.4.1 Lithophysal Rock 15
         3.1.4.2 Non-lithophysal Rock 16
      3.1.5 Rock Mass Density 16
      3.1.6 Properties of Swellex Rock Bolts 16
      3.1.7 Seismic Velocity Histories 16
   3.2 DESIGN CRITERIA AND CONSTRAINTS 18
      3.2.1 Criteria 18
      3.2.2 Constraints 18
   3.3 CODES AND STANDARDS 19

4. ASSUMPTIONS 20
   4.1 AVERAGE DEPTH OF REPOSITORY HOST HORIZON 20
   4.2 HORIZONTAL-TO-VERTICAL IN SITU STRESS RATIOS 20
   4.3 INITIAL GROUND RELAXATION 20
   4.4 FRICTION ANGLES OF LITHOPHYSAL ROCK 20
   4.5 TENSILE STRENGTH OF LITHOPHYSAL ROCK 21

5. METHODS OF GROUND SUPPORT DESIGN 22
   5.1 OVERVIEW OF DESIGN PROCESS 22
   5.2 REPOSITORY HOST HORIZON AND GEOTECHNICAL CHARACTERIZATION 23
   5.3 GROUND SUPPORT FUNCTIONS 25
   5.4 METHODS OF DESIGN CALCULATIONS 26
      5.4.1 Empirical Methods 26
         5.4.1.1 RMR System 26
         5.4.1.2 Q System 28
         5.4.1.3 Applicability of Empirical Methods 30

CONTENTS (Continued)

Page

5.4.2 Analytical Methods 31
5.4.2.1 Modeling of Emplacement Drifts 31
5.4.2.2 Loading and Boundary Conditions 32
5.4.2.3 Evaluation of Factor of Safety 35
5.4.3 Analysis of Uncertainties Associated with Design Inputs and Modeling 38

6. RESULTS OF DESIGN CALCULATION 39
6.1 STABILITY OF UNSUPPORTED EMPLACEMENT DRIFTS 39
6.1.1 Temperature Increase in Rock 39
6.1.2 Rock Displacement and Stress 41
6.1.2.1 Drift Closures 41
6.1.2.2 Stress in Rock Adjacent to Drifts 49
6.1.3 Assessment of Factor of Safety of Emplacement Drifts 56
6.1.3.1 Potential Yield Zone around Emplacement Drifts 56
6.1.3.2 Factor of Safety of Emplacement Drifts 56
6.1.4 Ground Reaction Curves 74
6.1.5 Initial Ground Relaxation 74
6.2 EMPIRICAL ANALYSIS OF GROUND SUPPORT NEEDS 80
6.3 SELECTION OF GROUND SUPPORT METHODS 81
6.3.1 Candidate Ground Support Components and Materials 81
6.3.1.1 Friction-type Rock Bolts 81
6.3.1.2 Perforated Steel Sheets 83
6.3.1.3 Candidate Ground Support Materials 84
6.3.2 Candidate Ground Support Methods 84
6.3.2.1 Lithophysal Rock 84
6.3.2.2 Non-lithophysal Rock 85
6.3.3 Initial Ground Support Methods 85
6.4 EVALUATION OF GROUND SUPPORT PERFORMANCE 86
6.4.1 Numerical Calibration of Swellex Bolt Pull Test 86
6.4.2 Performance of Swellex Bolts in Emplacement Drifts 88
6.4.2.1 Swellex Bolts in Lithophysal Rock 88
6.4.2.2 Swellex Bolts in Non-lithophysal Rock 89
6.4.3 Performance of Bernold-type Steel Sheets 100
6.4.3.1 Estimate of Support Load 100
6.4.3.2 Estimate of Stress and Factor of Safety 103
6.4.4 Prevention of Rockfall by Ground Support 104
6.5 UNCERTAINTY ANALYSIS 105
6.5.1 Uncertainty Associated with Design Inputs 105
6.5.1.1 Variations in Material Properties 105
6.5.1.2 Variations in Loading Conditions 106
6.5.1.3 Variations in Duration of Design Service Life 106
6.5.2 Uncertainty Associated with Calculation Methods 107
6.5.2.1 Continuum versus Discontinuum 107

CONTENTS (Continued)

Page

6.5.2.2 Model Dimensions 108

7. SUMMARY AND CONCLUSION 109

8. REFERENCES 111
8.1 DOCUMENTS CITED 111
8.2 CODES, STANDARDS, REGULATIONS, AND PROCEDURES 113
8.3 SOURCE DTNS CITED 113
8.4 OUTPUT DTN 114

FIGURES

Page

Figure 3-1. Time Histories of Velocity Components of Seismic Motion at Repository Horizon 17
Figure 5-1. Flow Diagram of Ground Support Design Process 22
Figure 5-2. Underground Layout and Geological Units by Panel 24
Figure 5-3. Fractures in the Wall of the ECRB in the Tptpmn Unit 25
Figure 5-4. Lithophysae and Fracturing in the Tptpll Unit 25
Figure 5-5. Estimated Ground Support Needs Based on Q Index 30
Figure 5-6. Time Histories of Rock Temperatures on Model Boundaries 33
Figure 5-7. Geometry and Boundary Conditions for FLAC Models 35
Figure 6-1. Temperature Contours around Emplacement Drifts at Various Years Following Waste Emplacement 40
Figure 6-2. Time Histories of Closures of Emplacement Drifts in Lithophysal Rock with Categories 1 and 5 under In Situ and Thermal Loads: (a) Ko=0.3; (b) Ko=1.0 43
Figure 6-3. Time Histories of Closures of Emplacement Drifts in Non-lithophysal Rock with Categories 1 and 5 under In Situ and Thermal Loads: (a) Ko=0.3; (b) Ko=1.0 44
Figure 6-4. Time Histories of Closures of Emplacement Drifts in Lithophysal Rock with Categories 1 and 5 under Seismic Load at Year=0: (a) Ko=0.3; (b) Ko=1.0 45
Figure 6-5. Time Histories of Closures of Emplacement Drifts in Lithophysal Rock with Categories 1 and 5 under Seismic Load at Year=50: (a) Ko=0.3; (b) Ko=1.0 46
Figure 6-6. Time Histories of Closures of Emplacement Drifts in Non-lithophysal Rock with Categories 1 and 5 under Seismic Load at Year=0: (a) Cat.=1; (b) Cat.=5 47
Figure 6-7. Time Histories of Closures of Emplacement Drifts in Non-lithophysal Rock with Categories 1 and 5 under Seismic Load at Year=50: (a) Cat.=1; (b) Cat.=5 48
Figure 6-8. Time Histories of Major Principal Stresses near Crown and Springline of Emplacement Drifts in Lithophysal Rock with Categories 1 and 5 under In Situ and Thermal Loads: (a) Ko=0.3; (b) Ko=1.0 50
Figure 6-9. Time Histories of Major Principal Stresses near Crown and Springline of Emplacement Drifts in Non-lithophysal Rock with Categories 1 and 5 under In Situ and Thermal Loads: (a) Ko=0.3; (b) Ko=1.0 51
Figure 6-10. Time Histories of Major Principal Stresses near Crown and Springline of Emplacement Drifts in Lithophysal Rock with Categories 1 and 5 under In Situ and Seismic Loads (Year=0): (a) Ko=0.3; (b) Ko=1.0 52
Figure 6-11. Time Histories of Major Principal Stresses near Crown and Springline of Emplacement Drifts in Lithophysal Rock with Categories 1 and 5 under In Situ, Thermal, and Seismic Load (Year=50): (a) Ko=0.3; (b) Ko=1.0 53
Figure 6-12. Time Histories of Major Principal Stresses near Crown and Springline of Emplacement Drifts in Non-lithophysal Rock with Categories 1 and 5 under In Situ and Seismic Loads (Year=0): (a) Ko=0.3; (b) Ko=1.0 54
Figure 6-13. Time Histories of Major Principal Stresses near Crown and Springline of Emplacement Drifts in Non-lithophysal Rock with Categories 1 and 5 under In Situ, Thermal, and Seismic Loads (Year=50): (a) Ko=0.3; (b) Ko=1.0 55

FIGURES (Continued)

Page

Figure 6-14. Potential Yield Zone and Contours of Strength-to-Stress Ratios around Emplacement Drifts in Lithophysal Rock with Category 1 and Ko=0.3: (a) at 0 Year; (b) at 50 Years. 58
Figure 6-15. Potential Yield Zone and Contours of Strength-to-Stress Ratios around Emplacement Drifts in Lithophysal Rock with Category 1 and Ko=1.0: (a) at 0 Year; (b) at 50 Years. 59
Figure 6-16. Potential Yield Zone and Contours of Strength-to-Stress Ratios around Emplacement Drifts in Lithophysal Rock with Category 5 and Ko=0.3: (a) at 0 Year; (b) at 50 Years. 60
Figure 6-17. Potential Yield Zone and Contours of Strength-to-Stress Ratios around Emplacement Drifts in Lithophysal Rock with Category 5 and Ko=1.0: (a) at 0 Year; (b) at 50 Years. 61
Figure 6-18. Potential Yield Zone and Contours of Strength-to-Stress Ratios around Emplacement Drifts in Non-lithophysal Rock with Category 1 and Ko=0.3: (a) at 0 Year; (b) at 50 Years. 62
Figure 6-19. Potential Yield Zone and Contours of Strength-to-Stress Ratios around Emplacement Drifts in Non-lithophysal Rock with Category 1 and Ko=1.0: (a) at 0 Year; (b) at 50 Years. 63
Figure 6-20. Potential Yield Zone and Contours of Strength-to-Stress Ratios around Emplacement Drifts in Non-lithophysal Rock with Category 5 and Ko=0.3: (a) at 0 Year; (b) at 50 Years. 64
Figure 6-21. Potential Yield Zone and Contours of Strength-to-Stress Ratios around Emplacement Drifts in Non-lithophysal Rock with Category 5 and Ko=1.0: (a) at 0 Year; (b) at 50 Years. 65
Figure 6-22. Average Factors of Safety for Unsupported Emplacement Drifts Based on Strength-to-stress Ratio: (a) in Lithophysal Rock, (b) in Non-lithophysal Rock 66
Figure 6-23. Development of Radial Displacements at Crown of Unsupported Emplacement Drifts in Category 1 Lithophysal Rock: (a) K_o=0.3, (b) K_o=1.0 67
Figure 6-24. Development of Radial Displacements at Crown of Unsupported Emplacement Drifts in Category 3 Lithophysal Rock: (a) K_o=0.3, (b) K_o=1.0 68
Figure 6-25. Development of Radial Displacements at Crown of Unsupported Emplacement Drifts in Category 5 Lithophysal Rock: (a) K_o=0.3, (b) K_o=1.0 69
Figure 6-26. Development of Radial Displacements at Crown of Unsupported Emplacement Drifts in Category 1 Non-lithophysal Rock: (a) K_o=0.3, (b) K_o=1.0 70
Figure 6-27. Development of Radial Displacements at Crown of Unsupported Emplacement Drifts in Category 3 Non-lithophysal Rock: (a) K_o=0.3, (b) K_o=1.0 71
Figure 6-28. Development of Radial Displacements at Crown of Unsupported Emplacement Drifts in Category 5 Non-lithophysal Rock: (a) K_o=0.3, (b) K_o=1.0 72
Figure 6-29. Factor of Safety for Unsupported Emplacement Drifts under Various Rock Conditions: (a) in Lithophysal Rock, (b) in Non-lithophysal Rock 73
Figure 6-30. Ground Reaction Curves for Unsupported Emplacement Drifts: (a) Lithophysal Rock; (b) Non-lithophysal Rock. 76
Figure 6-31. Configuration of a FLAC3D Model for Emplacement Drift 77

FIGURES (Continued)

Page

Figure 6-32. Vertical Displacements at Drift Crown during TBM Advance for Unsupported Emplacement Drifts in Category 1 Lithophysal Rock: (a) K_o=0.3; (b) K_o=1.0 78
Figure 6-33. Vertical Displacements at Drift Crown during TBM Advance for Unsupported Emplacement Drifts in Category 5 Lithophysal Rock: (a) K_o=0.3; (b) K_o=1.0 79
Figure 6-34. A Typical Split Set Rock Bolt 82
Figure 6-35. A Typical Swellex Rock Bolt 83
Figure 6-36. Bernold-type Perforated Steel Sheet 84
Figure 6-37. Final Ground Support Methods Recommended for Emplacement Drifts. 86
Figure 6-38. Configuration and Failure State of FLAC Model Simulation of a Pull Test of Swellex Bolts 87
Figure 6-39. Numerical Calibration of Super Swellex Bolt Pull Test 87
Figure 6-40. Axial Forces in Bolts Installed in Emplacement Drifts in Lithophysal Rock under In Situ and Thermal Loads: (a) K_o=0.3; (b) K_o=1.0 90
Figure 6-41. Axial Forces in Bolts Installed in Emplacement Drifts in Lithophysal Rock under In Situ and Thermal Loads for Cat.=1 and K_o=0.3: (a) at 0 years (b) at 50 years 91
Figure 6-42. Axial Forces in Bolts Installed in Emplacement Drifts in Lithophysal Rock under In Situ and Thermal Loads for Cat.=1 and K_o=1.0: (a) at 0 years (b) at 50 years 92
Figure 6-43. Axial Forces in Bolts Installed in Emplacement Drifts in Lithophysal Rock under In Situ and Thermal Loads for Cat.=5 and K_o=0.3: (a) at 0 years (b) at 50 years 93
Figure 6-44. Axial Forces in Bolts Installed in Emplacement Drifts in Lithophysal Rock under In Situ and Thermal Loads for Cat.=5 and K_o=1.0: (a) at 0 years (b) at 50 years 94
Figure 6-45. Axial Forces in Bolts Installed in Emplacement Drifts in Lithophysal Rock under In Situ and Seismic Loads: (a) Cat.=1; (b) Cat.=5. 95
Figure 6-46. Axial Forces in Bolts Installed in Emplacement Drifts in Lithophysal Rock under In Situ, Thermal, and Seismic Loads: (a) Cat.=1; (b) Cat.=5. 96
Figure 6-47. Axial Forces in Bolts Installed in Emplacement Drifts in Non-lithophysal Rock under In Situ and Thermal Loads: (a) K_o=0.3; (b) K_o=1.0. 97
Figure 6-48. Axial Forces in Bolts Installed in Emplacement Drifts in Non-lithophysal Rock under In Situ and Seismic Loads: (a) Cat.=1; (b) Cat.=5. 98
Figure 6-49. Axial Forces in Bolts Installed in Emplacement Drifts in Non-lithophysal Rock under In Situ, Thermal, and Seismic Loads: (a) Cat.=1; (b) Cat.=5. 99
Figure 6-50. Illustration of Potentially-loosen Rock on Periphery of an Emplacement Drift 101

TABLES

Page

Table 3-1. Time Histories of Rock Temperatures 14
Table 3-2. Thermal Properties of Lithophysal and Non-lithophysal Units 15
Table 3-3. Coefficient of Thermal Expansion for Non-Lithophysal and Lithophysal Rocks ... 15
Table 3-4. Rock Mass Mechanical Properties for Lithophysal Rock 15
Table 3-5. Rock Mass Mechanical Properties for Non-lithophysal Rock 16
Table 3-6. Dimensions and Properties for Stainless Steel Super Swellex Rock Bolts 17
Table 4-1. Rock Mass Strength Properties for Lithophysal Rock (Tptpll) 20
Table 5-1. Estimate of Ground Support Needs Based on RMR System 28
Table 6-1. Estimate of Ground Support Needs for Emplacement Drifts in Non-lithophysal Rock Based on RMR and Q Systems 81
Table 6-2. Estimated Stresses and Factors of Safety in Bernold-type Stainless Steel Sheets for Various Loading Conditions 103

ACRONYMS AND ABBREVIATIONS

ANSYS	ANSYS Computer Code
ASM	American Society for Metals
ASTM	American Society for Testing and Materials
BSC	Bechtel SAIC Company, LLC.
DOE	U.S. Department of Energy
DTN	Data Tracking Number
ECRB	Enhanced Characterization of the Repository Block
EDZ	Excavation-disturbed Zone
ESF	Exploratory Studies Facility
ESR	Excavation Support Ratio
FLAC	Fast Lagrangian Analysis of Continua
FLAC3D	3-Dimensional Fast Lagrangian Analysis of Continua
FS	Factor of Safety
GRC	Ground Reaction Curve
J_n	Joint Set Number
J_r	Joint Roughness Number
J_a	Joint Alteration Number
J_w	Joint Water Reduction Factor
LA	License Application
NGI	Norwegian Geotechnical Institute
PGA	Peak Ground Acceleration
Q	Rock Mass Quality Index
QARD	Quality Assurance Requirements and Description
RHH	Repository Host Horizon
RMR	Rock Mass Rating
RQD	Rock Quality Designation
SC	Safety Category
SCM	Software Configuration Management
SRF	Stress Reduction Factor
STSR	Strength-to-stress Ratio
TBM	Tunnel Boring Machine
TDMS	Technical Data Management System

Tptpll	Lower Lithophysal Unit
Tptpln	Lower Non-lithophysal Unit
Tptpmn	Middle Non-lithophysal Unit
Tptpul	Upper Lithophysal Unit

YMP	Yucca Mountain Project

1. INTRODUCTION

1.1 PURPOSE AND SCOPE

The purpose of this calculation is to analyze the stability of repository emplacement drifts during the preclosure period, and to provide a final ground support method for emplacement drifts for the License Application (LA). The scope of the work includes determination of input parameter values and loads, selection of appropriate process and methods for the calculation, application of selected methods, such as empirical or analytical, to the calculation, development and execution of numerical models, and evaluation of results.

Results from this calculation are limited to use for design of the emplacement drifts and the final ground support system installed in these drifts. The design of non-emplacement openings and their ground support systems is covered in the *Ground Control for Non-Emplacement Drifts for LA* (BSC 2004c).

1.2 QUALITY ASSURANCE

The Q-List designates the ground control system for emplacement drifts as 'not important to waste isolation', and 'not important to safety', and the Safety Category (SC) is 'Non-SC' (BSC 2003e, p. A-4). However, this document is prepared with a QA:QA status and all activities addressed in this calculation are subject to the requirements of the Quality Assurance Requirements and Description (QARD) (DOE 2004) since the ground control system for emplacement drifts will support the activities associated with the Waste Retrieval System which is classified as 'SC' (BSC 2003e, p. A-4) and subject to the QARD requirements.

The calculation is prepared per AP-3.12Q, *Design Calculations and Analysis*, and its requirements. All input data are identified and tracked in accordance with AP-3.15Q, *Managing Technical Product Inputs*. In addition, LP-SI.11Q-BSC, *Software Management*, is used for activities related to software usage.

This report is preliminary, intended to support LA design.

2. USE OF SOFTWARE

Two commercially available computer programs, FLAC (Fast Lagrangian Analysis of Continua) and FLAC3D (Fast Lagrangian Analysis of Continua in 3 Dimensions), are used to perform thermal, mechanical, and seismic analyses in the calculation. Descriptions of these codes and their qualification status are provided in the following subsections.

2.1 FLAC COMPUTER SOFTWARE

FLAC Version 4.0 (STN: 10167-4.0-00) is a two-dimensional explicit finite difference code which simulates the behavior of structures built of soil, rock, or other materials subjected to static, dynamic, and thermally-induced loads (Itasca Consulting Group 2002). Modeled materials respond to applied forces or boundary restraints according to prescribed linear or non-linear stress/strain laws and undergo plastic flow when a limiting yield condition is reached. FLAC is based upon a Lagrangian scheme which is well suited for large deflections and has been used primarily for analysis and design in mine engineering and underground construction. The explicit time-marching solution of the full equations of motion, including inertial terms, permits the analysis of progressive failure and collapse. A detailed discussion on the general features and fields of the FLAC computer software applications is presented in the user's manual (Itasca Consulting Group 2002).

FLAC was used in coupled thermomechanical and seismic analyses in this calculation. The validation test cases of Test 1, Test 3, Test 4, Test 5, and Test 7 documented in *the Software Implementation Report for FLAC Version 4.0* (BSC 2002a, Table 2) support the application of mechanical, thermomechanical, and dynamic analyses conducted for this calculation. The input and output files generated by FLAC are archived on a CD and submitted to the Technical Data Management System (TDMS) as an output Data Tracking Number (DTN: MO0310MWDGCCED.001) for this calculation. A listing of the input and output files can be found in the readme file of this DTN. The results are presented and described in Section 5.

FLAC Version 4.0 (BSC 2002c) was obtained from the Software Configuration Management (SCM) in accordance with the LP-SI.11Q-BSC procedure. FLAC is installed and run on stand-alone PCs with Windows 2000/NT 4.0 operating systems. FLAC Version 4.0 is qualified for use in design in accordance with the LP-SI.11Q-BSC procedure. The software was appropriate for the applications used in this analysis, and used only within the range of validation, as specified in the software qualification documentation.

2.2 FLAC3D COMPUTER SOFTWARE

FLAC3D Version 2.1 (STN: 10502-2.1-00) is a three-dimensional explicit finite difference code which simulates the behavior of structures built of soil, rock, or other materials subjected to static, dynamic, and thermally-induced loads (Itasca Consulting Group 2002). Modeled materials respond to applied forces or boundary restraints according to prescribed linear or non-linear stress/strain laws and undergo plastic flow when a limiting yield condition is reached. FLAC3D is based upon a Lagrangian scheme which is well suited for large deflections and has been used primarily for analysis and design in mine engineering and underground construction.

The explicit time-marching solution of the full equations of motion, including inertial terms, permits the analysis of progressive failure and collapse. A detailed discussion on the general features and fields of the FLAC3D computer software applications is presented in the user's manual (Itasca Consulting Group 2002).

FLAC3D was used in mechanical analysis in this calculation. The validation test cases of Test 1 and Test 2 documented in the *Software Implementation Report for FLAC3D Version 2.1* (BSC 2002b, Table 2-2) support the application of mechanical analyses conducted for this calculation. The input and output files generated by FLAC3D are archived on a CD and submitted to the TDMS as an output DTN (DTN: MO0310MWDGCCED.001) for this calculation. A listing of the input and output files can be found in the readme file of this DTN. The results are presented and described in Section 5.

FLAC3D Version 2.1 (BSC 2002d) was obtained from the Software Configuration Management (SCM) in accordance with the LP-SI.11Q-BSC procedure. FLAC is installed and run on stand-alone PCs with Windows 2000/NT 4.0 operating systems. FLAC3D Version 2.1 is qualified for use in design in accordance with the LP-SI.11Q-BSC procedure. The software was appropriate for the applications used in this analysis, and used only within the range of validation, as specified in the software qualification documentation.

2.3 SPREADSHEET SOFTWARE

Microsoft Excel 97 SR-2 spreadsheet software was used in displaying some of the FLAC and FLAC3D results graphically. In this application, results from the FLAC or FLAC3D analyses were used as inputs, and outputs were charts. There are no formulas used in the spreadsheets. Both the inputs and outputs (charts) in Excel are archived on a CD and submitted to the TDMS as an output DTN (DTN: MO0310MWDGCCED.001) for this calculation. A listing of the input and output files can be found in the readme file of this DTN.

Microsoft Excel 97 SR-2 is an exempt software product in accordance with the LP-SI.11Q-BSC procedure.

3. INPUTS

This section presents various input parameter values used in this calculation. Most of these values are selected from the *Input Parameters for Ground Support Design* document (BSC 2003a). Since the sources of these parameter values and the rationale for selection of them are discussed in that document, no further justifications on the use of these parameter values are provided in this section. For inputs selected from other than the *Input Parameters for Ground Support Design*, their sources will be identified along with the rational for selection.

3.1 DATA AND PARAMETERS

3.1.1 Time Histories of Rock Temperatures

Time histories of rock temperatures are listed in Table 3-1. These values reflect the effect of forced continuous ventilation at 15 m^3/s during the preclosure period of 50 years, and are obtained from DTN: MO0306MWDALAFV.000. The rock temperatures at 50 m above and below the drift center are extracted from the ANSYS output files associated with the ventilation model. These ANSYS output files were downloaded from the Technical Data Management Systems (TDMS) under DTN: MO0306MWDALAFV.000.

Table 3-1. Time Histories of Rock Temperatures

Time (years)	Temperatures (°C)		
	Drift Wall	50-m Above Drift Center[a]	50-m Below Drift Center[a]
0	22.28	21.68	23.08
0.01	36.64	21.68	23.08
1	71.80	21.68	23.08
2	72.22	21.68	23.08
5	70.42	21.71	23.10
7	68.63	21.81	23.19
10	66.32	22.09	23.45
20	59.88	23.42	24.72
30	54.32	24.68	25.96
50	46.78	26.53	27.81

Source: DTN: MO0306MWDALAFV.000, ANSYS-LA-Fine.xls, and la600c24.rth.
[a] Temperature data at the exact locations were obtained by linear interpolation from the source DTN.

3.1.2 Rock Thermal Properties

Thermal conductivity, specific heat, and dry bulk density for both lithophysal and non-lithophysal units are listed in Table 3-2 (BSC 2003a, Table 5-3), except for specific heat values, which are obtained from DTN: SN0307T0510902.003.

Table 3-2. Thermal Properties of Lithophysal and Non-lithophysal Units

Litho-Stratigraphic Unit	Thermal Conductivity (W/m·K)		Specific Heat[a] (J/kg·K)		
	Wet	Dry	25 - 94°C	95 - 114°C	115 - 325°C
Tptpmn	2.07	1.42	910	3000	990
Tptpll	1.89	1.28	930	3300	990

Source: BSC 2003a, Table 5-3; [a] DTN: SN0307T0510902.003, rock_mass_heat_capacity.xls.

3.1.3 Rock Mass Coefficient of Thermal Expansion

The mean rock mass coefficient of thermal expansion during heating for lithophysal and non-lithophysal rocks is tabulated in Table 3-3 (BSC 2003a, Table 5-4).

Table 3-3. Coefficient of Thermal Expansion for Non-Lithophysal and Lithophysal Rocks

Temperature Range (°C)	Value (10^{-6}/°C)[a]
25 - 50	7.50
50 - 75	8.80
75 - 100	9.06
100 - 125	9.80
125 - 150	10.61
150 - 175	11.83
175 - 200	13.77
200 - 225	17.27

Source: BSC 2003a, Table 5-4. [a] Values from heating cycle.

3.1.4 Rock Mass Mechanical Properties

3.1.4.1 Lithophysal Rock

Rock mass properties for lithophysal rock are listed in Table 3-4 (BSC 2003a, Table 5-8).

Table 3-4. Rock Mass Mechanical Properties for Lithophysal Rock

Parameter	Lithophysal Rock (Tptpul and Tptpll)					
Rock Mass Lithophysal Porosity Category	1	2	3	4	5	6
Lithophysal Porosity (%)	25-30	20-25	15-20	10-15	<10	N/A
Poisson's Ratio	0.22	0.22	0.22	0.22	0.22	0.22
Modulus of Elasticity (GPa)	1.9	6.4	10.8	15.3	19.7	1.0
Unconfined Compressive Strength (MPa)	10	15	20	25	30	6
Cohesion (MPa)	2.07	3.11	4.14	5.18	6.21	1.24
Friction Angle (degrees)	45	45	45	45	45	45

Source: BSC 2003a, Table 5-8.

3.1.4.2 Non-lithophysal Rock

Rock mass properties for non-lithophysal (Tptpmn) rock are listed in Table 3-5. These values are determined based on the rock mass classification. Details on how these values are estimated are presented in the *Subsurface Geotechnical Parameters Report* (BSC 2003b, Section 8.5, Table 8-41 and Section 8.5.2.3).

Table 3-5. Rock Mass Mechanical Properties for Non-lithophysal Rock

Parameter	Non-lithophysal Rock (Tptpmn)				
Rock Mass Quality Category	1	2	3	4	5
Cumulative Frequency Distribution (%)	10	30	50	70	90
Geologic Strength Index (GSI)	50.48	55.49	59.03	62.33	66.79
Rock Mass Quality (Q' or Q_p)	2.05	3.59	5.31	7.67	12.58
Elastic Modulus (GPa)	10.25	13.66	16.74	20.23	26.18
Poisson's Ratio[a]	0.19	0.19	0.19	0.19	0.19
Global Compressive Strength (MPa)	33.50	39.67	44.42	49.50	57.71
Cohesion (MPa)	7.60	8.69	9.53	10.39	11.75
Friction Angle (degrees)	40.15	42.29	43.64	44.92	46.66
Tensile Strength (MPa)	0.08	0.12	0.16	0.21	0.32

Source: BSC 2003b, Section 8.5, Table 8-41; [a] BSC 2003b, Section 8.5.2.3.

3.1.5 Rock Mass Density

A rock mass saturated bulk density of 2,410 kg/m^3 is used to estimate overburden and in situ stress state. This value is for the rock unit of Tptpln, and is the highest value of lithostratigraphic units (BSC 2001, Table 4-2). Therefore, use of this value is conservative for the purpose of this calculation.

3.1.6 Properties of Swellex Rock Bolts

Swellex steel rock bolts are proposed for use in emplacement drifts. Their thermal and mechanical properties are listed in Table 3-6. These property values are selected from various sources. The source information is also provided in Table 3-6.

3.1.7 Seismic Velocity Histories

Seismic velocity histories for the mean annual exceedance probability of 1×10^{-4} (10,000 years) are shown in Figure 3-1 (DTN: MO0306SDSAVDTH.000, MatH1.vth, MatH2.vth, and MatV.vth). Details on how these seismic velocity histories are applied in numerical calculations are described in Section 5.4.2.2.3.

Table 3-6. Dimensions and Properties for Stainless Steel Super Swellex Rock Bolts

Parameter	Value	Source
Diameter of Rock Bolt (m)	0.054	Atlas Copco 2003, p. 10.
Thickness of (m)	0.003	Atlas Copco 2003, p. 10.
Density (kg/m^3)	8,000	ASM International 1990, Table 21, p. 871, for 316 type stainless steel.
Young's Modulus of Stainless Steel (GPa)	193	ASM International 1990, Table 21, p. 871, for 316 type stainless steel.
Tensile Strength (MPa)	620	ASTM A 276-03, Table 2, p. 4, for 316 type steel.
Limit Axial Force (kN)	298	Calculated from $620\times10^6\times\pi/4\times(0.054^2-0.048^2)/1000=298$ kN.
Coefficient of Thermal Expansion (m/m·°C)	15.9×10^{-6}	ASM International 1990, Table 21, p. 871, for 316 type stainless steel at a temperature range of 0 to 100°C.
Bond Stiffness (N/m/m)	3×10^8	Calibrated from pull test data. See Section 6.4.1.
Bond Strength (N/m)	2.75×10^5	Calibrated from pull test data. See Section 6.4.1.

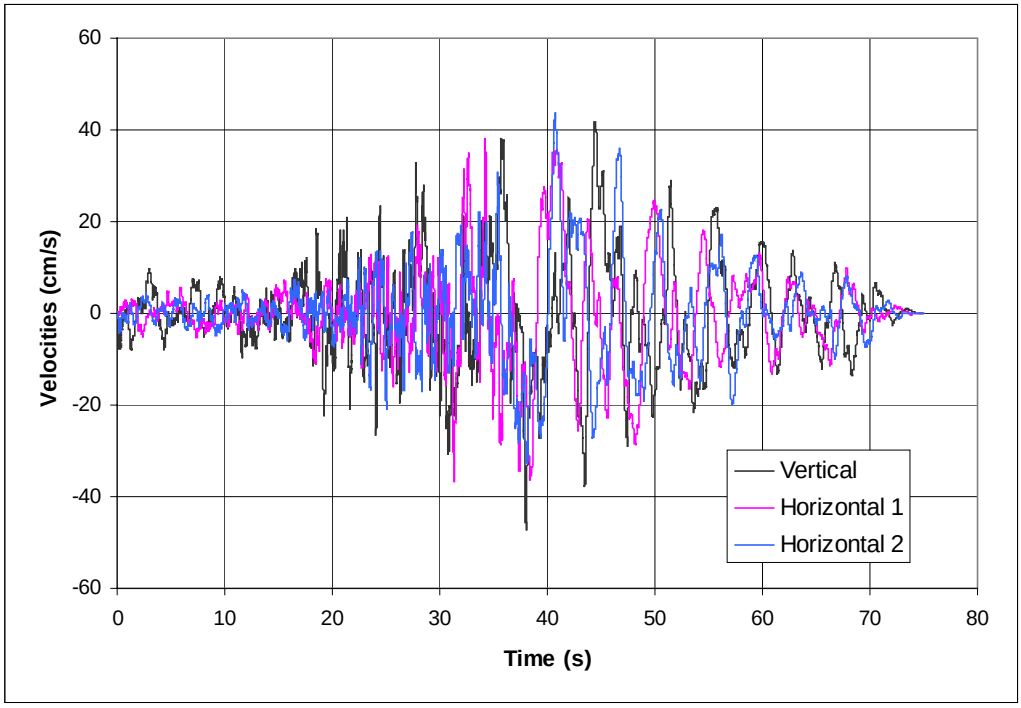

Source: DTN: MO0306SDSAVDTH.000, MatH1.vth, MatH2.vth, and MatV.vth.

Figure 3-1. Time Histories of Velocity Components of Seismic Motion at Repository Horizon

3.2 DESIGN CRITERIA AND CONSTRAINTS

3.2.1 Criteria

The following criteria are applicable to the design of ground support system in emplacement drifts:

3.2.1.1 The repository must be designed so that any or all of the emplaced waste could be retrieved on a reasonable schedule starting at any time up to 50 years after waste emplacement operations are initiated. (10 CFR 63 2002, Section 63.111(e)(1)).

3.2.1.2 The ground control system shall be designed to maintain adequate operating envelopes through permanent closure for emplacement drifts (Minwalla 2003, Section 4.5.2.1).

3.2.1.3 The ground control system shall accommodate geologic mapping of emplacement drifts (Minwalla 2003, Section 4.5.2.1).

3.2.1.4 The system shall be designed for the appropriate worst case combination of in situ, thermal, seismic, construction, and operational loads (Minwalla 2003, Section 4.5.2.1).

3.2.1.5 The ground control system for emplacement drifts shall consider the following factors of safety margin in design (Minwalla 2003, Section 4.5.2.1):

Load Type	Concrete	Steel
Static Loads (in situ+thermal)	2.0 – 2.5	1.4 – 1.8
Static plus Dynamic Loads (in situ+thermal+seismic)	N/A	1.2 – 1.5

3.2.1.6 The ground control system shall use materials having acceptable long-term effects on waste isolation (Minwalla 2003, Section 4.5.2.2).

3.2.1.7 The ground control system shall be designed to withstand a design basis earthquake (Minwalla 2003, Section 4.5.2.2).

3.2.1.8 The ground control system shall be designed to prevent rock falls that could potentially result in personnel injury (Minwalla 2003, Section 4.5.2.3).

3.2.1.9 The ground control system for emplacement drifts shall be designed to function without planned maintenance during the operational life, while providing for the ability to perform unplanned maintenance in the emplacement drifts on an as-needed basis (Minwalla 2003, Section 4.5.2.6).

3.2.2 Constraints

The following design constraints are applicable to the prediction of deformation profile of emplacement drifts (Sun 2002, Section 2.2):

3.2.2.1 Drift Spacing: The nominal emplacement drift spacing shall be 81 meters (265.8 ft), drift center line to drift center line.

3.2.2.2 Excavated Diameter: The nominal excavated diameter of emplacement drifts shall be 5.5 meters (18.0 ft).

3.2.2.3 Design Thermal Load: The ground control system shall be designed for a design thermal load of 1.45 kW/m (1508.4 Btu/hr·ft), averaged over a fully loaded emplacement drift at the time of completion of loading an entire emplacement drift.

3.2.2.4 Design Seismic Load: The ground control system shall be designed for a design basis seismic load for the mean annual exceedance probability of 1×10^{-4} (10,000 years).

3.3 CODES AND STANDARDS

The following codes and standards are applicable to this calculation:

ASTM A 240/A 240M-03b	*Standard Specification for Chromium and Chromium-Nickel Stainless Steel Plate, Sheet, and Strip for Pressure Vessels and for General Applications*
ASTM A 276-03	*Standard Specification for Stainless Steel Bars and Shapes*
ASTM F 432-95 (Reapproved 2001)	*Standard Specification for Roof and Rock Bolts and Accessories*

4. ASSUMPTIONS

Assumptions used in this calculation are described in this section.

4.1 AVERAGE DEPTH OF REPOSITORY HOST HORIZON

The average depth of repository host horizon is assumed to be 400 m measured from the center of an emplacement drift (BSC 2003a, Tables 5-2a to 5-2c). Depth of emplacement drifts varies from drift to drift. The depths near the centers of Panels 1, 3 East and 3 West are 296 m, 259 m, and 372 m, respectively. Use of a depth of 400 m for calculating in situ stress at the emplacement drift horizon will result in a higher stress than anticipated since estimated in situ stress is proportional to the depth, and therefore, is conservative for the purpose of the calculation. Used in Section 6.

4.2 HORIZONTAL-TO-VERTICAL IN SITU STRESS RATIOS

The upper and lower bounds of horizontal-to-vertical in situ stress ratio are assumed to be 1.0 and 0.3 (Sun 2002, Table 3-2). The basis of these values for the repository ground support design is provided in the cited reference. Used in Section 6.

4.3 INITIAL GROUND RELAXATION

An initial ground relaxation value of 60 percent is assumed (Sun 2002, Table 6-1). This results in 40 percent of the pre-excavation in situ stress being imposed on the final ground support. The basis for use of this value is provided in the cited reference. Used in Section 6.4.2.

4.4 FRICTION ANGLES OF LITHOPHYSAL ROCK

Friction angle (ϕ) of lithophysal rock (Tptpll) listed in Table 3-4 is 45 degrees. To have a conservative assessment of drift stability, a friction angle of 35 degrees is assumed and used in Section 6 of this calculation for the lithophysal rock. Values of cohesion (c) corresponding to a friction angle of 35 degrees (see Table 4-1) are estimated based on the unconfined compressive strength (UCS) values for each category identified in Table 3-4 and Mohr-Coulomb yield criterion, using the following equation (Hoek et al. 2000, Eq. 8.15, p. 92):

$$c = \frac{q_u(1-\sin\phi)}{2\cos\phi} \qquad \text{(Eq. 4-1)}$$

where q_u = unconfined compressive strength, MPa

Table 4-1. Rock Mass Strength Properties for Lithophysal Rock (Tptpll)

Rock Mass Category	1	2	3	4	5	6
UCS (MPa)	10	15	20	25	30	6
Friction Angle (Degrees)	35	35	35	35	35	35
Cohesion (MPa)	2.60	3.90	5.21	6.51	7.81	1.56

4.5 TENSILE STRENGTH OF LITHOPHYSAL ROCK

Tensile strength is assumed to be equal to a half of cohesion for various categories of the lithophysal rock. For example, tensile strength of Category 1 rock mass is equal to 1.04 MPa since cohesion for this category rock mass is 2.07 MPa as indicated in Table 3-4. This value is about 10% of the corresponding UCS value, and is considered reasonable for the lithophysal rock mass. Used in Section 6.

5. METHODS OF GROUND SUPPORT DESIGN

This section provides a description of the process and methods used in the design of ground support for emplacement drifts.

5.1 OVERVIEW OF DESIGN PROCESS

The process of ground support design for emplacement drifts involves identification of ground support functional and performance requirements, interfacing with performance assessment for criteria of acceptable ground support materials, interfacing with subsurface design for layout and site geologic information, development of methods for design calculations, selection of design inputs, conducting calculations and analyses, evaluation of results, and development of drawings and specifications. A flow diagram of the ground support design process is illustrated in Figure 5-1. This calculation covers all elements of the design process, except the development of drawings and specifications

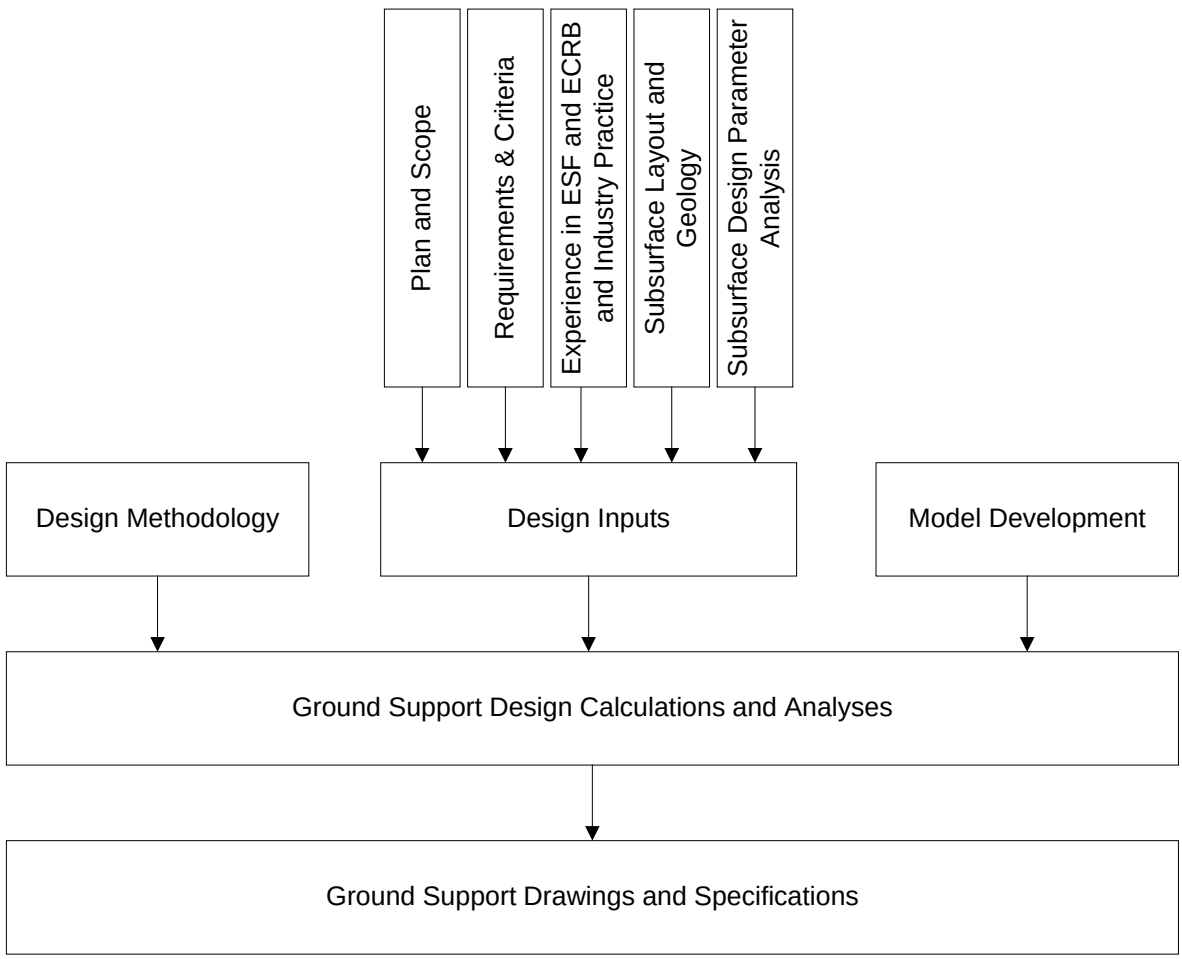

Figure 5-1. Flow Diagram of Ground Support Design Process

5.2 REPOSITORY HOST HORIZON AND GEOTECHNICAL CHARACTERIZATION

According to the *Underground Layout Configuration* calculation (BSC 2003d, Section 7.1.7), the repository host horizon (RHH) will be located in the lower part of the lithophysal zone of the densely welded devitrified lithophysal-rich tuff unit and the entire densely welded devitrified lithophysal-poor tuff unit of the Topopah Spring Tuff. The RHH contains four lithostratigraphic units, namely the upper lithophysal unit (Tptpul), the middle non-lithophysal unit (Tptpmn), the lower lithophysal unit (Tptpll), and the lower non-lithophysal unit (Tptpln). The underground layout and the geological units within each panel is shown in Figure 5-2 (BSC 2003d, Figure II-2). Of the total emplacement areas, approximately 85% will lie within the Tptpll and Tptpul units combined and the rest 15% will be located in the Tptpmn and Tptpln units (BSC 2003d, Table II-2).

Geological mapping was conducted in the Exploratory Studies Facility (ESF) tunnel and the Enhanced Characterization of the Repository Block (ECRB) drift to characterize the rock units within the RHH. The data collected were analyzed using two empirical rock mass classification systems, the Geomechanics Rock Mass Rating (RMR) system (Bieniawski 1989) and the Rock Mass Quality (Q) system of Norwegian Geotechnical Institute (NGI) (Barton et al. 1974). The geotechnical characteristics of the four lithostratigraphic units can be summarized as follows (Board 2003, Section 3.4):

Tptpul Unit. The Tptpul unit on average has a RQD rating of 36 (poor), a RMR value of 57 (fair) and a Q value of 14 (good). Its lithophysae content ranges from 10 to 40 percent by volume. These cavities have an average diameter of 10 cm. Fractures are hard to distinguish, with an average of only one joint set. Keyblock-type failures are not likely to occur in this unit, though some horizontal cooling joints are observed.

Tptpmn Unit. The Tptpmn unit has a mean horizontal RQD rating ranging from 60 to 62 (fair), and a RMR value of 60 (fair). It is characterized by less than 3 percent lithophysae by volume. This unit has an average of three to three plus random joint sets, with predominately two vertical joint sets and one horizontal joint set. The horizontal joint set, or vapor-phase partings, is the primary cause of potential formation of keyblocks. A typical fracture pattern in the Tptpmn unit is shown in Figure 5-3.

Tptpll Unit. The Tptpll unit has a horizontal RQD rating of 42 (poor), a Q rating of 7.9 (fair), and a RMR value of 57 (fair). Its content of lithophysae varies from 5 to 30 percent by volume, with a size ranging from 5 to 130 cm. The larger lithophysal cavities tend to be irregular or ellipsoidal features that exhibit prismatic fracturing. The unit has an average of two plus random joint sets; however no keyblock problems are expected. Typical lithophysae and fracturing in the Tptpll are shown in Figure 5-4.

Tptpln Unit. The Tptpln has a RQD rating ranging from 62 to 67 (fair), a RMR value of 60 (fair), and a Q value of 12.3 (good). This unit contains less than 3 percent lithophysal cavities by volume. It has an average of three joint sets, with no keyblock problems anticipated.

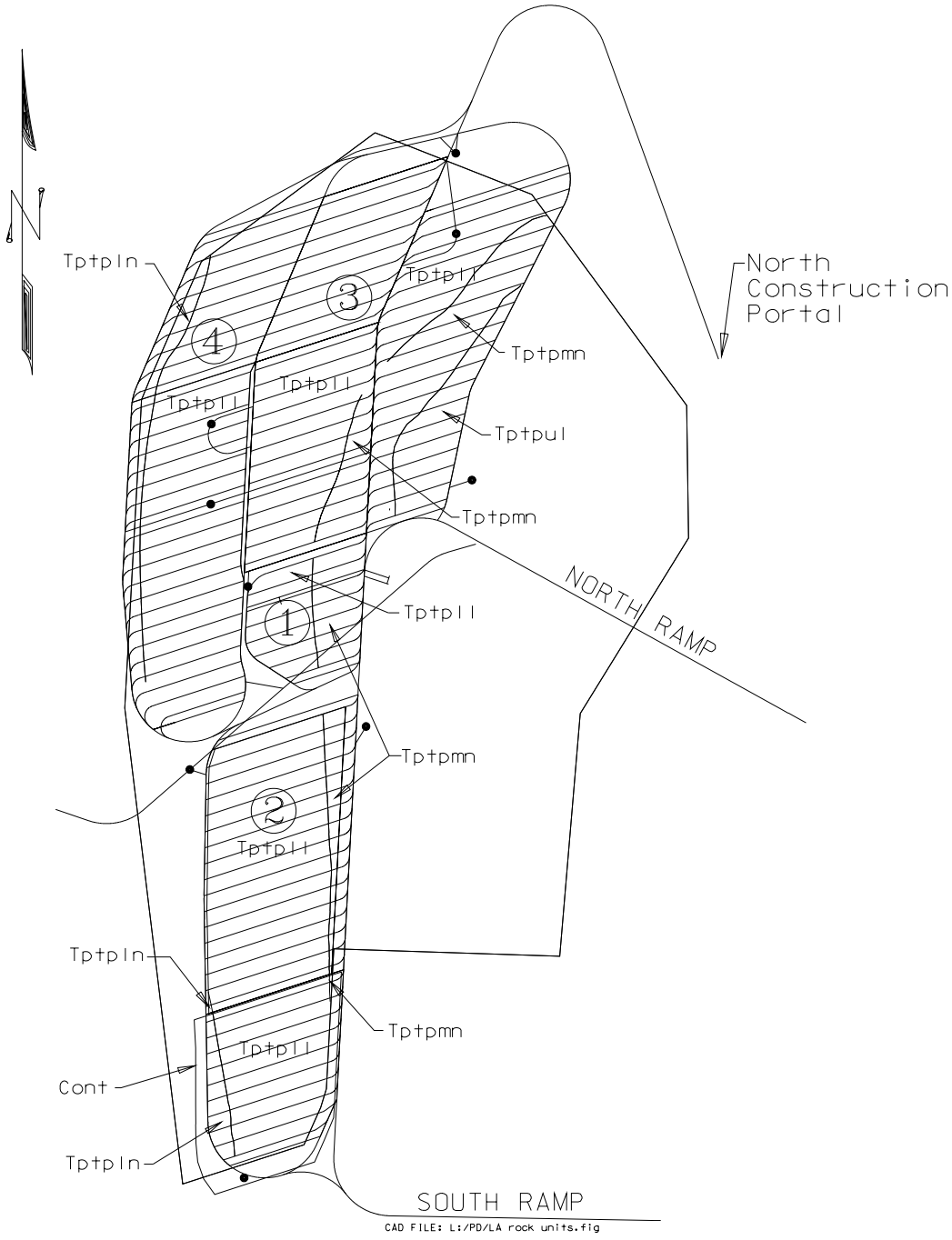

Source: BSC 2003d, Figure II-2.

Figure 5-2. Underground Layout and Geological Units by Panel

Source: Board 2003, Figure 8.

Figure 5-3. Fractures in the Wall of the ECRB in the Tptpmn Unit

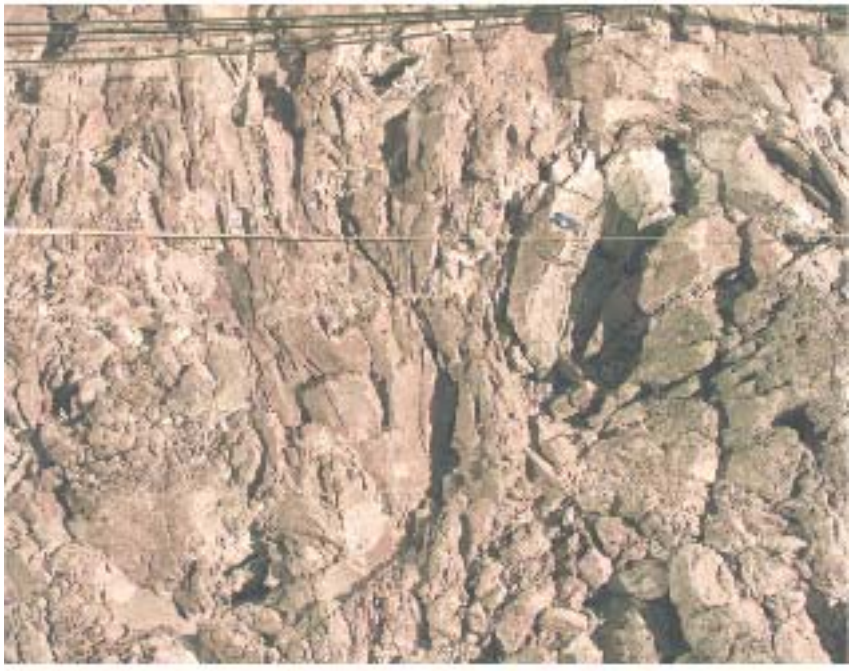

Source: Board 2003, Figure 10b.

Figure 5-4. Lithophysae and Fracturing in the Tptpll Unit

5.3 GROUND SUPPORT FUNCTIONS

Ground support for emplacement drifts has the following functional and performance requirements (see Section 3.2.1 and Board 2003, Section 7.3):

- Ensure stable conditions for personnel and environmental safety during construction and the preclosure period
- Limit rock loosening or sagging to acceptable levels, so that operational envelopes are maintained
- Prevent rock loosening and potential rockfall onto waste packages during the preclosure period
- Allow for geological mapping, performance confirmation activities (which may include remote observation and possible field testing), waste retrieval operations, and closure operations (which may include installation of permanent drip shields)
- Use materials with acceptable long-term effects on waste isolation
- To be functional without planned maintenance during the preclosure period.

These functional and performance requirements should be addressed in the design and selection of ground support system for emplacement drifts.

5.4 METHODS OF DESIGN CALCULATIONS

Both empirical and analytical methods are employed in the design calculations. The empirical methods are primarily tools for assessing the needs for ground support of emplacement drifts as well as for its selection. Design issues such as personnel safety, constructibility, and geologic mapping requirements should be factored into the design of the ground support system at this stage. With the aid of computer modeling, the stability of the unsupported opening should also be analyzed to further assessing the needs for ground support. Applicable thermal and seismic loads should be considered in the design in addition to the in situ loading conditions. The ground support system recommended should either cover most ground conditions or else be adaptable to varying ground conditions. Its performance should be further analyzed using analytical methods to make sure that design requirements are met. Based on empirical estimates, design issues, and computer modeling results, the final ground support system should be developed.

5.4.1 Empirical Methods

Two empirical methods used in the design calculation are Rock Mass Rating (RMR) classification system (Bieniawski 1989) and Rock Mass Quality (Q) system of Norweigian Geotechnical Institute (NGI) (Barton et al. 1974).

5.4.1.1 RMR System

The RMR system was developed by Bieniawski (1989). This engineering classification of rock masses, especially evolved for rock engineering applications, provides a general rock mass rating (RMR) increasing with rock quality from 0 to 100. It is based upon the following six parameters:

- strength of the rock

- drill core quality or RQD
- joint and fracture spacing
- joint conditions
- ground water conditions
- orientation of joints

These parameters not only are measurable in the field but can also be obtained from borings. Joints are the major factor in this classification system; four of the six parameters (RQD, joint spacing, joint conditions, and orientation of joints) are related to joint characteristics. Increments of rock mass rating corresponding to each parameter are summed to determine RMR.

The RMR values for various rock units at the repository host horizon are generally available from the ESF and ECRB. In case these RMR values are not available, empirical correlation can be used to estimate RMR values based on known rock mass modulus. The empirical correlation used in this calculation is as follows (Barton 2002, Eq. 8):

$$RMR = 40 \log E_m + 10 \qquad \text{(Eq. 5-1)}$$

where E_m = rock mass modulus in GPa

Once the RMR values are determined, the rock mass quality for each rock unit considered can be judged based on the guidelines provided by Bieniawski (1989, Tables 4.1 and 4.2). Recommendation for the excavation scheme and rock support needs can be made by following the guidelines presented in Table 5-1 (Bieniawski 1989, Table 4.4).

Details on how to apply the RMR classification system to the preliminary design of ground support for rock tunnels such as those in repository emplacement drifts can be found in the *Engineering Rock Mass Classifications* (Bieniawski 1989, Section 4).

Table 5-1. Estimate of Ground Support Needs Based on RMR System

Rock mass class	Excavation	Rock bolts (20 mm diameter, fully grouted)	Shotcrete	Steel sets
I - Very good rock *RMR*: 81-100	Full face, 3 m advance.	Generally no support required except spot bolting.		
II - Good rock *RMR*: 61-80	Full face , 1-1.5 m advance. Complete support 20 m from face.	Locally, bolts in crown 3 m long, spaced 2.5 m with occasional wire mesh.	50 mm in crown where required.	None.
III - Fair rock *RMR*: 41-60	Top heading and bench 1.5-3 m advance in top heading. Commence support after each blast. Complete support 10 m from face.	Systematic bolts 4 m long, spaced 1.5 - 2 m in crown and walls with wire mesh in crown.	50-100 mm in crown and 30 mm in sides.	None.
IV - Poor rock *RMR*: 21-40	Top heading and bench 1.0-1.5 m advance in top heading. Install support concurrently with excavation, 10 m from face.	Systematic bolts 4-5 m long, spaced 1-1.5 m in crown and walls with wire mesh.	100-150 mm in crown and 100 mm in sides.	Light to medium ribs spaced 1.5 m where required.
V – Very poor rock *RMR*: < 20	Multiple drifts 0.5-1.5 m advance in top heading. Install support concurrently with excavation. Shotcrete as soon as possible after blasting.	Systematic bolts 5-6 m long, spaced 1-1.5 m in crown and walls with wire mesh. Bolt invert.	150-200 mm in crown, 150 mm in sides, and 50 mm on face.	Medium to heavy ribs spaced 0.75 m with steel lagging and forepoling if required. Close invert.

Source: Bieniawski 1989, Table 4.4.

5.4.1.2 Q System

The Q system, developed in Norway by Barton, Lien, and Lunde (1974), provides for the design of rock support for tunnels and large underground chambers. The system utilizes the following six factors:

- RQD
- Number of joint sets
- Joint roughness
- Joint alteration
- Joint water condition

- Stress condition

The factors are combined in the following way to determine the rock mass quality (Q) as (Barton et al. 1974, Eq. 1),

$$Q = \left(\frac{RQD}{J_n}\right)\left(\frac{J_r}{J_a}\right)\left(\frac{J_w}{SRF}\right) \quad \text{(Eq. 5-2)}$$

where RQD = rock quality designation
J_n = joint set number
J_r = joint roughness number
J_a = joint alteration number
J_w = joint water reduction factor
SRF = stress reduction factor (dependent on loading conditions)

The three ratios in the equation - RQD/Jn, Jr/Ja, and Jw/SRF - represent block size, minimum inter-block shear strength, and active stress, respectively (Barton et al. 1974, p. 202).

Similar to the RMR values, Q indices for various rock units at the repository host horizon are generally available from the ESF and ECRB. In case these Q indices are not available, empirical correlation can be used to estimate Q indices based on given rock mass modulus. The empirical correlation used in this calculation is as follows (Hoek et al. 2000, Eqs. 8.16 and 8.19):

$$Q = Q' \times \frac{J_w}{SRF} = e^{\frac{RMR-44}{9}} \times \frac{J_w}{SRF} \quad \text{(Eq. 5-3)}$$

where

$$Q' = \left(\frac{RQD}{J_n}\right)\left(\frac{J_r}{J_a}\right)$$

The RMR value in Eq. 5-3 is estimated from the given rock mass modulus using Eq. 5-1.

The Q index is used with the Equivalent Dimension, defined as the largest of span, diameter, and height divided by the excavation support ratio (ESR). ESR is roughly analogous to the inverse of the factor of safety used in engineering design. The ESR reflects the degree of safety and ground support required for an excavation as determined by the purpose, presence of machinery, personnel, etc., to meet safety requirements. In essence, the safety factor of an opening can be increased by reducing the ESR value. The ESR values for various underground openings can be estimated based on Barton et al. (1974, Table 7). As recommended by Hardy and Bauer (1991, Section 12.7.1) an ESR value of 1.3 is appropriate for the Yucca Mountain repository drifts.

The Equivalent Dimension is plotted against Q on the design chart (Figure 5-5) to determine the required rock support category (Hoek et al. 2000, Figure 4.3). Thermal or seismic loads can be included in an implicit way, by increasing the stress reduction factor, thereby requiring a higher degree of support.

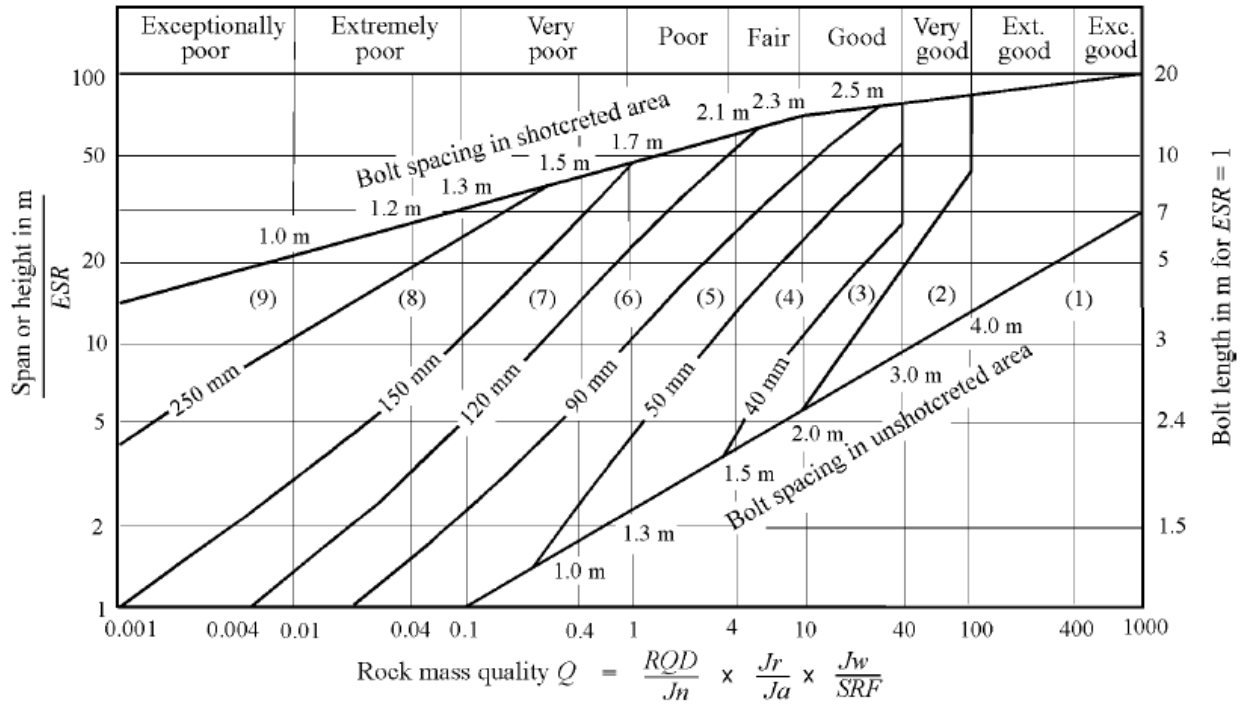

REINFORCEMENT CATEGORIES

1) Unsupported
2) Spot bolting
3) Systematic bolting
4) Systematic bolting with 40-100 mm unreinforced shotcrete
5) Fibre reinforced shotcrete, 50 - 90 mm, and bolting
6) Fibre reinforced shotcrete, 90 - 120 mm, and bolting
7) Fibre reinforced shotcrete, 120 - 150 mm, and bolting
8) Fibre reinforced shotcrete, > 150 mm, with reinforced ribs of shotcrete and bolting
9) Cast concrete lining

Source: Hoek et al. 2000, Figure 4.3.

Figure 5-5. Estimated Ground Support Needs Based on Q Index

5.4.1.3 Applicability of Empirical Methods

Empirical methods are usually applicable to mining or tunneling in jointed rock mass. The non-lithophysal rock is certainly a good example of this type of rock, and use of the RMR and Q approaches for emplacement drifts in the non-lithophysal rock is considered to be conventional.

For the emplacement drifts excavated in the lithophysal rock, however, use of the RMR or Q approach for the ground support design is non-conventional, and there are no sufficient data or field experiences available to support this application. This is primarily due to the fact that the lithophysal rock contains some air-filled large cavities and is hard to be characterized using the RMR or Q index since a RQD value is defined for a rock with fractures not with voids. Therefore, these empirical methods are not used in this calculation for evaluating the requirements of ground support for emplacement drifts in the lithophysal rock. Selection of ground support methods for this rock type is based on experiences and observations from the construction of the ESF and the ECRB tunnels, and assessment from numerical analyses.

5.4.2 Analytical Methods

Analytical methods, mainly numerical methods, are used in this calculation to evaluate the stability of emplacement drifts because the loading conditions such as thermal and seismic are complex and their effect is difficult to analyze with either empirical methods or closed-form solutions. Use of numerical methods to simulate the behavior of unsupported emplacement drifts is generally considered as one of the important steps during the analysis process for ground support design for this project. Usually, the presence of ground support, such as rock bolts, in a drift excavated in a hard or competent rock has a relatively small impact on the predicted deformation and stress of rock mass in the vicinity of a drift. Modeling an unsupported drift is valuable for understanding the fundamental behavior of the drift subjected to various loading conditions without the effects of incorporating the ground support into the model.

5.4.2.1 Modeling of Emplacement Drifts

Emplacement drifts excavated in both lithophysal and non-lithophysal rock units are modeled using a two-dimensional continuum approach. Use of this approach for the ground support design calculation is consistent with the conventional practice in mining or tunneling industry. In a continuum approach, the effect of geologic features, such as fractures or lithophysae, in the rock mass is “lumped” into a thermomechanical constitutive model that represents the overall equivalent effect of these features. In a discontinuum approach, fractures or lithophysae are modeled explicitly as interfaces or cavities. The difference between these techniques is therefore the level of detail that is necessary in the model to adequately capture the deformation and failure mechanisms (Board 2003, Section 5.3).

From a ground support design perspective, stability of emplacement drifts is judged by overall rock mass displacements and stresses. Two-dimensional continuum approach that uses equivalent rock mass properties and constitutive model may provide good tools for bounding analyses and also allow ease of parametric examination and model interpretation. Therefore, it is appropriate for use in ground support design related analyses.

The FLAC computer code is employed in the two-dimensional analyses. In FLAC models, rock mass properties which reflect the effects of lithophysae and fractures on rock mass properties are used. These property values are presented in Tables 3-5 and 3-6 for the lithophysal and non-lithophysal rocks, respectively. The behavior of rock mass is judged using the Morh-Coulomb yield criterion. Figure 5-6 illustrates the configuration of a FLAC model. The vertical dimension of the model is 100 m, and the horizontal is 81 m, equal to one time the drift spacing.

In addition to FLAC models, a three-dimensional continuum model using the FLAC3D computer code is also developed to evaluate the effect of TBM advance on rock deformation. The results from this FLAC3D model provide some justification for the ground relaxation value considered in the modeling of ground support components, such as rock bolts. In the FLAC3D model, the advance rate is taken to be four times the bolt spacing ($4\times1.25=5.0$ m) per excavation cycle. This is close to one time the drift diameter of 5.5 m. Ground support is installed at the end of each excavation cycle, at a distance of 5.0 m from the tunnel face. The ground relaxation is then estimated based on these conditions and predicted vertical displacements at the drift crown during TBM advance.

5.4.2.2 Loading and Boundary Conditions

Loads considered in the evaluation of stability of emplacement drifts include in situ stress, thermal, and seismic.

5.4.2.2.1 In Situ Stress Load

Average initial vertical stress (σ_v) at the center of an emplacement drift is estimated using the following expression (Goodman 1980, Eq. 4.1):

$$\sigma_v = -\sum_{i=1}^{n} \rho_i g h_i \qquad \text{(Eq. 5-4)}$$

where ρ_i = average bulk density of the *i*th layer of rock mass, kg/m^3
h_i = thickness of the *i*th layer of rock mass above an opening, m
g = gravitational acceleration, m/s^2
n = total number of overlaying layers of rock mass, dimensionless

The negative sign in Eq. 5-4 indicates a compressive stress. Average initial horizontal stress (σ_h) at the same location is estimated as:

$$\sigma_h = K_0 \sigma_v \qquad \text{(Eq. 5-5)}$$

where K_0 = horizontal-to-vertical stress ratio, dimensionless.

Given that a bulk density of 2,410 kg/m^3 (Section 3.1.8), a gravitational acceleration of 9.81 m/s^2, a depth or thickness measured from the center of emplacement drifts to the ground surface of 400 m (Section 4.1), and a horizontal-to-vertical stress ratio of 0.3 (Section 4.2), the initial vertical and horizontal stresses at the center of emplacement drifts prior to excavation are estimated to be about -9.46 MPa and -2.84 MPa, respectively.

For bounding analyses, the rounded lower and upper bound K_o values of 0.3 and 1.0, respectively, are used.

As shown in Figure 5-6, for stress analysis, the lower boundary of the FLAC model is fixed in both the vertical and horizontal directions, and the two lateral boundaries are fixed in the horizontal direction. Overburden is applied on the upper boundary.

5.4.2.2.2 Thermal Load

A design thermal load for LA design is 1.45 kW/m (Section 3.2.2.3). Instead of performing a thermal analysis to determine temperature distributions with time for this calculation, time-dependent temperatures from a ventilation model were employed. These time-dependent temperatures, as shown in Figure 5-6, which was generated based on Table 3-1,were determined using this thermal load, and reflect the effect of forced ventilation of 15 m^3/s during the preclosure period of 50 years (DTN: MO0306MWDALAFV.000).

In the FLAC models (see Figure 5-7), time histories of temperatures on the model boundaries (see Section 3.1.1, Table 3-1, and Figure 5-6) are applied as time-dependent boundary conditions. Two lateral boundaries are adiabatic due to a thermal symmetry, meaning that there is no heat flow across these boundaries. The temperature distributions within rock are calculated based on these thermal boundary conditions using a thermal analysis logic built in FLAC code. Thermally-induced stresses within rock at a given time are then estimated from the changes in temperature and rock mass coefficient of thermal expansion through a thermomechanical analysis.

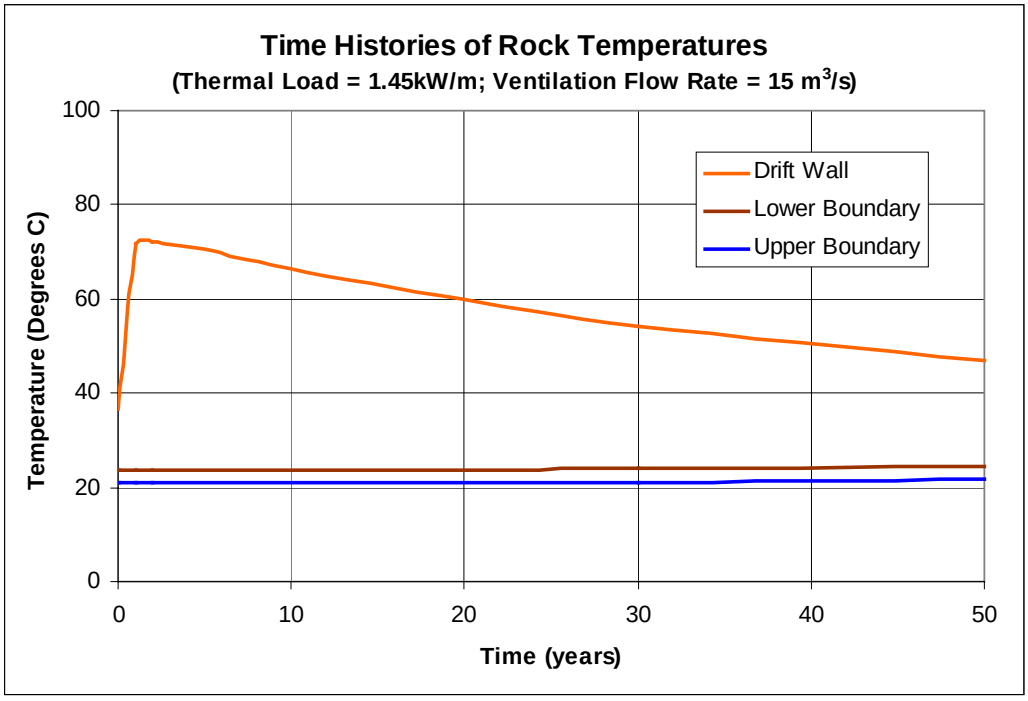

Source: MO0306MWDALAFV.000.

Figure 5-6. Time Histories of Rock Temperatures on Model Boundaries

5.4.2.2.3 Seismic Load

Seismic load corresponding to a mean annual exceedance probability of 1×10^{-4} (10,000 year), as mentioned in Section 3.1.7, are used as a basis for determination of the effect of seismic motions on stability of emplacement drifts and performance of ground support. This load is time-dependent, resulting in transient variations in displacements and stresses in rock mass and installed ground support components. The seismic load is considered in the FLAC models by applying seismically-induced stresses (both normal and shear tractions) to the lower boundary of a model (see Figure 5-6). These boundary stresses are calculated based on time-dependent ground velocities (P- and S-plane waves or vertical and horizontal velocities), as shown in Figure 3-1, using the following equations (Itasca Consulting Group 2002, FLAC Version 4.0, *Optional Features*, Equations 3.12 and 3.13):

$$t_n = 2\rho C_p v_n$$
$$t_s = 2\rho C_s v_s \qquad \text{(Eq. 5-6)}$$

where t_n = normal traction, Pa
t_s = shear traction, Pa
ρ = rock mass density, kg/m^3
C_p = speed of P-wave propagation through the rock, m/s
C_s = speed of S-wave propagation through the rock, m/s
v_n = normal particle velocity history, m/s
v_s = shear particle velocity history, m/s

C_p and C_s are given by (Itasca Consulting Group 2002, FLAC Version 4.0, *Optional Features*, Equations 3.14 and 3.15):

$$C_p = \sqrt{\frac{K + 4G/3}{\rho}} \quad \text{(Eq. 5-7)}$$

$$C_s = \sqrt{\frac{G}{\rho}} \quad \text{(Eq. 5-8)}$$

where K = bulk modulus of the rock mass, N/m^2
G = shear modulus of the rock mass, N/m^2

The factor 2 in Equation 5-7 is due to quiet or viscous boundary. Both P- and S-waves are applied simultaneously. The boundary conditions used in the dynamic analysis of the FLAC models are illustrated in Figure 5-7. Quiet boundaries, as indicated in Figure 5-7 as viscous boundaries, are used on all outside boundaries. These boundaries prevent outgoing seismic waves from reflecting back into the model. Quiet boundaries are combined with free-field boundaries on two lateral boundaries, as also shown in Figure 5-7. The free-field boundaries perform one-dimensional simulation of vertically propagating plane waves that represent motions of truncated, semi-infinite medium. They prevent distortion of vertically propagating plane waves along the quiet boundaries.

In order to reduce computational time, only portion of the velocity time histories that covers 5 to 95 percent of energy bracket is used. The dynamic time corresponding to this portion of velocity time histories is from 9.78 to 58.79 seconds (DTN: MO0306SDSAVDTH.000, MatH1.dur, MatH2.dur, and MatV.dur).

5.4.2.2.4 Operational Loads

Operational loads, such as waste package weight and invert material weight, are not considered in this calculation due to the preliminary nature of the design. Exclusion of these loads are believed to result in a conservative estimate of the rock displacements since these loads are expected to offset some of the displacements caused by excavation and heating. In addition, these loads act on the invert structure, not on ground support components.

5.4.2.2.5 Combined Loads

Combined in situ stress, thermal, and seismic loads are considered in the calculation. A load factor of unity is used. Seismic load is applied at a time of 0 and 50 years following heating.

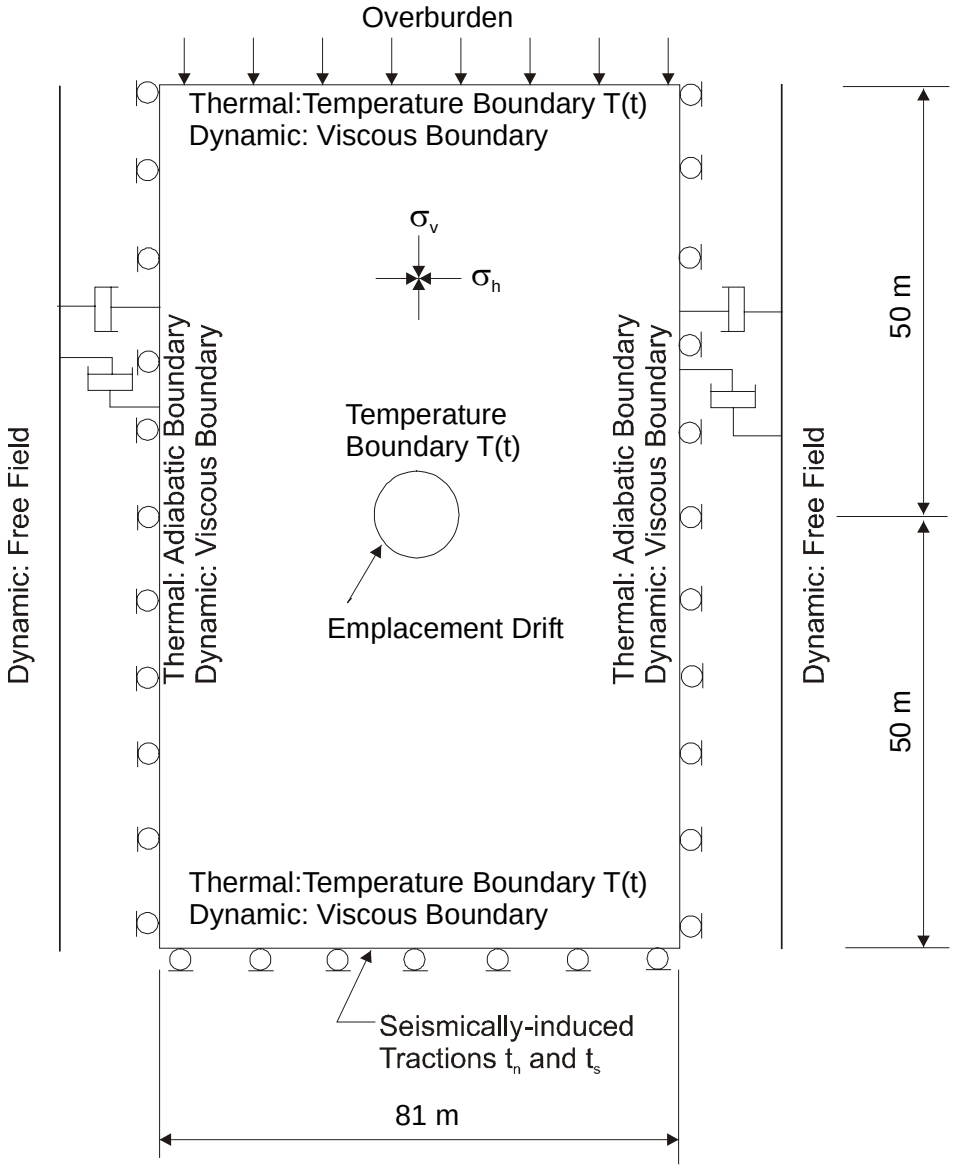

Figure 5-7. Geometry and Boundary Conditions for FLAC Models

5.4.2.3 Evaluation of Factor of Safety

5.4.2.3.1 Factor of Safety regarding Drift Stability

Stability of unsupported emplacement drifts can be evaluated using the concept of factor of safety. Factor of safety can be estimated using either stress or displacement criterion. In structural design, stress or displacement criterion is clearly specified, and determination of factor of safety for a structural member can be easily achieved. In tunnel design, however, there is no well-defined stress or displacement criterion regarding the opening stability. Evaluation of

factor of safety for an unsupported emplacement drift requires the development of a different approach suitable to tunnel design. The factor of safety estimated in this calculation is based on both stress and critical state criteria. The approach is described as follows.

- Factor of Safety Based on Shear Strength or Stress Criterion

Factor of safety, based on stress criterion, is defined as the average ratio of rock mass shear strength to shear stresses in rock adjacent to the drift. Shear strength of rock mass is determined by cohesion and frictional angle if the Mohr-Coulomb yield criterion is used. This yield criterion is expressed as (Goodman 1980, Eq. 3.7):

$$\tau_p = c + \sigma \tan\phi \qquad \text{(Eq. 5-9)}$$

where τ_p = shear strength, Pa
c = cohesion, Pa
σ = normal stress, Pa
ϕ = angle of internal friction, degree

Shear stress (τ) at each nodal point or centroid of an element in a numerical model of the specific category rock mass is calculated as:

$$\tau = \frac{\sigma_1 - \sigma_3}{2} \qquad \text{(Eq. 5-10)}$$

where σ_1 and σ_3 = major and minor principal stresses, respectively, Pa

Hence, a strength-to-stress ratio (STSR) at a given point can be estimated as:

$$STSR = \frac{\tau_p}{\tau} \qquad \text{(Eq. 5-11)}$$

Strength-to-stress ratios vary from point to point, and usually are lower near a drift wall and higher away from the wall. Using the lowest STSR value for a specific point as a yardstick of factor of safety to judge the entire drift performance is too conservative, and may lead to over-design. A more reasonable approach is to use an average value of STSR over a representative or critical region of emplacement drift. This average value of STSR can then be judged as a factor of safety for a drift under a specific loading condition.

There are many ways to determine a representative region over which a factor of safety is estimated. For example, an annulus around an emplacement drift is considered adequate for this calculation since this is the area in which the stability is most concerned. The thickness of the annulus may be determined based on the anticipated area of reinforcement by installed ground support.

- Factor of Safety Based on Critical State Criterion

Critical state criterion is also used in judging the stability of emplacement drifts. This criterion is applied in a different way than that used in the stress criterion. In this approach, rock displacements or deformation rates at a point of interest, say the crown, are monitored by gradually reducing values of cohesion and frictional angle for a specific rock type until the displacements or velocities diverge, indicating that the drift cannot achieve equilibrium or stable condition. The drift stability corresponding to this condition is at the critical state. Once the drift reaches the critical state, the rock displacements go to infinite or the velocities become non-zero. The reduced values of cohesion and frictional angle associated with the critical state are then compared to those so-called baselined values, as listed in Table 4-1 or Table 3-5, for a specific rock mass category. The ratio of the baselined shear strength to the reduced one is defined as the factor of safety for an emplacement drift as

$$FS = \frac{\tau_p}{\tau_r} = \frac{c_p + \sigma \tan \phi_p}{c_r + \sigma \tan \phi_r} \qquad \text{(Eq. 5-12)}$$

where τ_p = baselined shear strength, Pa
τ_r = reduced shear strength, Pa
c_p = baselined cohesion, Pa
c_r = reduced cohesion, Pa
ϕ_p = baselined frictional angle, degree
ϕ_r = reduced frictional angle, degree
σ = normal stress, Pa

If normal stress remains constant and c and tanϕ in the denominator of Eq. 5-12 are reduced with the same percentage, the factor of safety will then be proportional to

$$FS = \frac{c_p}{c_r} \qquad \text{(Eq. 5-13)}$$

or

$$FS = \frac{\tan \phi_p}{\tan \phi_r} \qquad \text{(Eq. 5-14)}$$

In the calculation, rock mass strength properties, c and tanϕ, are reduced at an interval of 5 to 10 percent to evaluate the factor of safety of emplacement drifts. This results in a series of reduced cohesion and frictional angle pairs. For each pair of cohesion and frictional angle, a FLAC model is run. The rock vertical displacements at the crown are monitored. The final run will show that the drift becomes unstable. To get more accurate results, percentage of reduction in each interval strength should be small. In this calculation a minimum percentage used is 5 percent, and considered reasonable for the purpose of ground support design.

To more realistically simulate the behavior of rock mass once it reaches the yield limit, a strain-softening plasticity model is used. In the Mohr-Coulomb model, the cohesion, frictional angle,

and tensile strength remain constant, while in the strain-softening plasticity model, these strength properties vary or decrease with plastic strain. The material will behave linearly up to the point of yield. Upon yield it softens and attains a residual strength instantly. In this calculation, the residual cohesion is equal to half of the given or 'peak' cohesion, the residual frictional angle remains unchanged, and the residual tensile strength is set to zero. These residual strength values remain constant during the plastic deformation.

5.4.2.3.2 Factor of Safety regarding Ground Support Performance

Similar to a structural design, factor of safety of a ground support component can be evaluated using the following expression:

$$FS = \frac{Strength}{Stress} \quad or \quad \frac{Anchorage \;\; Capacity}{Force} \qquad \text{(Eq. 5-15)}$$

For rock bolts, the strength can be either tensile strength or shear strength, depending on the type of bolts used, and for friction-type bolts, both stress conditions should be examined.

In most underground excavations, use of Equation 5-15 to evaluate the factor of safety may cause confusing. This is because, first, the axial forces in bolts are difficult to be calculated accurately; second, the function of fully-grouted or friction-type rock bolts is to reinforce rock mass like steel rebars in reinforced concrete. If slippage occurs on the interface between bolt and rock, the bolt will lose its intended function even though the bolt itself does not yield.

5.4.3 Analysis of Uncertainties Associated with Design Inputs and Modeling

Uncertainties in input data and design approaches exist. Attempts are made in the design calculation to minimize uncertainties by selecting the bounding input values or loads and conservative approaches. A more comprehensive sensitivity studies that address uncertainties associated with variations in data, loading conditions, and modeling approaches will be covered in a separate scoping analysis. Therefore, details on the uncertainties analysis will not be discussed in this calculation.

6. RESULTS OF DESIGN CALCULATION

This section presents the results of design analyses performed for emplacement drifts. These include empirical and analytical analyses. In the empirical analysis, both the RMR and Q approaches are used for the ground support needs for emplacement drifts in the lithophysal and non-lithophysal rocks. In the analytical analysis, numerical modeling is conducted using the bounding rock mass properties and loading conditions consisting of in situ, thermal, and seismic loads.

For ground support design purposes, the concept of ground reaction curve (GRC) is used to examine the interaction between rock bolts and rock. The visualization of GRC can also serve as an additional check of the stability of unsupported emplacement drifts, and to quantify the potential load that may be induced in rock bolts due to further ground convergence after bolt installation.

Unless otherwise indicated, the term “ground support” or “ground control” used in this section is referred to as the final ground support. When the initial ground support is discussed, it will be explicitly indicated.

6.1 STABILITY OF UNSUPPORTED EMPLACEMENT DRIFTS

This section presents the results of assessment of stability of unsupported emplacement drifts. The assessment is based on numerical analysis using the FLAC computer code. The analysis evaluates temperature increases in rock following waste emplacement, displacement and stress in the vicinity of an unsupported emplacement drift opening, factor of safety, ground reaction curves (GRC), and ground relaxation prior to ground support installation.

6.1.1 Temperature Increase in Rock

Temperatures in rock around an emplacement drift increase due to heating by waste packages. The distributions of rock temperatures at different years following waste emplacement are presented in Figure 6-1. These temperature contours are regenerated by FLAC based on the time-dependent boundary temperatures obtained from an ANSYS ventilation model (Section 3.1.1). With these temperatures, thermally-induced displacements and stresses in rock are calculated through thermomechanical analyses.

It can be seen that the peak temperature on drift wall is recorded at 2 years after waste emplacement, but the heat front continues to propagate. As a result, the heated rock volume increases with time over a period of 50 years considered, which dictates the continuous changes in rock displacements and stresses. In general, the increase in temperatures (less than 50°C) is not significant owing to the effect of forced ventilation during the preclosure period.

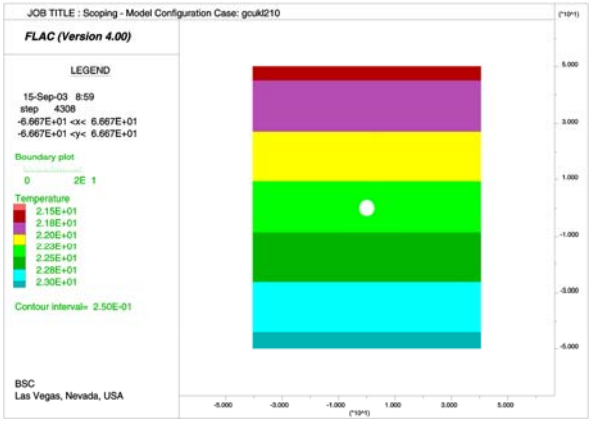

(a) initially

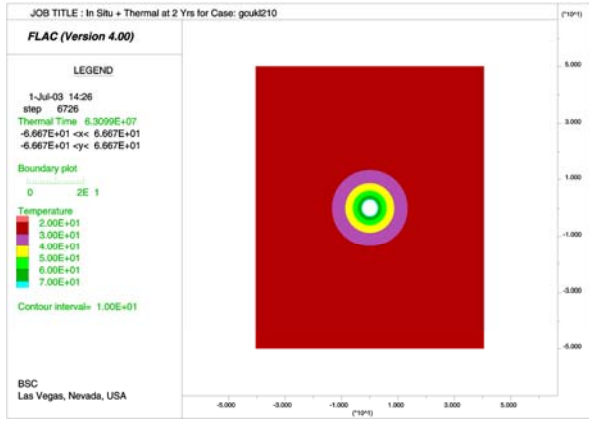

(b) at 2 years

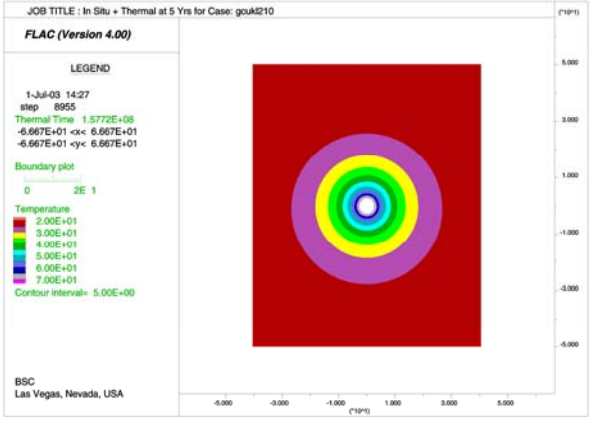

(c) at 5 years

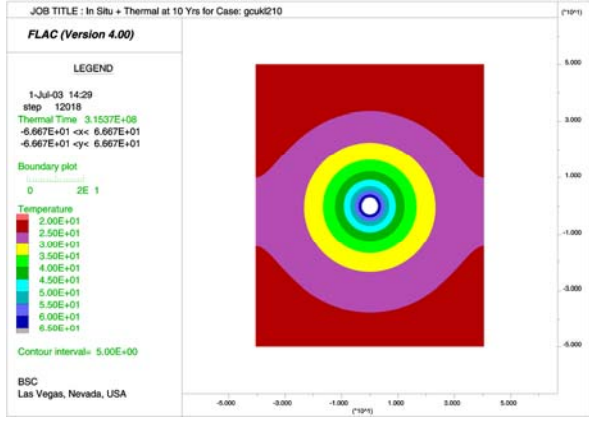

(d) at 10 years

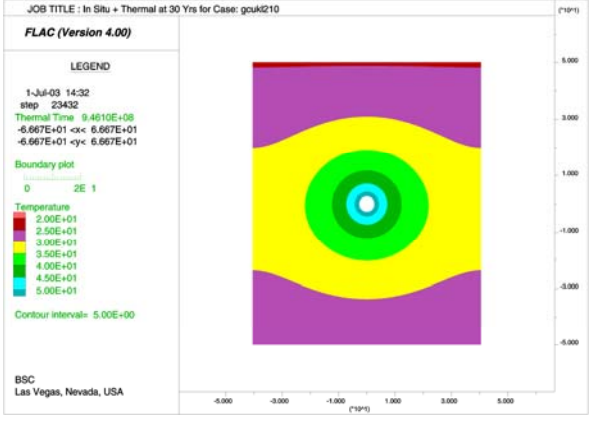

(e) at 30 years

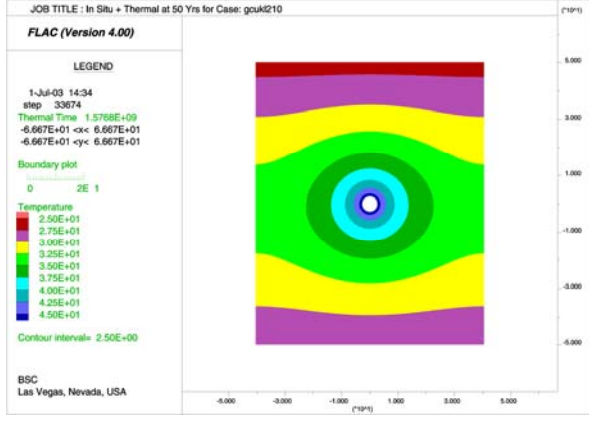

(f) at 50 years

Note: Temperature in °C.

Figure 6-1. Temperature Contours around Emplacement Drifts at Various Years Following Waste Emplacement

6.1.2 Rock Displacement and Stress

Drift closures, defined as the relative displacements between two points of interest on the surface of a drift, are commonly used to evaluate the status of drift stability. The magnitude of stress near the vicinity of drift may also provide some information on the drift stability since excess overstress in rock may result in yielding or failure in rock. Therefore, predicted displacement and stress around an unsupported emplacement drift are examined closely to judge its stability under anticipated loading conditions.

6.1.2.1 Drift Closures

Both vertical and horizontal drift closures are predicted for in situ, thermal, and seismic loading conditions. The vertical closure is defined as the relative displacements between the invert and the crown, while the horizontal closure is defined as those between the walls or springlines. The positive closure indicates that two reference points move toward each other, i.e., a reduction in dimension.

For emplacement drifts in the lithophysal rock, analyses were performed by considering the upper and lower bounds of rock mass properties. For examples, only the rock mass properties associated with the categories 1 and 5 were used. Responses associated with other categories of rock mass properties are anticipated to be bounded by those cases considered. It is noted that, as indicated in Table 3-4, there is a category 6 for the lithophysal rock, and this category rock mass is associated with the excavation-disturbed zone (EDZ). Observations from the ECRB have not indicated a assembly of rock mass represented by this category (see Section 5.2). Therefore, category 6 rock mass is not considered representative as a low bound, and excluded from consideration in this calculation. Cases which include the effect of EDZ using the category 6 rock mass properties will be presented in an ongoing scoping analysis.

Time histories of the drift vertical and horizontal closures are illustrated in Figures 6-2a and 6-2b for unsupported emplacement drifts in the lithophysal rock subjected to in situ and thermal loads corresponding to the initial horizontal-to-vertical stress ratio (K_o) of 0.3 and 1.0, respectively. The maximum vertical closures are predicted to range from about 38 mm with K_o=1.0 to about 55 mm at K_o=0.3 for category 1 rock mass, and from about 3 mm with K_o=1.0 to about 5 mm at K_o=0.3 for category 5 rock mass. The maximum horizontal closures are expected to vary from about 4 mm with K_o=0.3 to about 39 mm at K_o=1.0 for category 1 rock mass, and from about 1 mm with K_o=0.3 to about 4 mm at K_o=1.0 for category 5 rock mass. It appears that the rock deformation is induced primarily by in situ stress during excavation. Thermally-induced deformation is minimal (a maximum of about 2 mm for all cases analyzed) because the increase in temperature during the preclosure ventilation period is very small.

Similarly, the drift closures for emplacement drifts in the non-lithophysal rock were also predicted with the bounding rock mass properties, as shown in Figure 6-3a and 6-3b for K_o=0.3 and K_o=1.0, respectively. The maximum vertical closures are predicted to range from about 7 mm with K_o=1.0 to about 10 mm at K_o=0.3 for category 1 rock mass, and from about 3 mm with K_o=1.0 to about 4 mm at K_o=0.3 for category 5 rock mass. The maximum horizontal closures are shown to vary from about 1 mm with K_o=0.3 to about 8 mm at K_o=1.0 for category 1 rock mass, and from about 1 mm with K_o=0.3 to about 4 mm at K_o=1.0 for category 5 rock mass.

Again, it can be seen from Figures 6-2 and 6-3 that the rock deformation is induced primarily by excavation under the in situ stress. Thermally-induced deformation is very small.

Drift closures induced by seismic motions were calculated for emplacement drifts in both the lithophysal and non-lithophysal rocks, and are presented in Figures 6-4 through 6-7. It is indicated that seismically-induced rock deformation is not significant. The maximum closures due to seismic loadings are predicted to vary from less than 10 mm for the category 1 lithophysal rock to less than 5 mm for the category 1 non-lithophysal rock. The results also indicate that the rock is not expected to behave much differently if the seismic motions occur at the beginning of waste emplacement (year=0) or at 50 years following waste emplacement. This is because that the effect of heating by waste on rock mass behavior is minimized by the use of continuous ventilation during the preclosure period.

Combining the rock displacements induced by in situ and thermal loads with those caused by seismic load results in the maximum anticipated drift closures of about 65 mm for the weakest lithophysal rock (category=1) and about 15 mm for the weakest non-lithophysal rock (category=1).

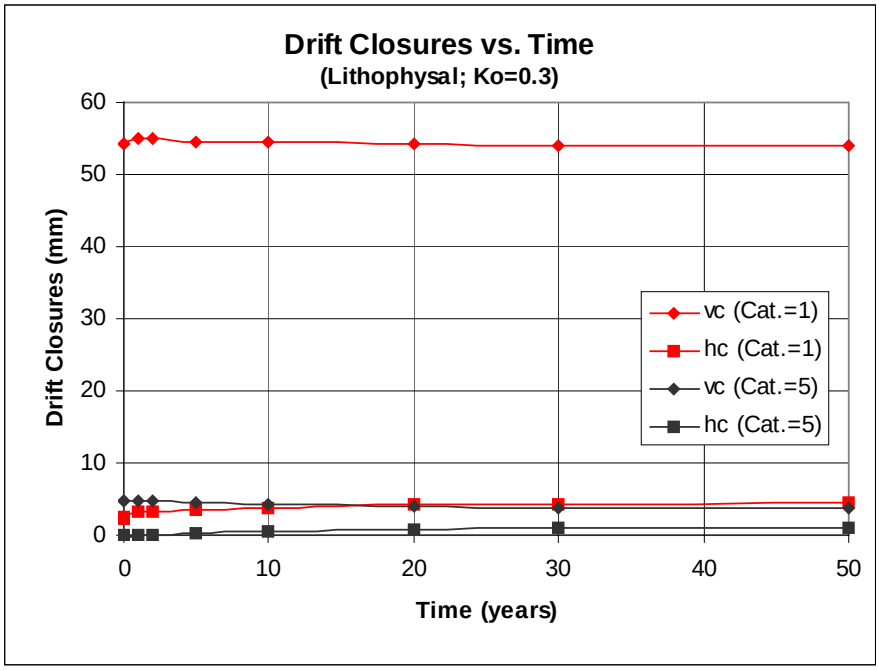

(a)

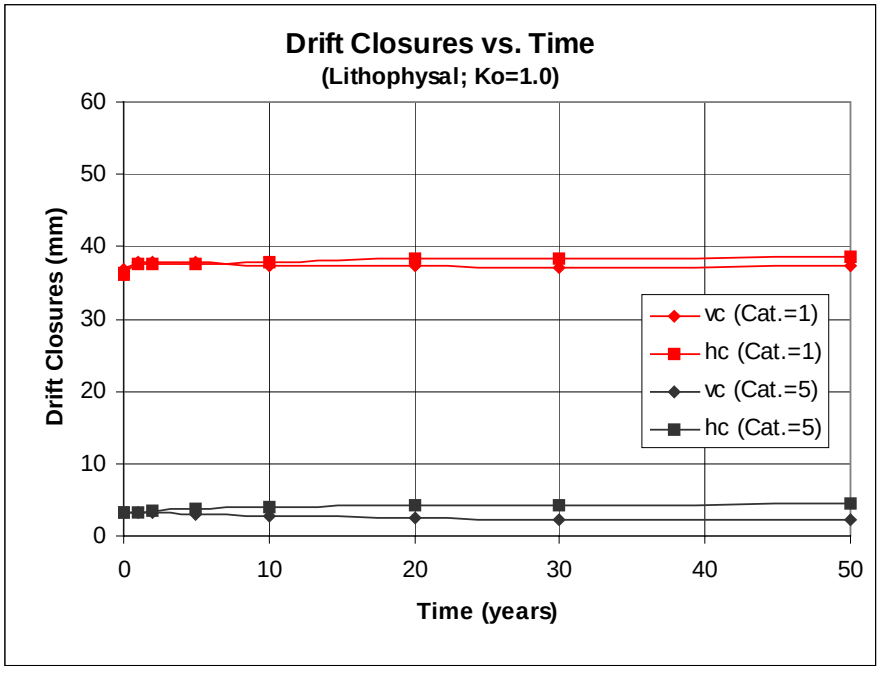

(b)

Figure 6-2. Time Histories of Closures of Emplacement Drifts in Lithophysal Rock with Categories 1 and 5 under In Situ and Thermal Loads: (a) Ko=0.3; (b) Ko=1.0

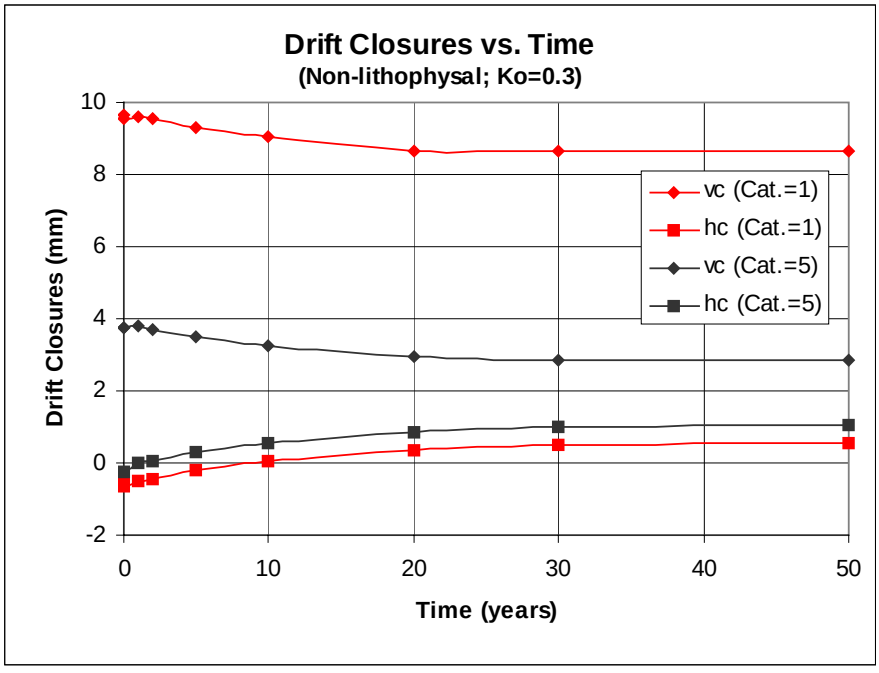

(a)

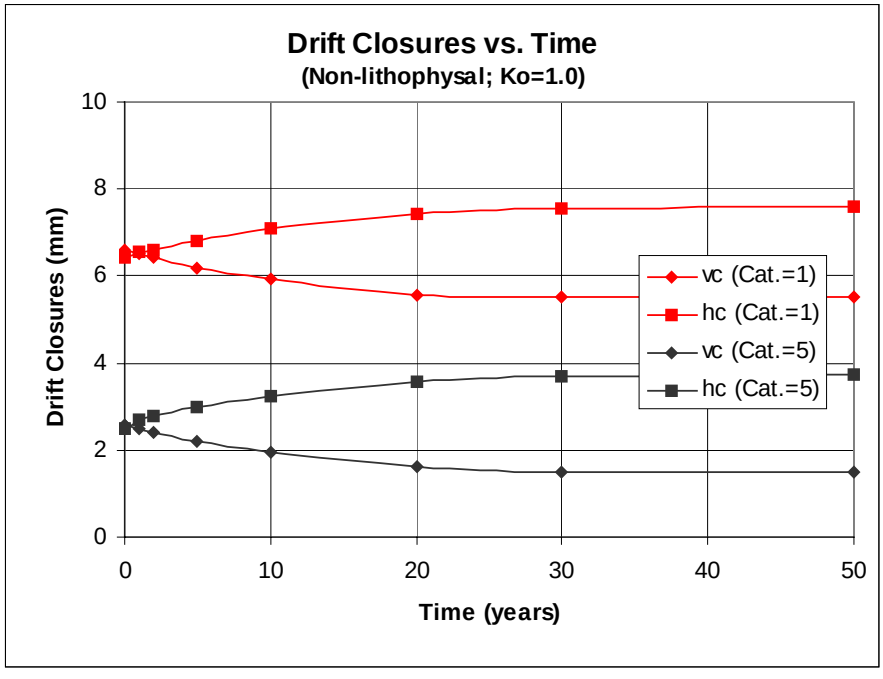

(b)

Figure 6-3. Time Histories of Closures of Emplacement Drifts in Non-lithophysal Rock with Categories 1 and 5 under In Situ and Thermal Loads: (a) Ko=0.3; (b) Ko=1.0

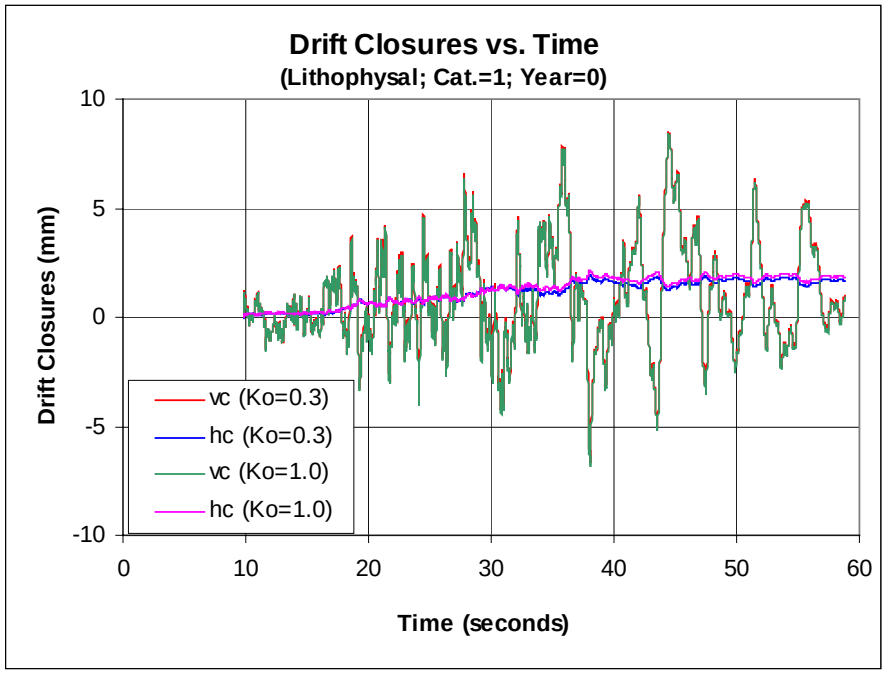

(a)

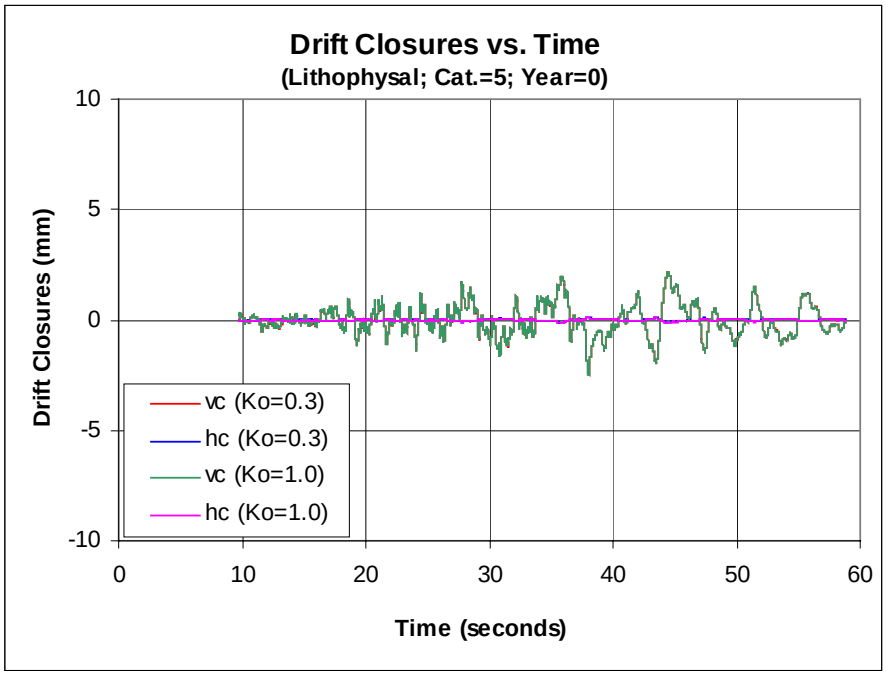

(b)

Figure 6-4. Time Histories of Closures of Emplacement Drifts in Lithophysal Rock with Categories 1 and 5 under Seismic Load at Year=0: (a) Ko=0.3; (b) Ko=1.0

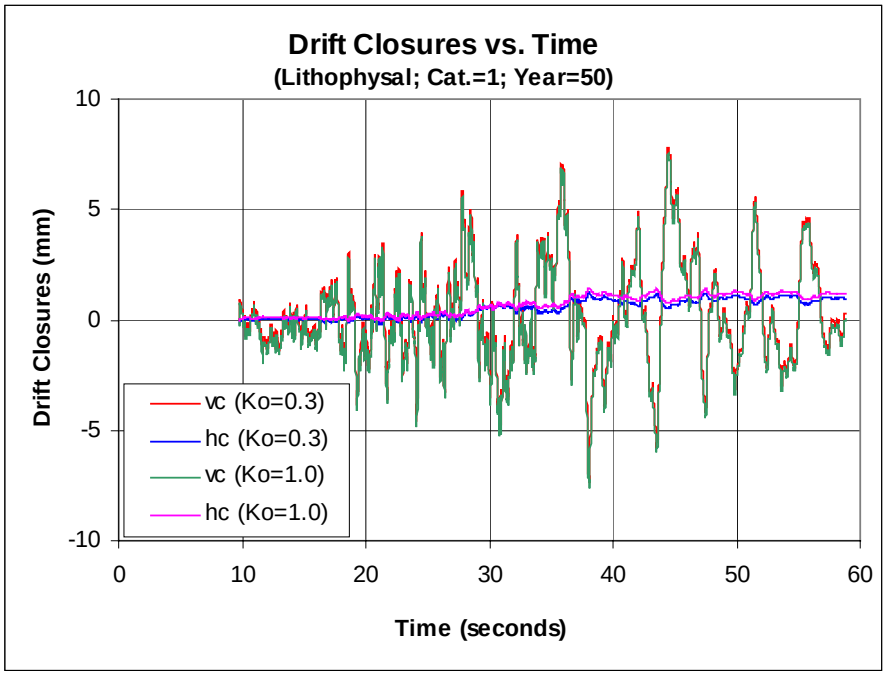

(a)

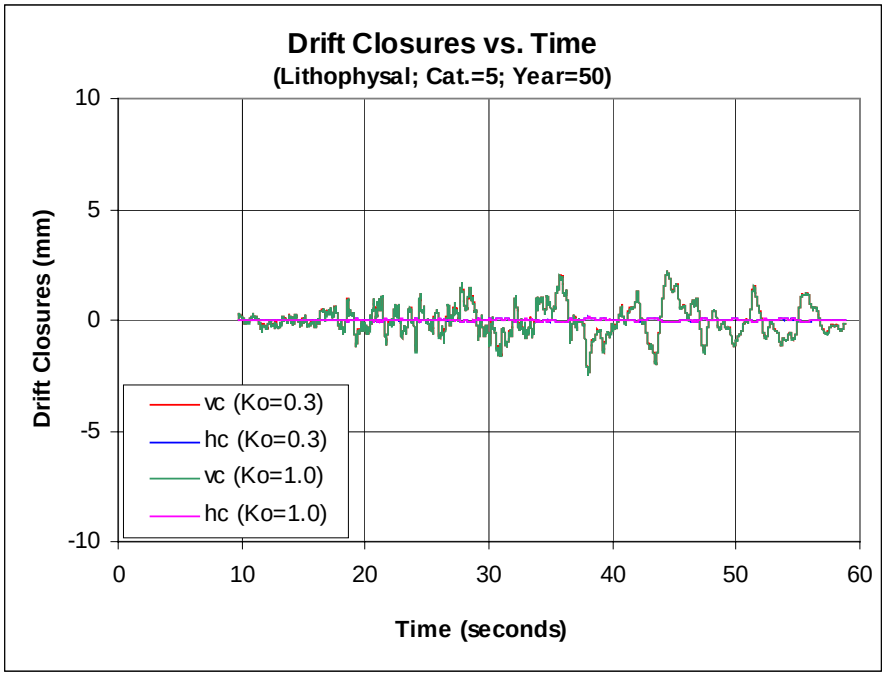

(b)

Figure 6-5. Time Histories of Closures of Emplacement Drifts in Lithophysal Rock with Categories 1 and 5 under Seismic Load at Year=50: (a) Ko=0.3; (b) Ko=1.0

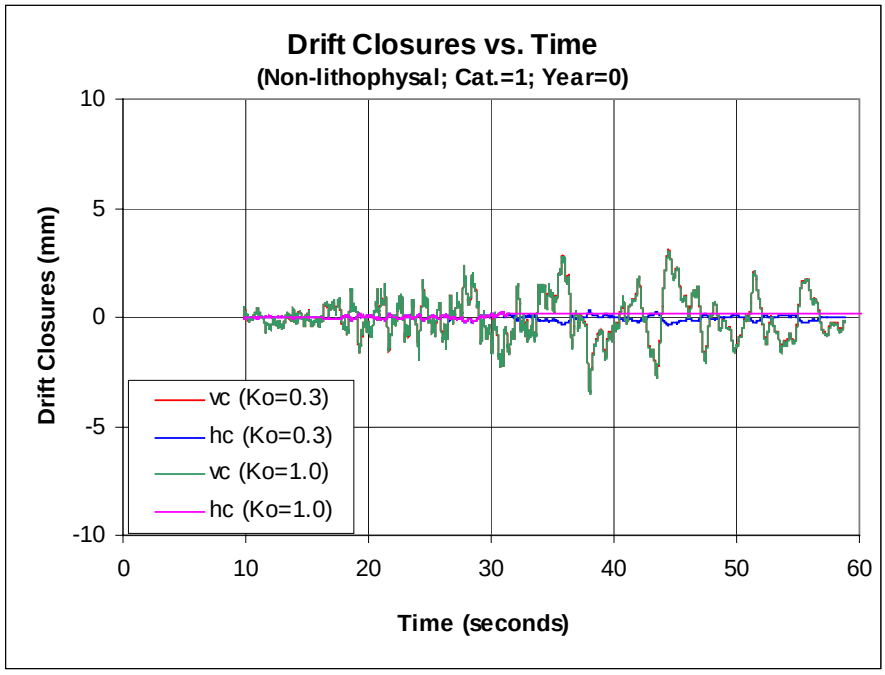

(a)

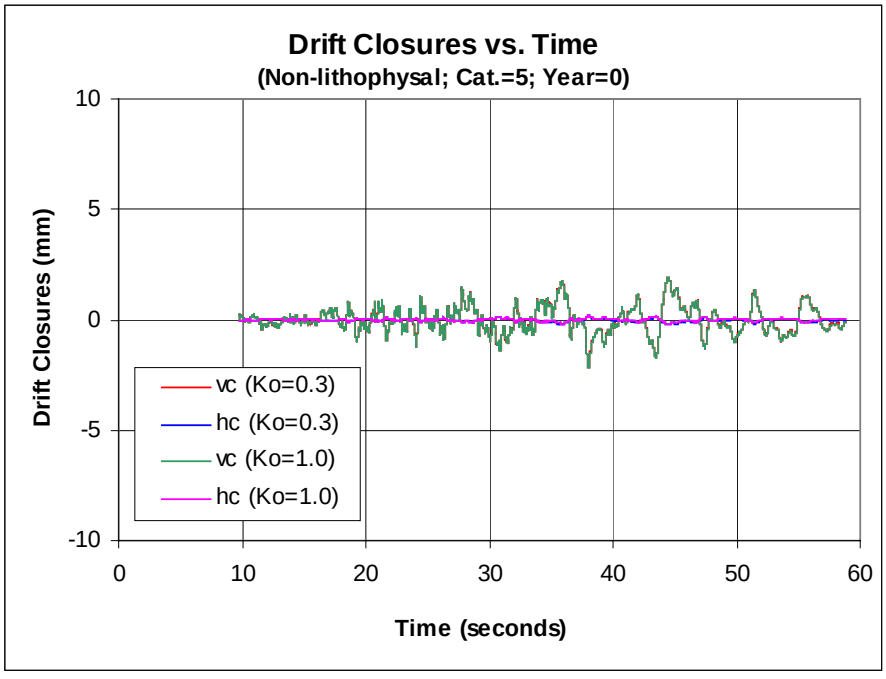

(b)

Figure 6-6. Time Histories of Closures of Emplacement Drifts in Non-lithophysal Rock with Categories 1 and 5 under Seismic Load at Year=0: (a) Cat.=1; (b) Cat.=5

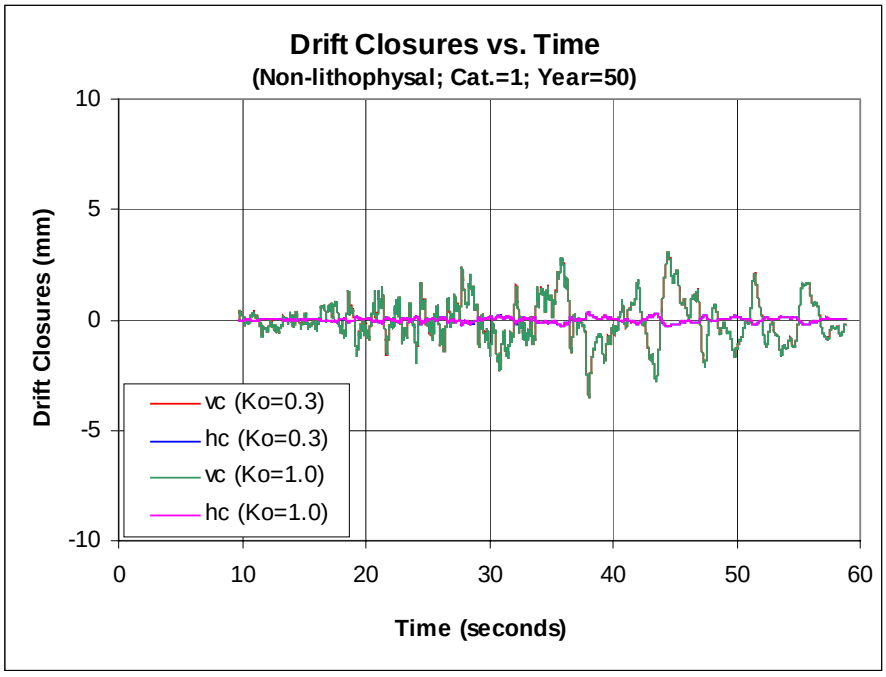

(a)

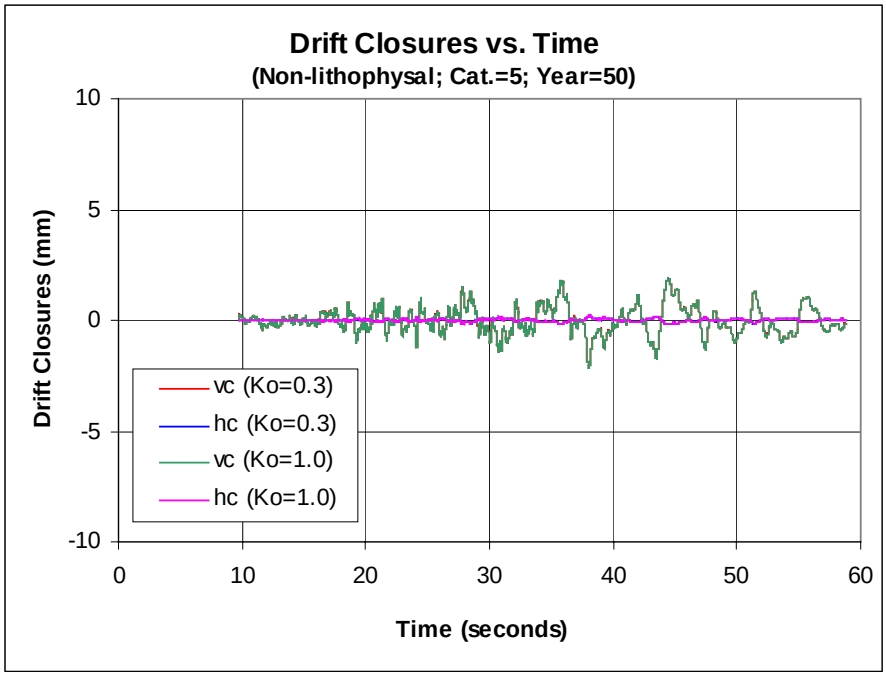

(b)

Figure 6-7. Time Histories of Closures of Emplacement Drifts in Non-lithophysal Rock with Categories 1 and 5 under Seismic Load at Year=50: (a) Cat.=1; (b) Cat.=5

6.1.2.2 Stress in Rock Adjacent to Drifts

Stresses in rock adjacent to emplacement drifts were predicted to assist in evaluation of stability of these drifts subjected to in situ, thermal, and seismic loads. Areas where the magnitude of stresses is critical to the stability of emplacement drifts are those near the crown and the springlines. The major principal stresses in these areas are examined very closely to ensure that any potential unstable conditions are prevented by appropriate ground support measures.

Time histories of the major principal stresses at the crown and the springline are shown in Figures 6-8a and 6-8b for unsupported emplacement drifts in the lithophysal rock subjected to in situ and thermal loads corresponding to the initial horizontal-to-vertical stress ratio (K_o) of 0.3 and 1.0, respectively. It is indicated that stresses change with temperature, especially in category 5 rock mass, though the magnitude of change is not substantial because the variation in temperature is not great. The maximum major principal stresses are expected to vary from about 17 to 20 MPa for category 1 rock to about 20 to 28 MPa for category 5 rock.

Time histories of the major principal stresses at the crown and the springline are shown in Figures 6-9a and 6-9b for unsupported emplacement drifts in the non-lithophysal rock subjected to in situ and thermal loads corresponding to the initial horizontal-to-vertical stress ratio (K_o) of 0.3 and 1.0, respectively. Similar to what is observed for the lithophysal rock, stresses change with temperature. The maximum major principal stresses are expected to vary from about 22 to 24 MPa for category 1 rock to about 31 MPa for category 5 rock.

During seismic shaking, stresses fluctuate with seismic velocities, as illustrated in Figures 6-10 and 6-11 for the lithophysal rock and in Figures 6-12 and 6-13 for the non-lithophysal rock, respectively. The magnitude of fluctuation in stresses varies with locations. Near the crown of emplacement drifts, the variations are small, while near the springlines, the changes are great. The maximum fluctuation in the major principal stresses near the springline is predicted to vary from about 2 MPa for category 1 lithophysal rock to about 6 MPa for category 5 lithophysal rock (see Figures 6-10a and 6-10b). For emplacement drifts in the non-lithophysal rock, the maximum fluctuation is predicted to vary from about 6 MPa for category 1 rock to about 9 MPa for category 5 rock (see Figures 6-12a and 6-12b). These results suggest that the stronger the rock is, the greater the variations in stress will be.

Combining the stresses induced by in situ, thermal, and seismic loads, the maximum major principal stresses in the lithophysal rock are expected to vary from about 19 to 22 MPa for category 1 rock to about 26 to 34 MPa for category 5 rock. In the non-lithophysal rock, the maximum major principal stresses are expected to vary from about 28 to 30 MPa for category 1 rock to about 40 MPa for category 5 rock.

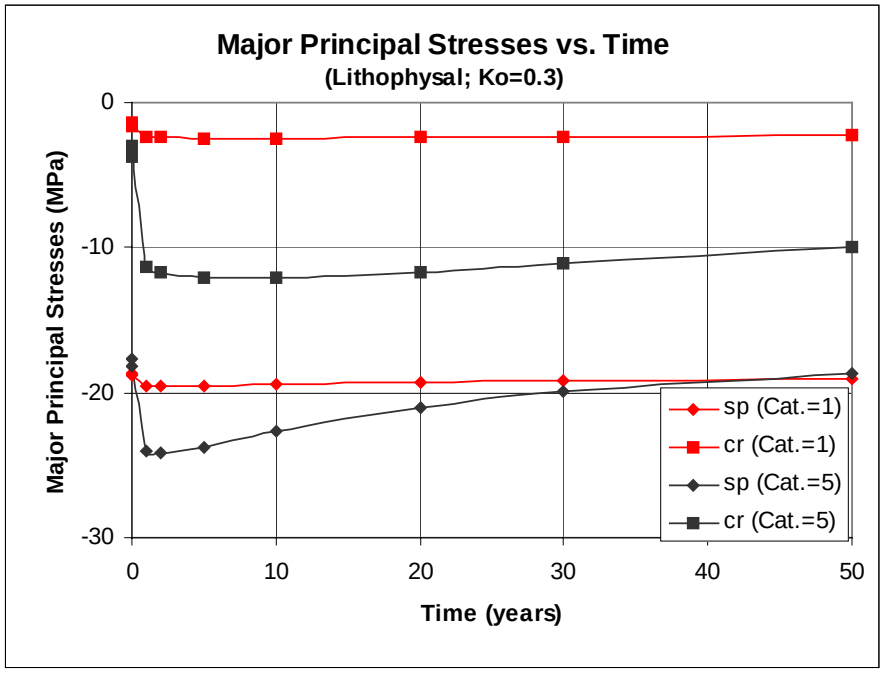

(a)

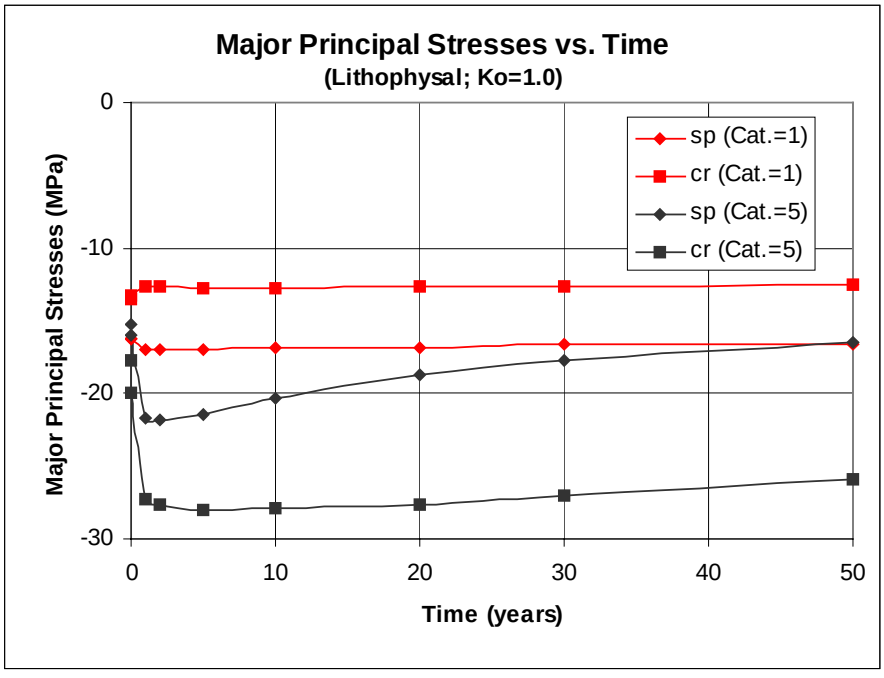

(b)

Figure 6-8. Time Histories of Major Principal Stresses near Crown and Springline of Emplacement Drifts in Lithophysal Rock with Categories 1 and 5 under In Situ and Thermal Loads: (a) Ko=0.3; (b) Ko=1.0

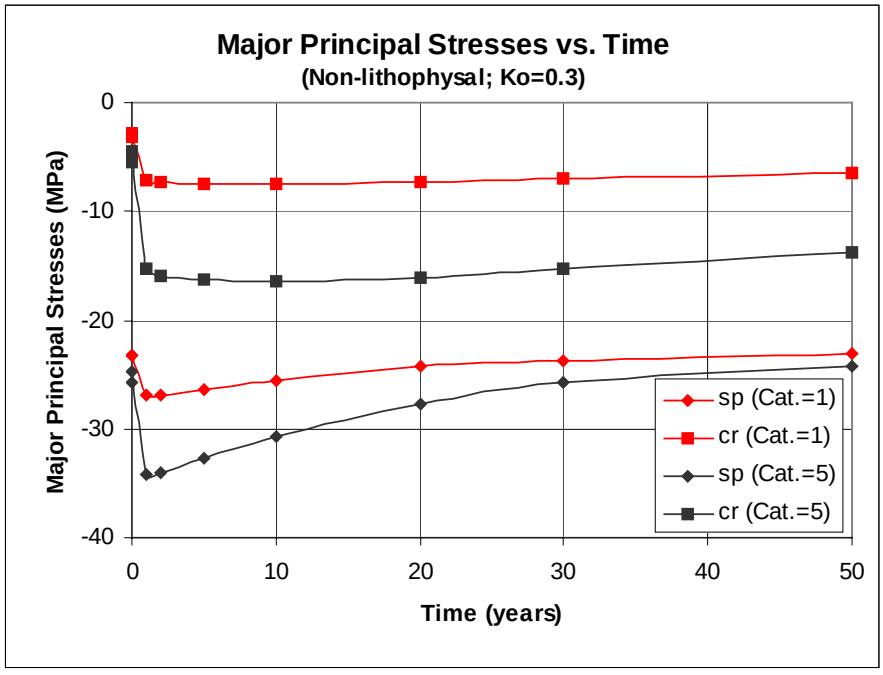

(a)

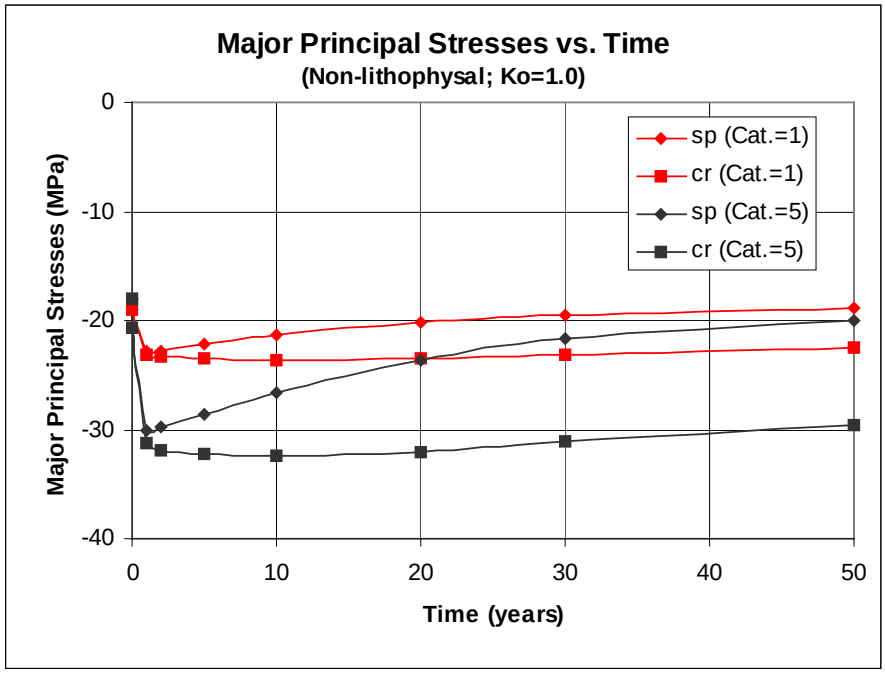

(b)

Figure 6-9. Time Histories of Major Principal Stresses near Crown and Springline of Emplacement Drifts in Non-lithophysal Rock with Categories 1 and 5 under In Situ and Thermal Loads: (a) Ko=0.3; (b) Ko=1.0

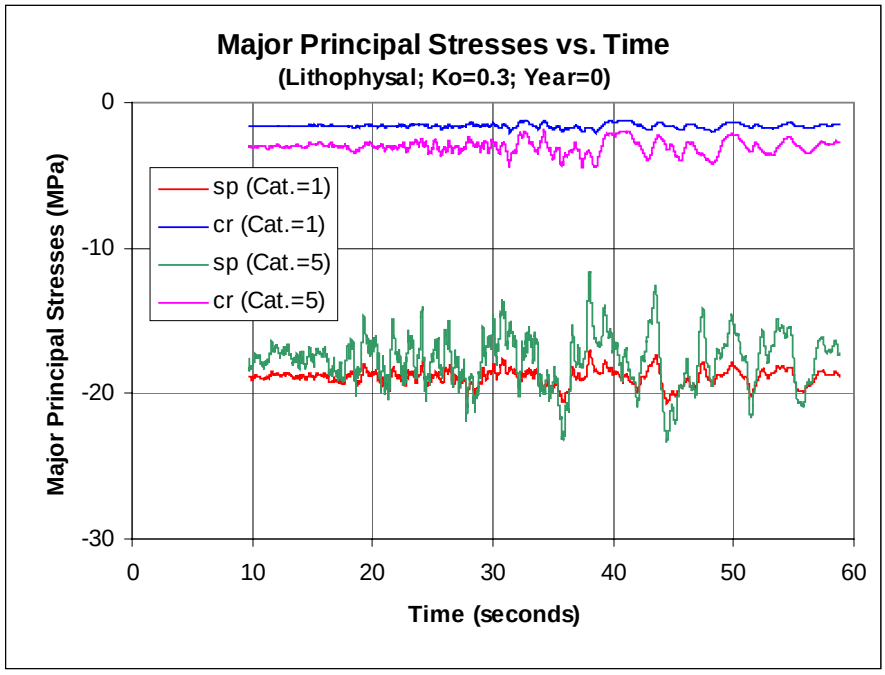

(a)

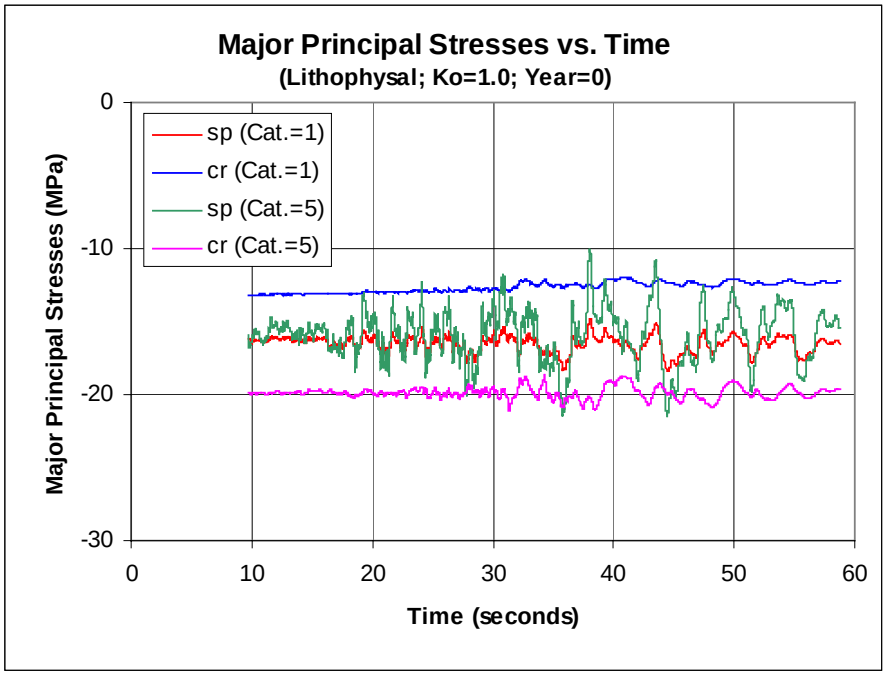

(b)

Figure 6-10. Time Histories of Major Principal Stresses near Crown and Springline of Emplacement Drifts in Lithophysal Rock with Categories 1 and 5 under In Situ and Seismic Loads (Year=0): (a) Ko=0.3; (b) Ko=1.0

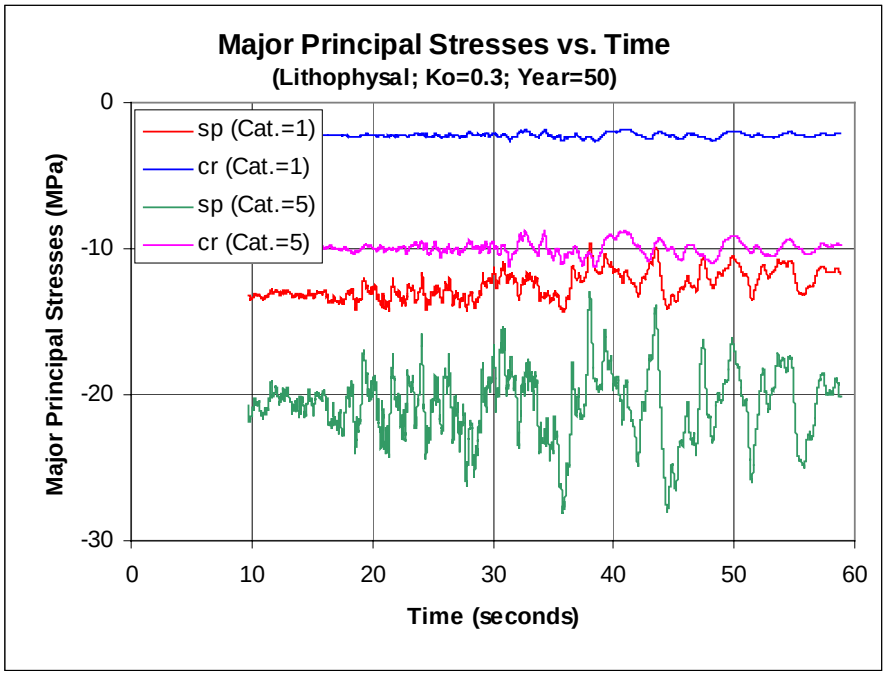

(a)

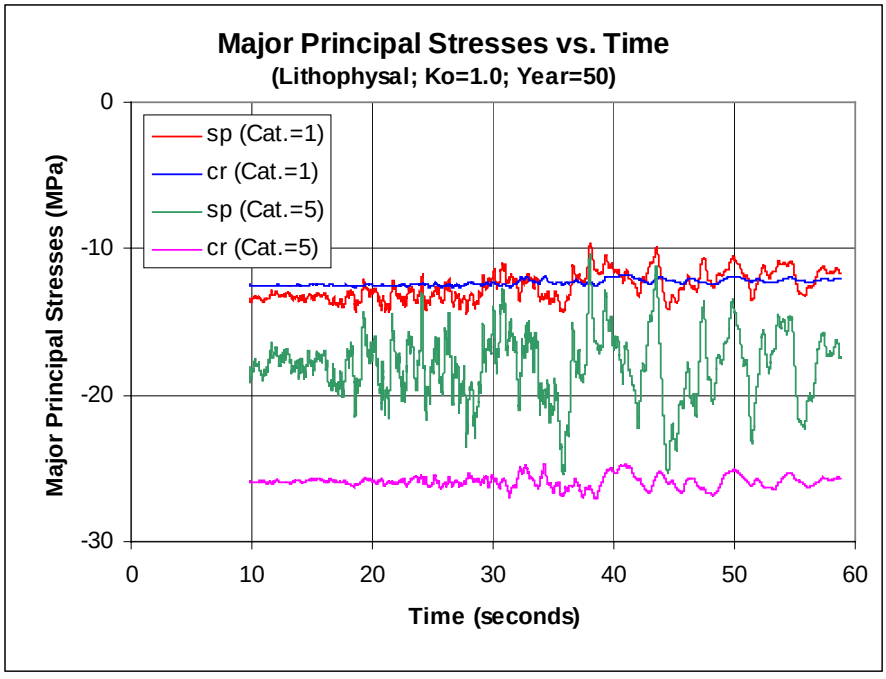

(b)

Figure 6-11. Time Histories of Major Principal Stresses near Crown and Springline of Emplacement Drifts in Lithophysal Rock with Categories 1 and 5 under In Situ, Thermal, and Seismic Load (Year=50): (a) Ko=0.3; (b) Ko=1.0

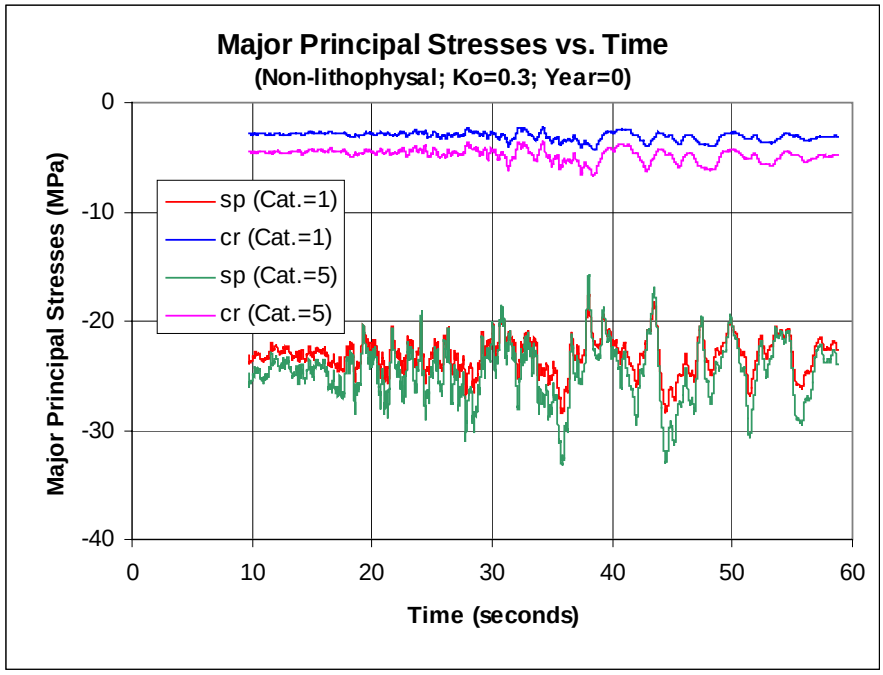

(a)

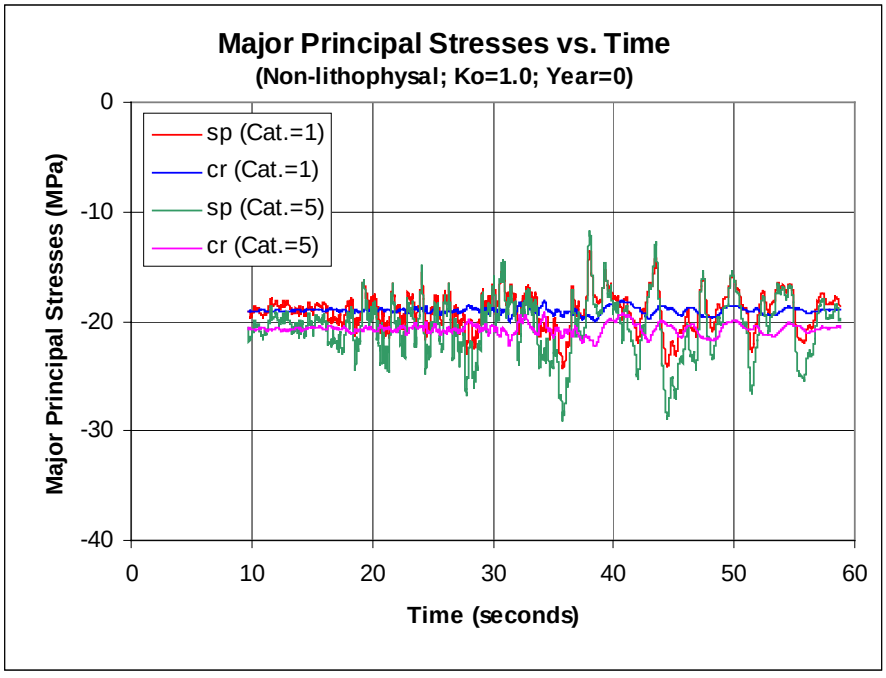

(b)

Figure 6-12. Time Histories of Major Principal Stresses near Crown and Springline of Emplacement Drifts in Non-lithophysal Rock with Categories 1 and 5 under In Situ and Seismic Loads (Year=0): (a) Ko=0.3; (b) Ko=1.0

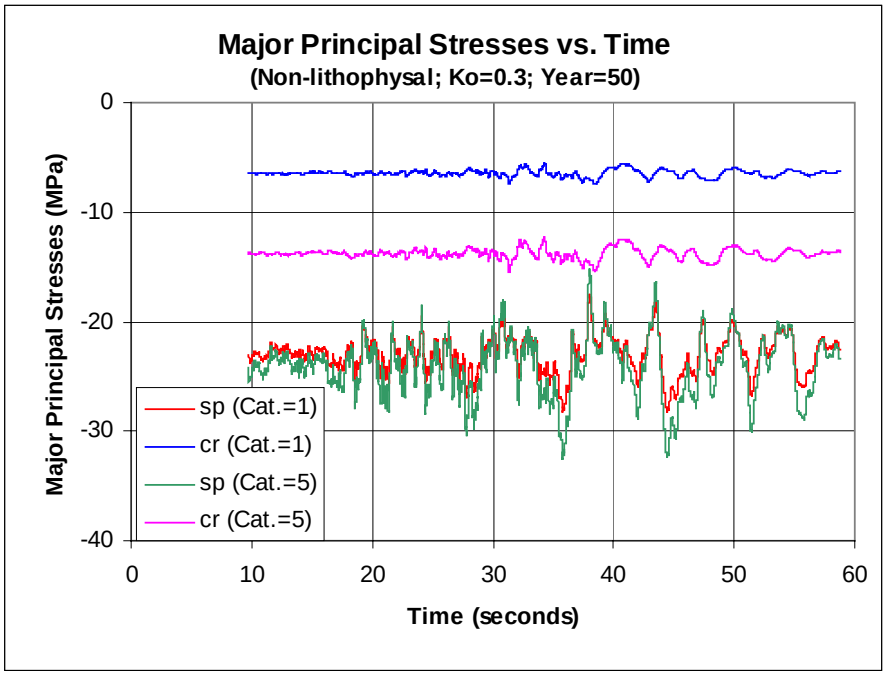

(a)

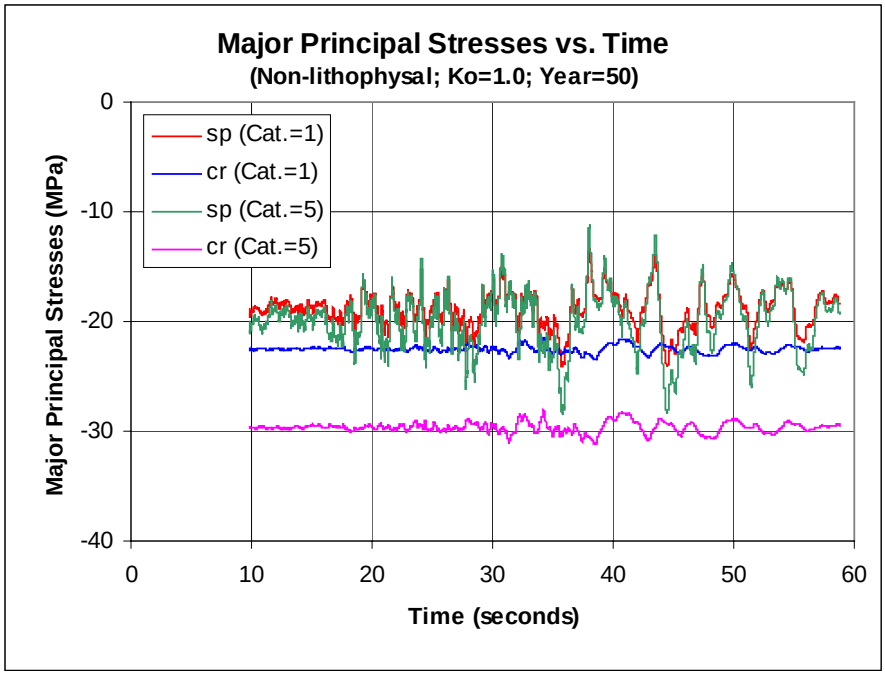

(b)

Figure 6-13. Time Histories of Major Principal Stresses near Crown and Springline of Emplacement Drifts in Non-lithophysal Rock with Categories 1 and 5 under In Situ, Thermal, and Seismic Loads (Year=50): (a) Ko=0.3; (b) Ko=1.0

6.1.3 Assessment of Factor of Safety of Emplacement Drifts

There are several ways to assess the stability of unsupported emplacement drifts. One commonly used method is to examine the potential yield zone around an opening. Another is to evaluate the factor of safety of the excavation under various loading conditions. Results of these stability analyses for emplacement drifts are presented in the following two subsections.

6.1.3.1 Potential Yield Zone around Emplacement Drifts

Potential yield zones around emplacement drifts in the lithophysal rock are predicted from the FLAC analyses, and plotted in Figures 6-14 through 6-17. The depth of potential yield zone for the lithophysal rock is estimated to be about 1 m for category 1 and K_o=0.3, and yield in tension may occur near the drift crown due to low horizontal stresses assumed (see Figure 6-14a). For all other cases, the depth of potential yield zone is well under 1 m.

Comparing the distribution of potential yield zone induced by excavation (Figure 6-14a) to that following 50 years of heating (Figure 6-14b), it is seen that heating slightly expands the overstress zone near the drift wall, but generally does not alter much the distribution of stresses. This observation also applies to other cases considered.

For emplacement drifts in the non-lithophysal rock, potential yield zones associated with all rock categories and initial stress ratios (K_o) are anticipated to be less than about 1 m deep (see Figures 6-18 through 6-21). Heating following waste emplacement does not change much the stress conditions, as observed for the lithophysal rock.

Overall, the emplacement drift openings in both the lithophysal and non-lithophysal rocks are stable judged by the stress conditions and the depth of potential zones.

6.1.3.2 Factor of Safety of Emplacement Drifts

6.1.3.2.1 Average Factor of Safety Based on Strength-to-stress Ratio

Mohr-Coulomb strength-to-stress ratios (STSR) for unsupported emplacement drifts in both the lithophysal and non-lithophysal rocks are shown in Figures 6-14 through 6-21. Since stresses are higher near the springline than near the crown when K_o=0.3, a higher STSR is predicted near the crown than near the springline. When K_o=1.0, the stress condition is close to a hydrostatic state, and the predicted STSRs are nearly uniform around an emplacement drift opening.

Using these STSR distributions, an overall factor of safety is estimated for an emplacement drift under a specific loading condition. The estimated factor of safety is an average value of STSRs over an annulus around the drift. The thickness of the annulus selected is 3 m, which is equal to the proposed bolt length (see Section 6.3.2). Due to changes in stresses during heating, the estimated factors of safety are time-dependent. Time histories of the average factors of safety are shown in Figures 6-22a and 6-22b for emplacement drifts in the lithophysal and non-lithophysal rocks, respectively.

It is indicated that an overall factor of safety for emplacement drifts varies from 2.2 to 5.8 in the lithophysal rock, and from 5.1 to 8.1 in the non-lithophysal rock. Heating in rock will slightly

improve the overall factors of safety when the initial horizontal-to-vertical stress ratio is low (K_o=0.3), but not change much if the initial stress that a drift is subjected to is hydrostatic (K_o=1.0).

As discussed Section 6.1.2.1, stresses fluctuate during seismic shaking. Both the major and the minor principal stresses are expected to change in the same trend, either both increase or both decrease. This will result in a minimal variation in shear stresses. The average factors of safety under seismic loading condition is not expected to be significantly different from those under combined in situ and thermal loading conditions. Therefore, the factors of safety discussed above may also serve as reasonable estimates for emplacement drifts subjected to seismic loading condition.

6.1.3.2.2 Factor of Safety Based on Critical State Criterion

Average factors of safety estimated based on the strength-to-stress ratios presented above may offer some useful clue on stability of unsupported emplacement drifts, but they only rely on the stress criterion. An alternative approach based on critical state criterion, as discussed in Section 5.4.2.3.1, may provide a more comprehensive assessment of the factor of safety of emplacement drifts since it may allow both the stress and displacement criteria to be used.

A series of analyses were conducted using the FLAC models to evaluate the behavior of unsupported drifts in a given rock mass category with a series of reduced strength values. Plots of the radial or vertical displacements at the crown versus numerical steps with different strength reduction factors (SRF) are shown in Figures 6-23 through 6-28 for emplacement drifts in the lithophysal and non-lithophysal rocks. These plots were generated for the in situ loading condition only. They may also represent for the drifts subjected to other loading conditions based on the analyses discussed in Section 6.1.2 since the stability of unsupported emplacement drifts are primarily determined by in situ loading condition whereas thermal and seismic loads have insignificant effect.

As indicated in Figures 6-23a and 6-23b, when rock mass strength is reduced by 55 percent (SRF=0.45) unsupported emplacement drifts in category 1 lithophysal rock will be unstable for both K_o=0.3 and K_o=1.0. This gives a safety factor of 2.2 (1/0.45=2.2) for this rock type. Similarly, based on the results for emplacement drifts in categories 3 and 5 lithophysal rocks, as shown in Figures 6-24 and 6-25, respectively, the factors of safety can be estimated to be 4 (1/0.25=4) and 5 (1/0.2=5), respectively. A relation of safety factor and rock mass category for the lithophysal rock is shown in Figure 6-29a. Compared to those presented in Figure 6-22a based on the strength-to-stress ratios, it appears that these two approaches can generate reasonable and consistent results.

Similar analyses for emplacement drifts in the non-lithophysal rock indicate that the factors of safety, as shown in Figure 6-29b, vary from 5 to 10 for various rock mass categories considered. These results suggest that emplacement drifts excavated in the non-lithophysal rock are expected to be more stable than in the lithophysal rock.

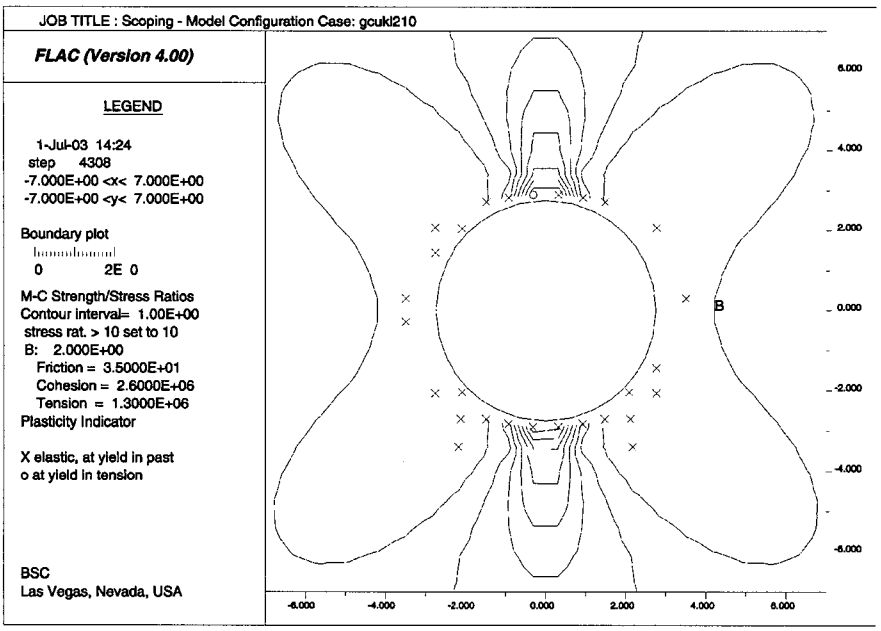

(a)

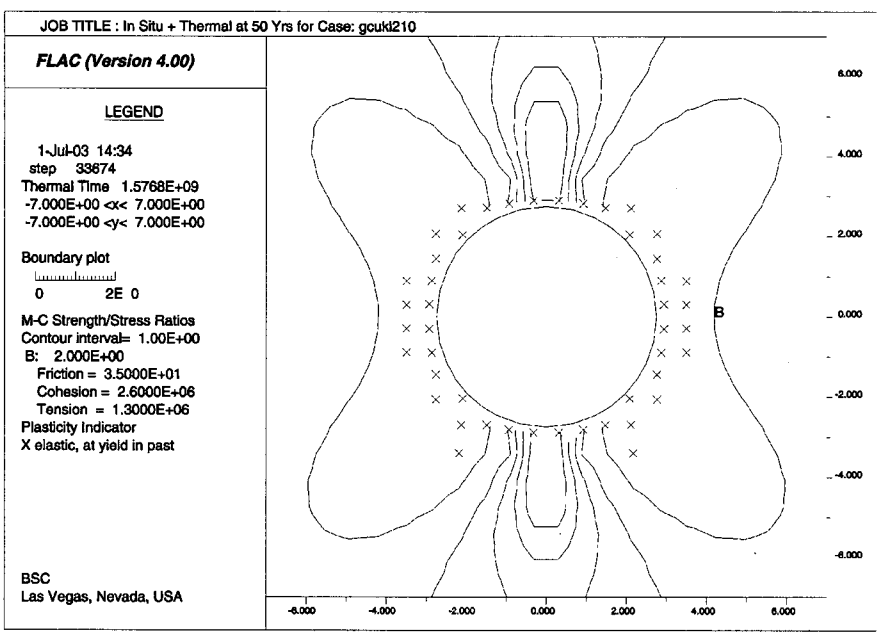

(b)

Figure 6-14. Potential Yield Zone and Contours of Strength-to-Stress Ratios around Emplacement Drifts in Lithophysal Rock with Category 1 and Ko=0.3: (a) at 0 Year; (b) at 50 Years.

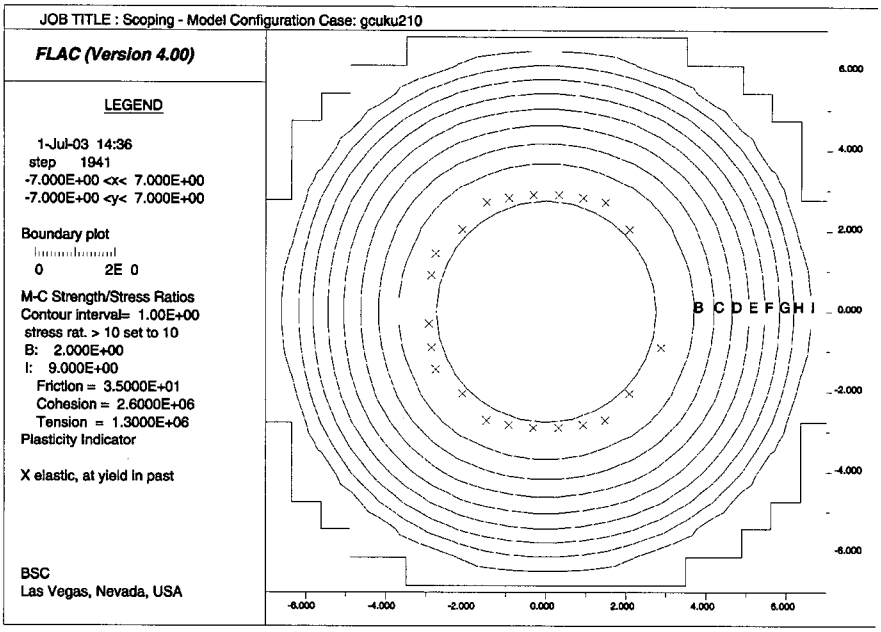

(a)

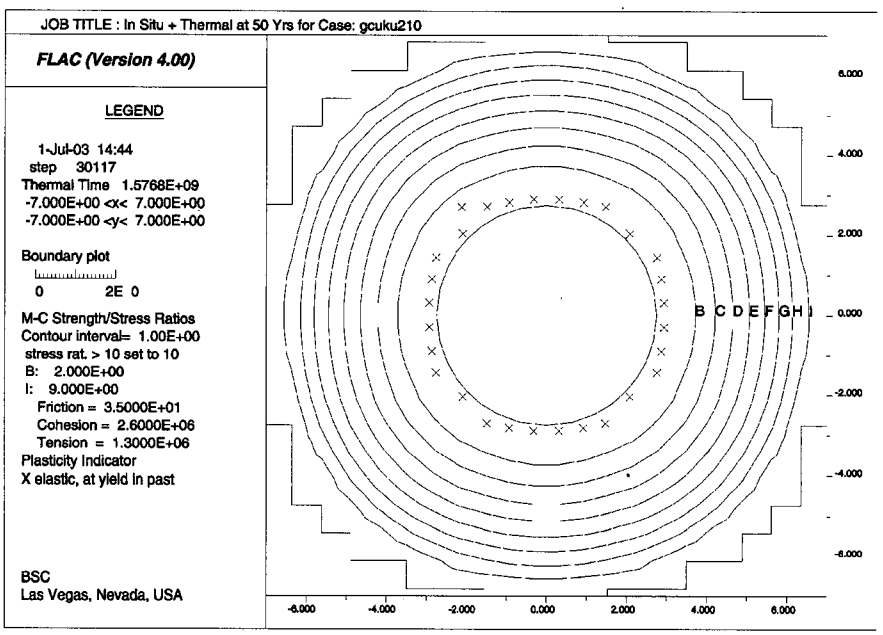

(b)

Figure 6-15. Potential Yield Zone and Contours of Strength-to-Stress Ratios around Emplacement Drifts in Lithophysal Rock with Category 1 and Ko=1.0: (a) at 0 Year; (b) at 50 Years.

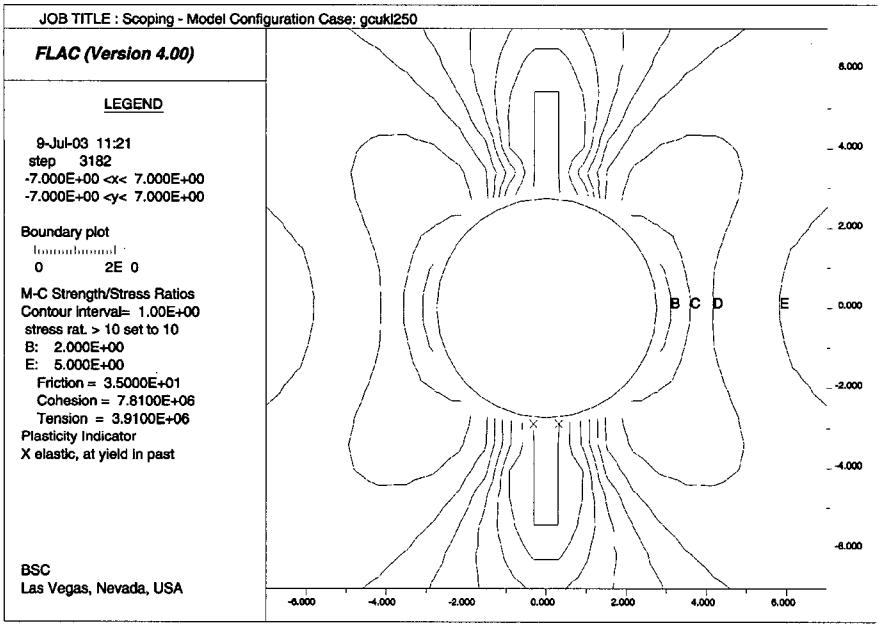

(a)

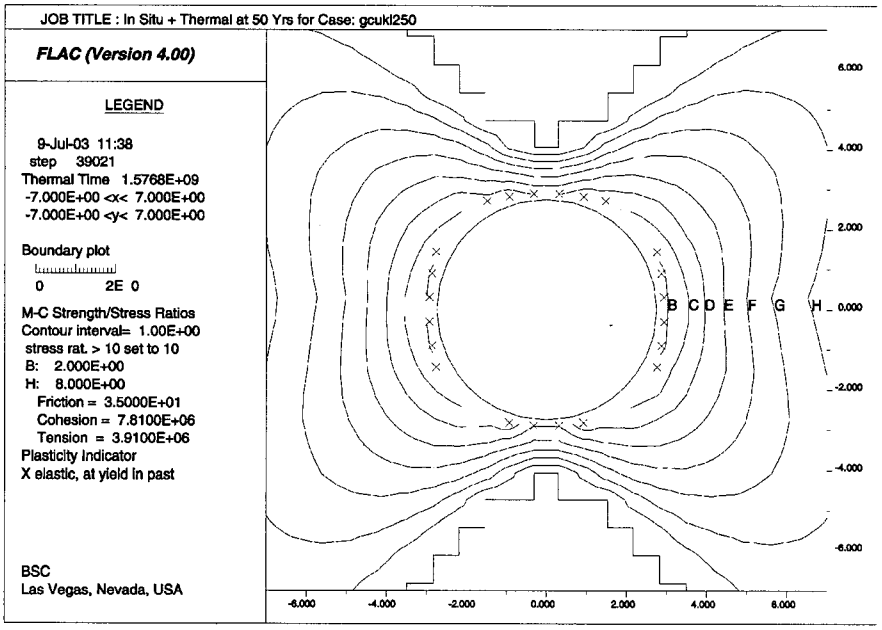

(b)

Figure 6-16. Potential Yield Zone and Contours of Strength-to-Stress Ratios around Emplacement Drifts in Lithophysal Rock with Category 5 and Ko=0.3: (a) at 0 Year; (b) at 50 Years.

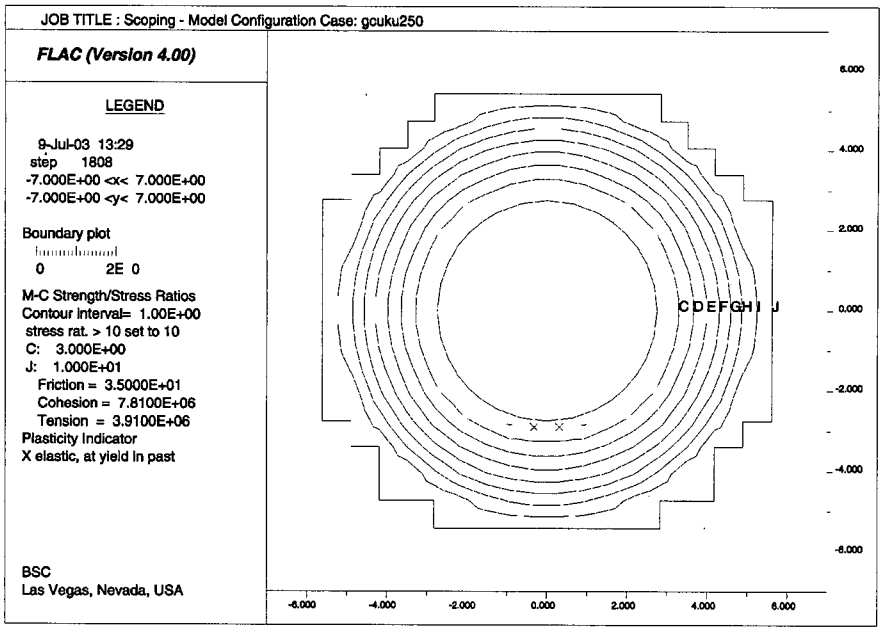

(a)

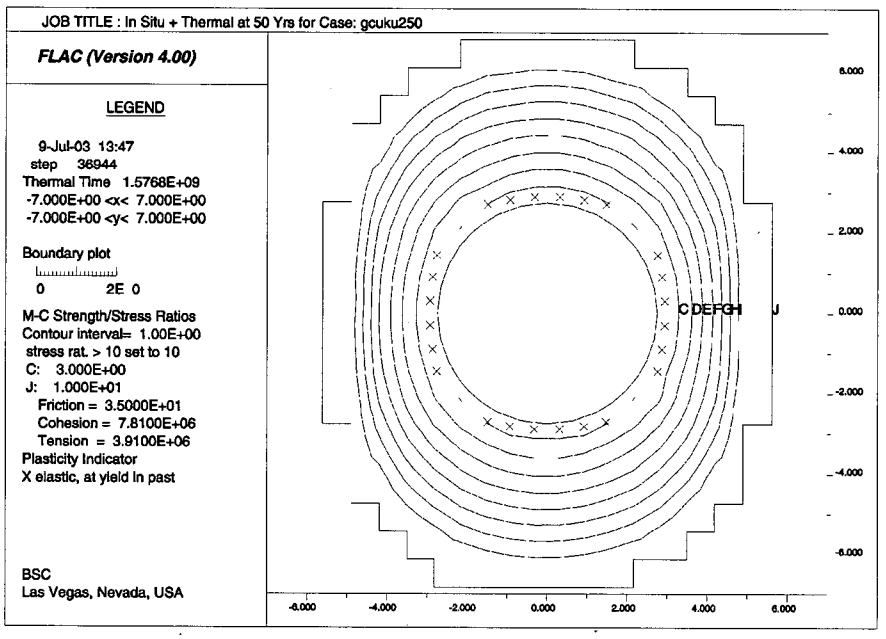

(b)

Figure 6-17. Potential Yield Zone and Contours of Strength-to-Stress Ratios around Emplacement Drifts in Lithophysal Rock with Category 5 and Ko=1.0: (a) at 0 Year; (b) at 50 Years.

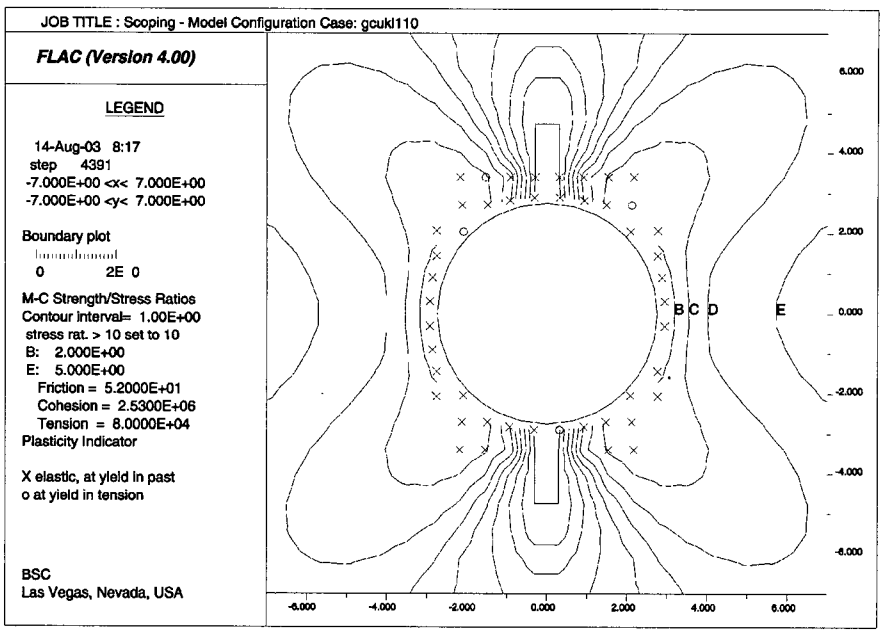

(a)

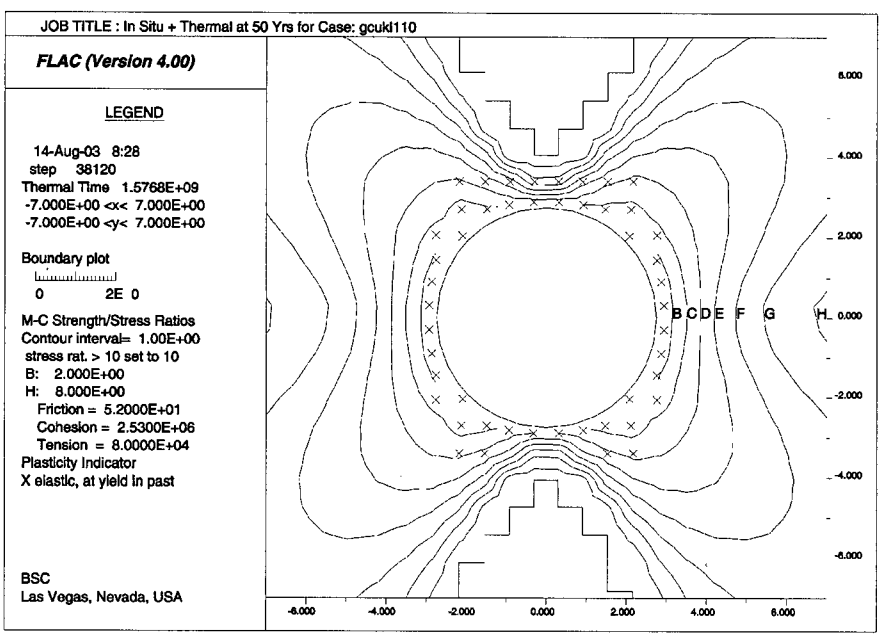

(b)

Figure 6-18. Potential Yield Zone and Contours of Strength-to-Stress Ratios around Emplacement Drifts in Non-lithophysal Rock with Category 1 and Ko=0.3: (a) at 0 Year; (b) at 50 Years.

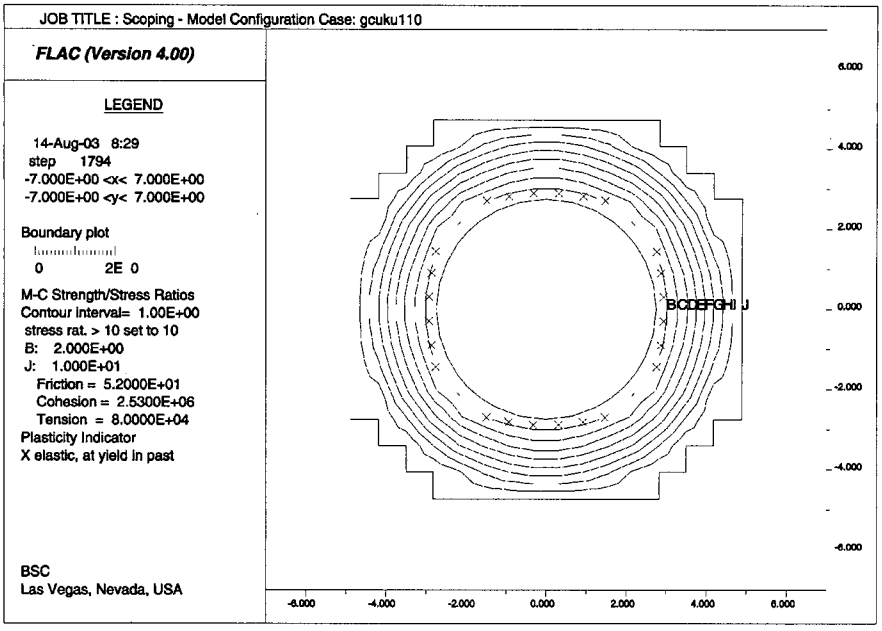

(a)

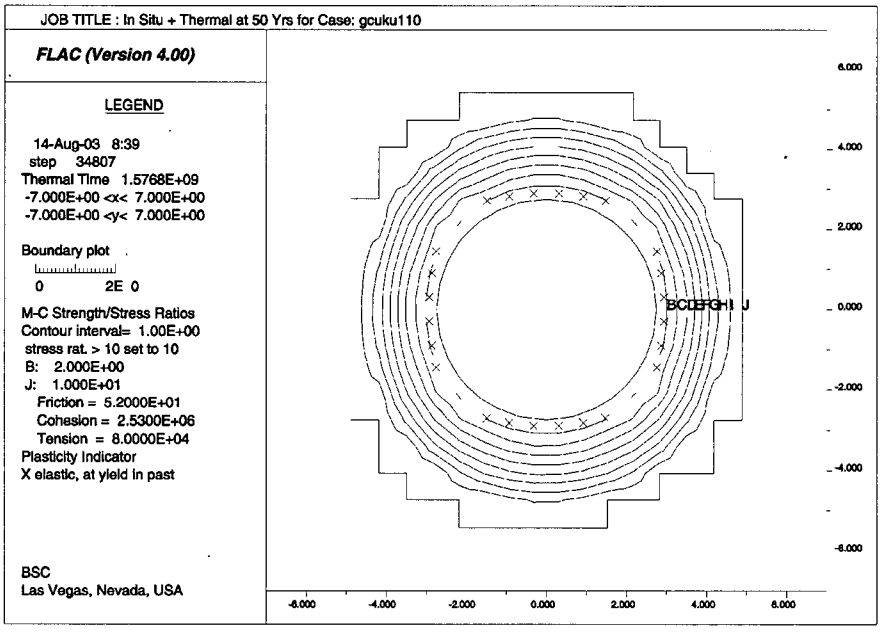

(b)

Figure 6-19. Potential Yield Zone and Contours of Strength-to-Stress Ratios around Emplacement Drifts in Non-lithophysal Rock with Category 1 and Ko=1.0: (a) at 0 Year; (b) at 50 Years.

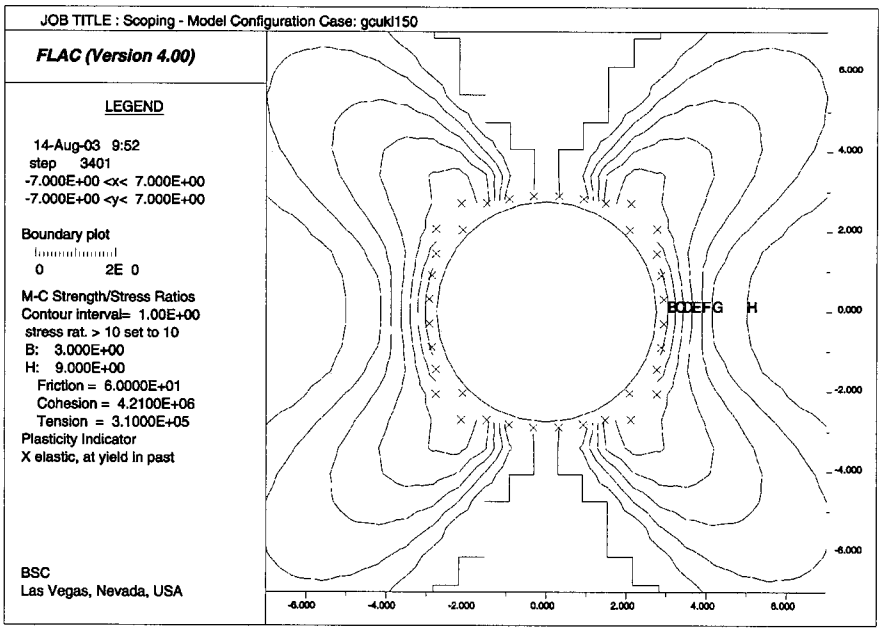

(a)

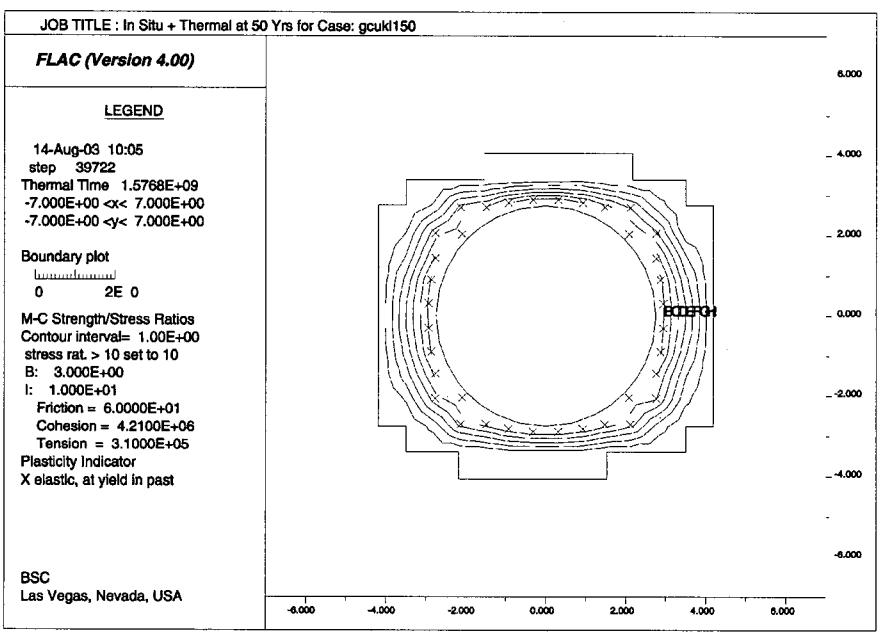

(b)

Figure 6-20. Potential Yield Zone and Contours of Strength-to-Stress Ratios around Emplacement Drifts in Non-lithophysal Rock with Category 5 and Ko=0.3: (a) at 0 Year; (b) at 50 Years.

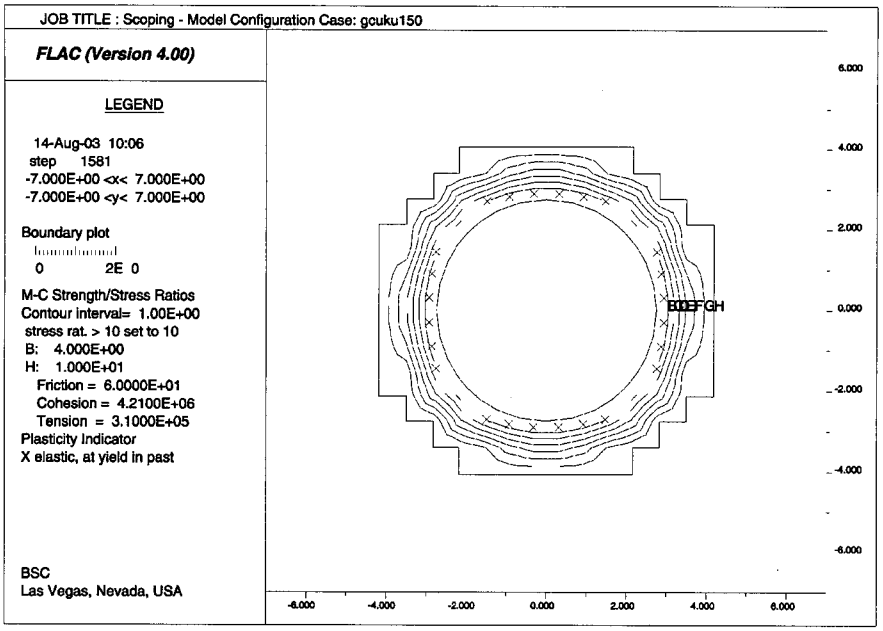

(a)

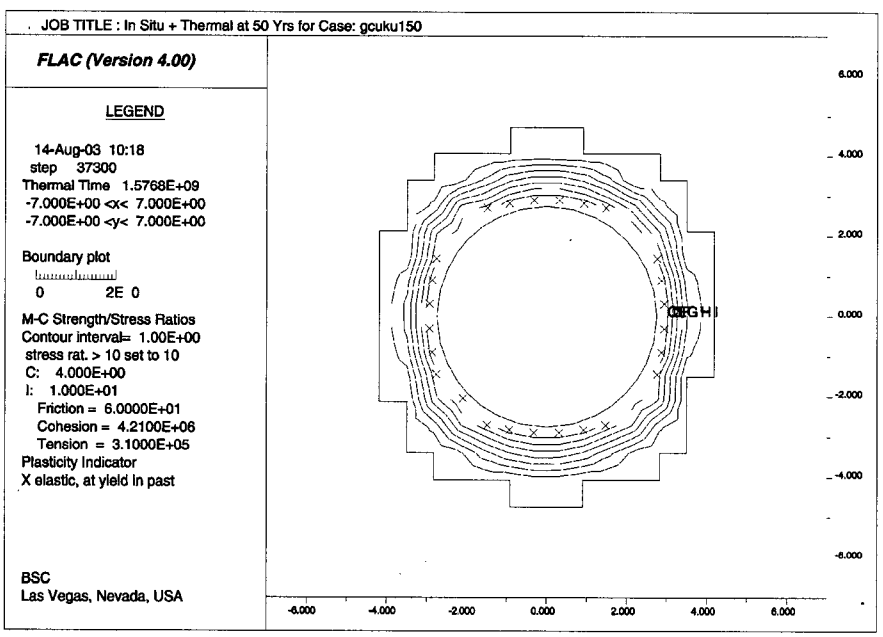

(b)

Figure 6-21. Potential Yield Zone and Contours of Strength-to-Stress Ratios around Emplacement Drifts in Non-lithophysal Rock with Category 5 and Ko=1.0: (a) at 0 Year; (b) at 50 Years.

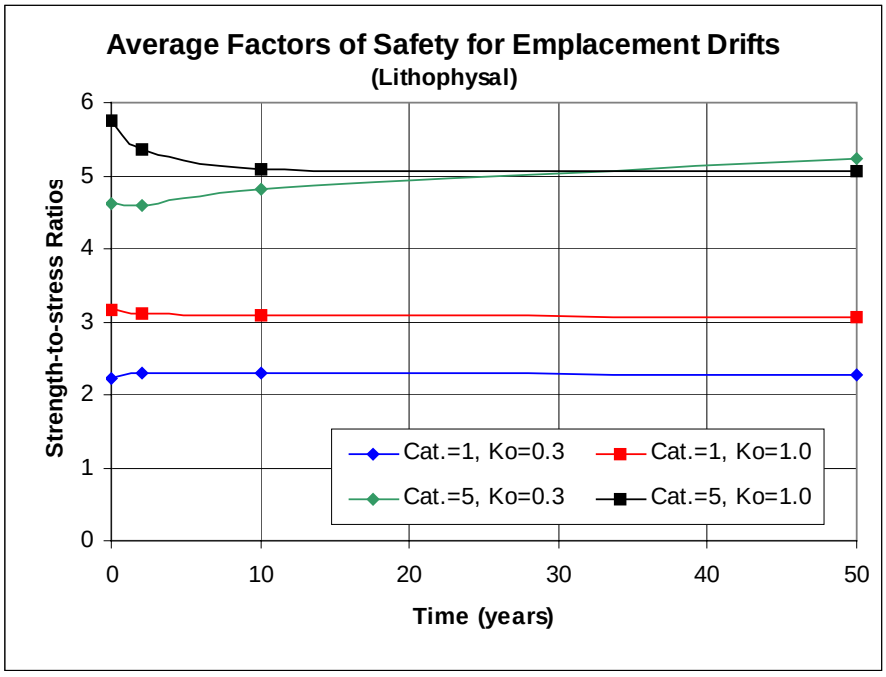

(a)

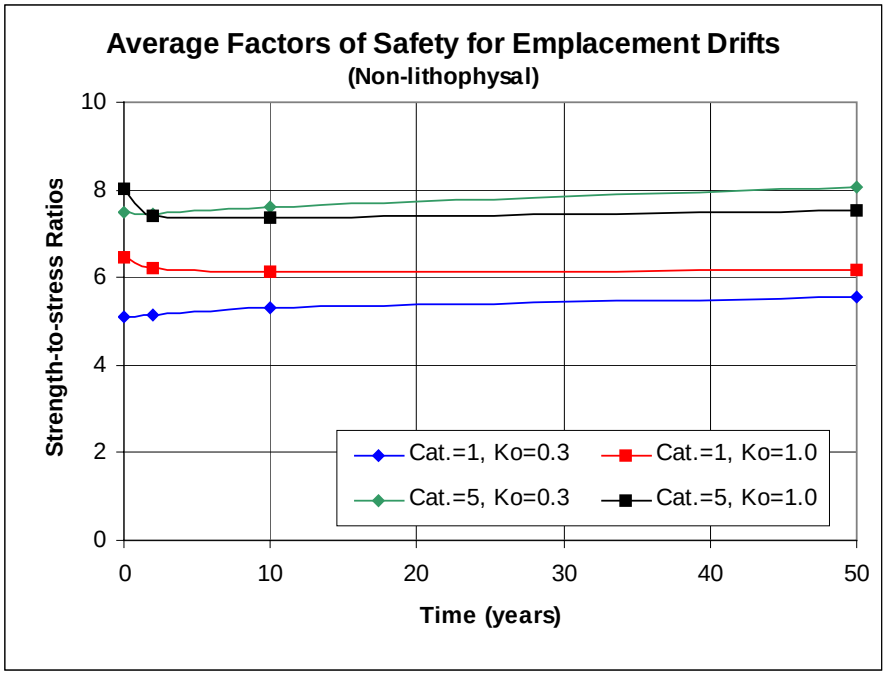

(b)

Figure 6-22. Average Factors of Safety for Unsupported Emplacement Drifts Based on Strength-to-stress Ratio: (a) in Lithophysal Rock, (b) in Non-lithophysal Rock

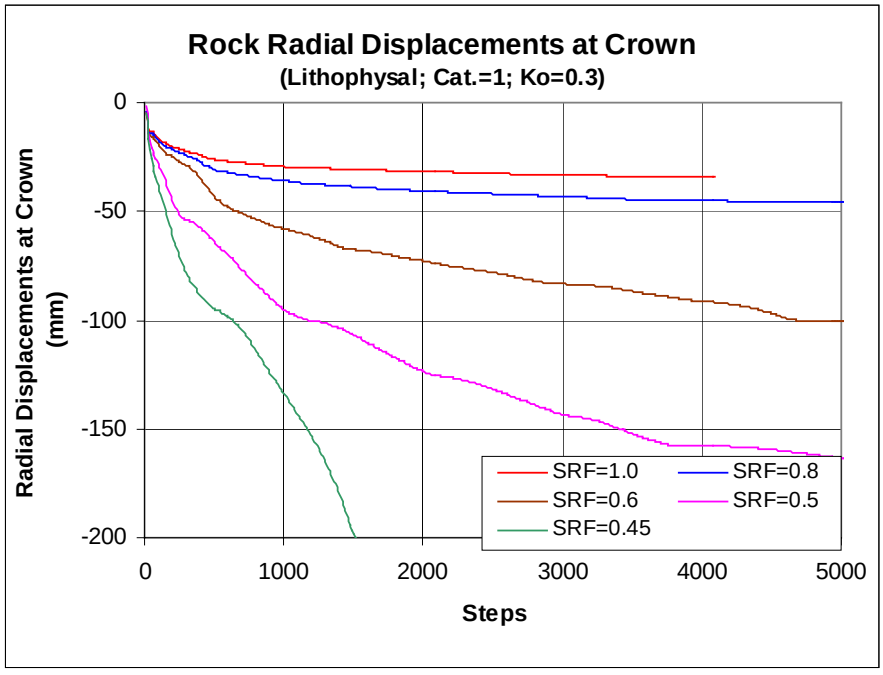

(a)

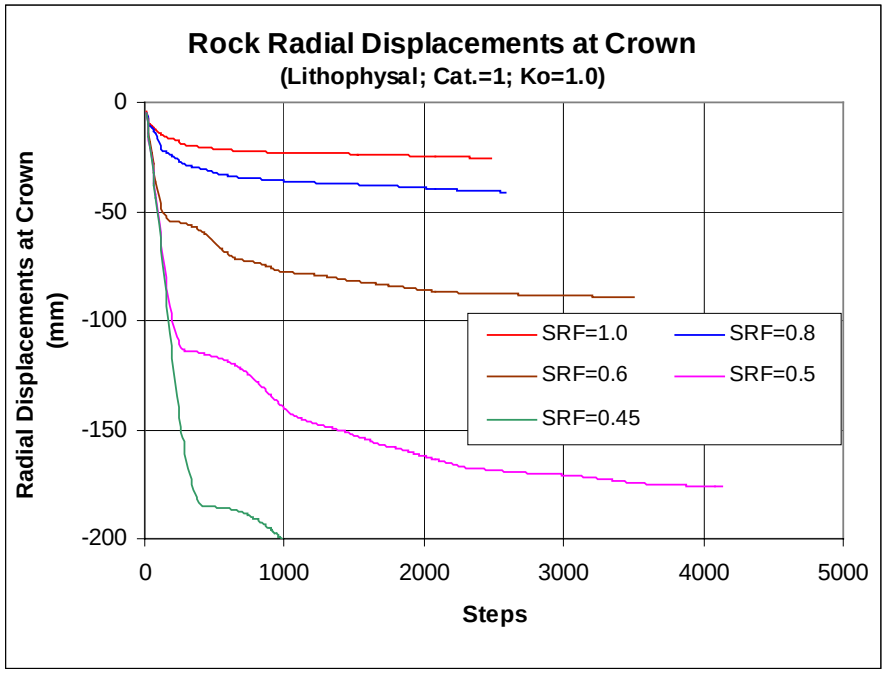

(b)

Figure 6-23. Development of Radial Displacements at Crown of Unsupported Emplacement Drifts in Category 1 Lithophysal Rock: (a) K_o=0.3, (b) K_o=1.0

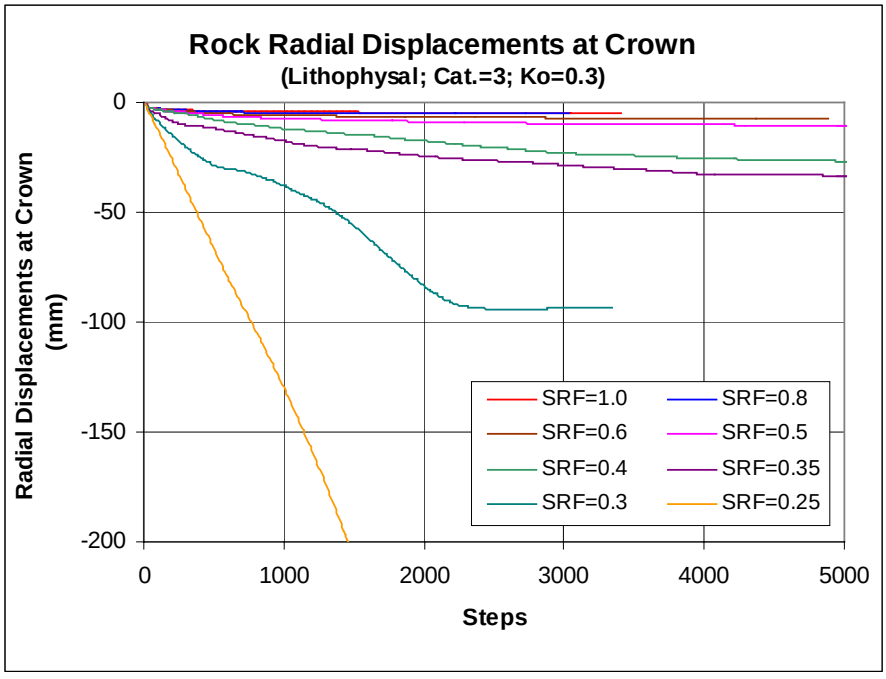

(a)

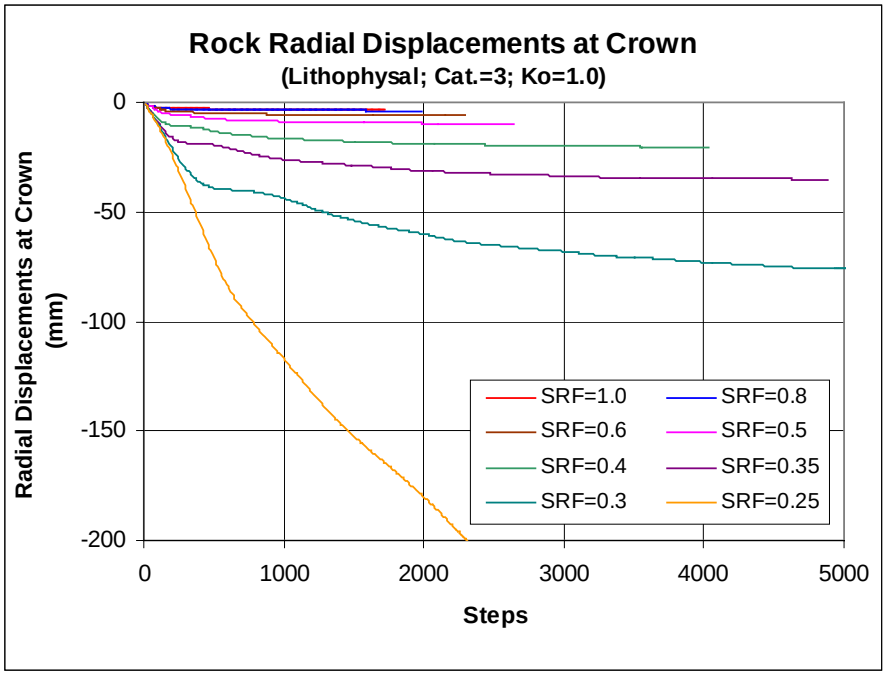

(b)

Figure 6-24. Development of Radial Displacements at Crown of Unsupported Emplacement Drifts in Category 3 Lithophysal Rock: (a) K_o=0.3, (b) K_o=1.0

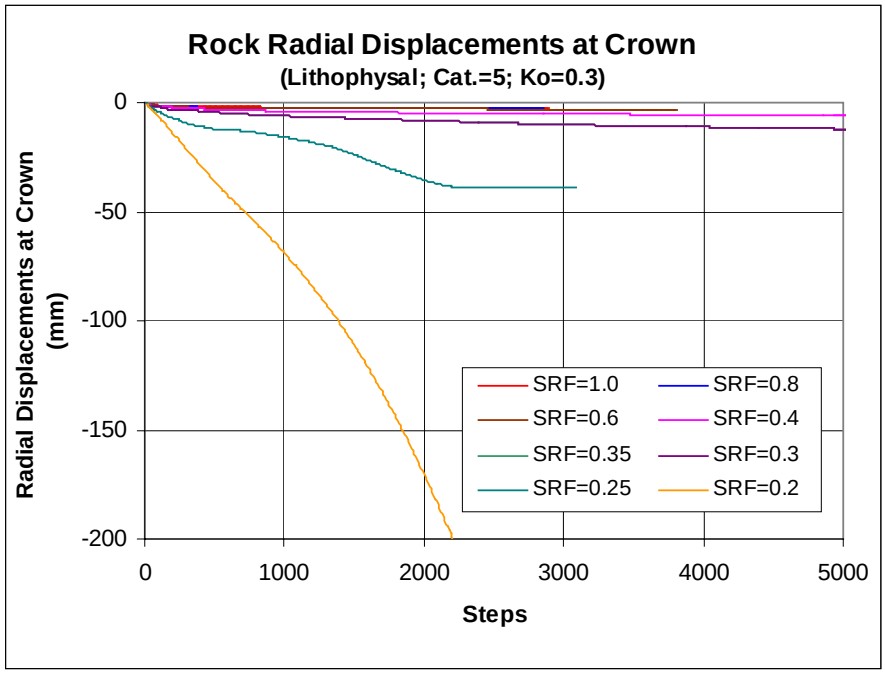

(a)

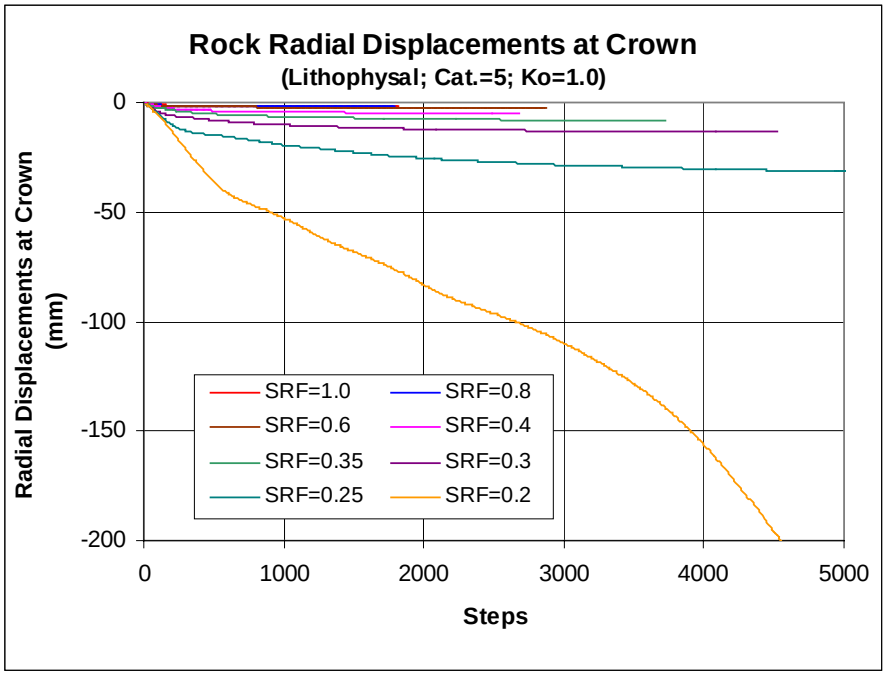

(b)

Figure 6-25. Development of Radial Displacements at Crown of Unsupported Emplacement Drifts in Category 5 Lithophysal Rock: (a) K_o=0.3, (b) K_o=1.0

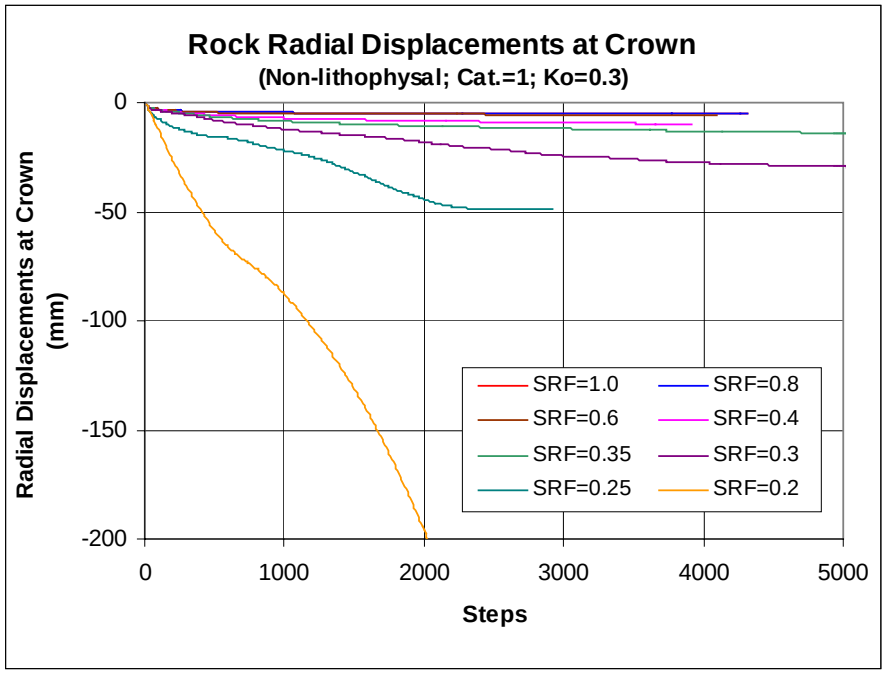

(a)

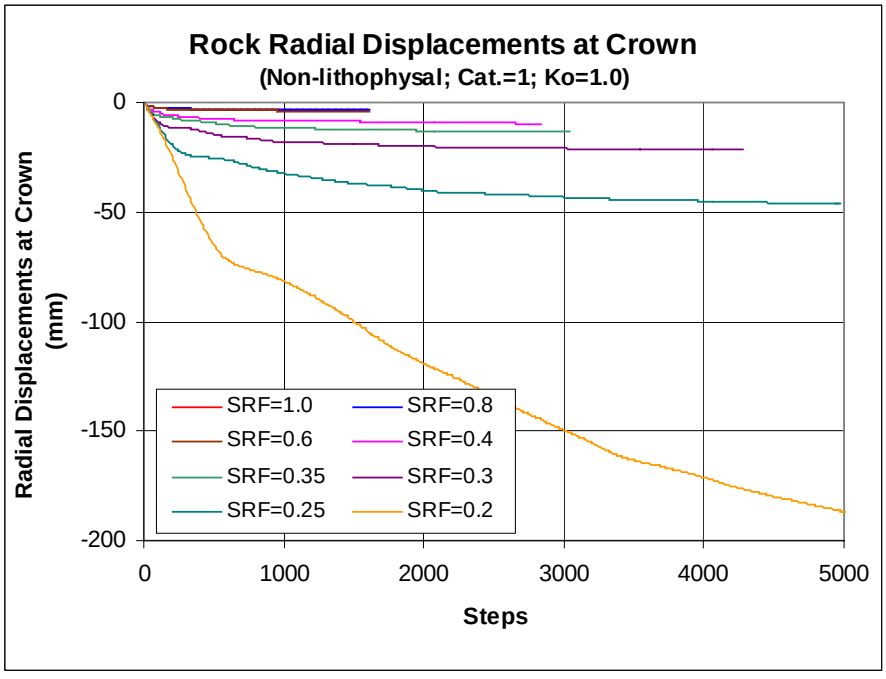

(b)

Figure 6-26. Development of Radial Displacements at Crown of Unsupported Emplacement Drifts in Category 1 Non-lithophysal Rock: (a) K_o=0.3, (b) K_o=1.0

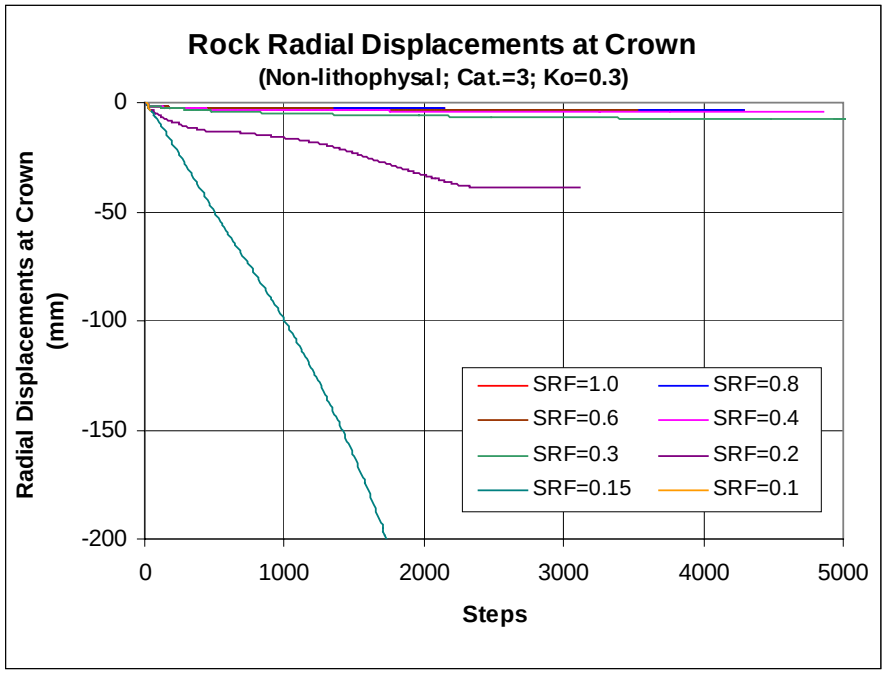

(a)

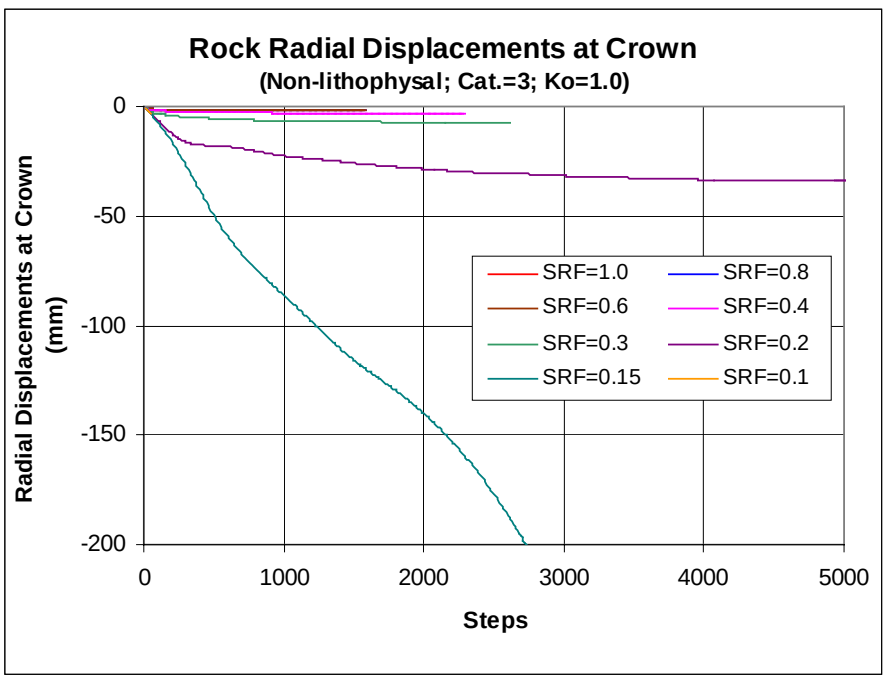

(b)

Figure 6-27. Development of Radial Displacements at Crown of Unsupported Emplacement Drifts in Category 3 Non-lithophysal Rock: (a) K_o=0.3, (b) K_o=1.0

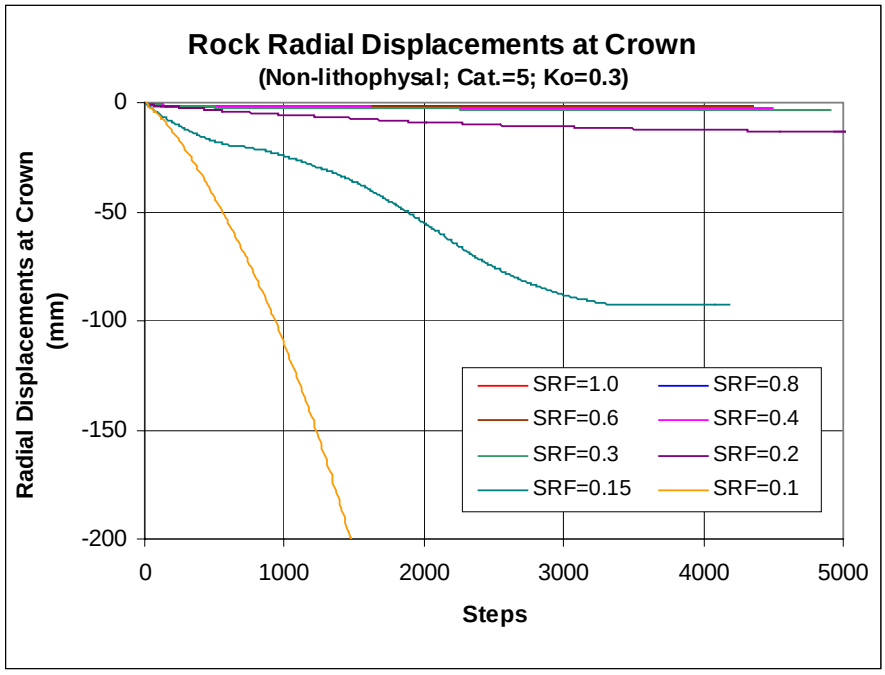

(a)

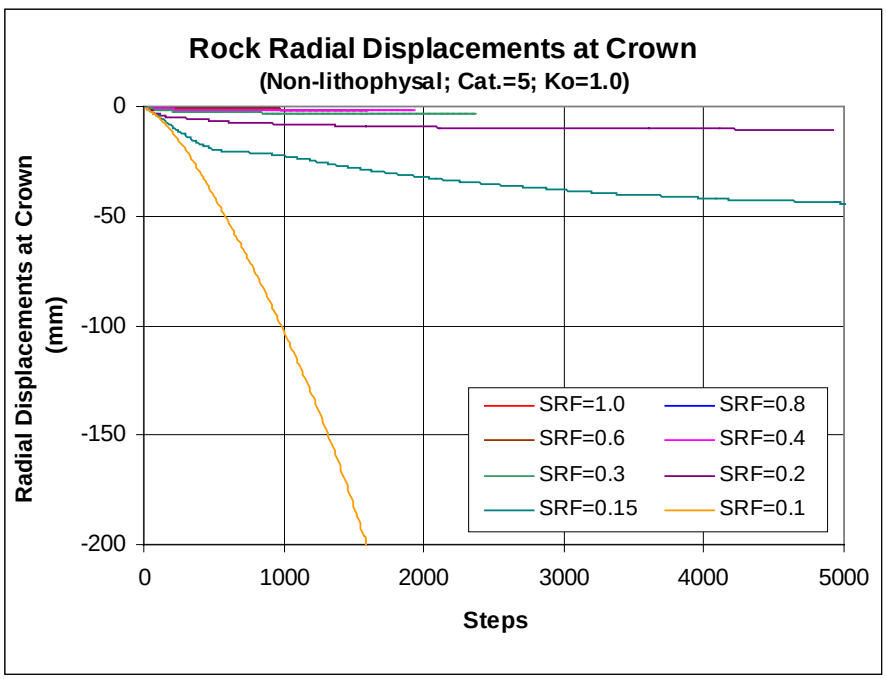

(b)

Figure 6-28. Development of Radial Displacements at Crown of Unsupported Emplacement Drifts in Category 5 Non-lithophysal Rock: (a) K_o=0.3, (b) K_o=1.0

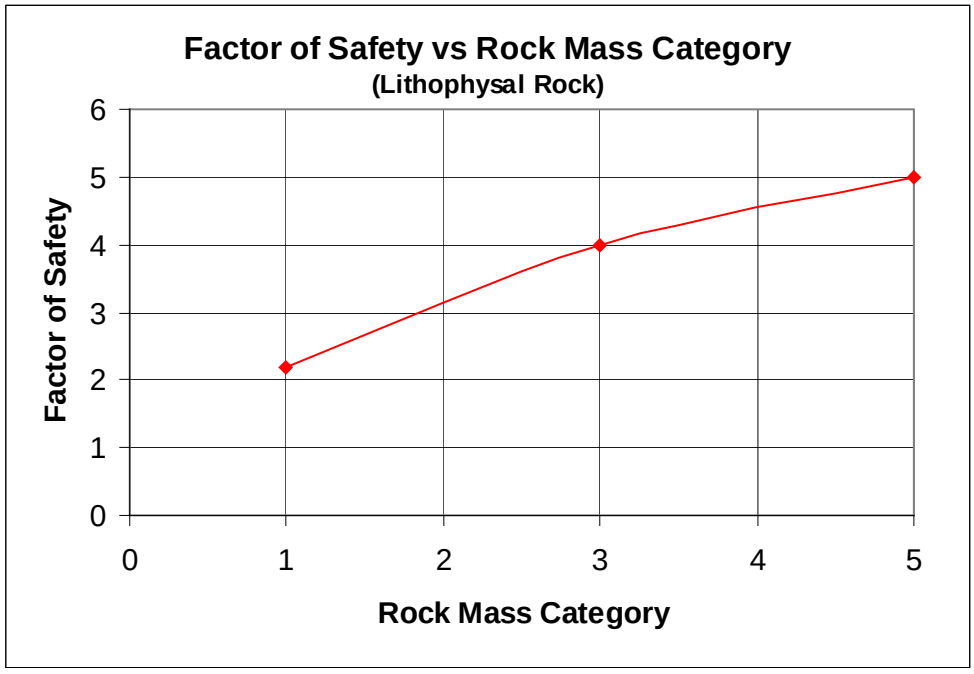

(a)

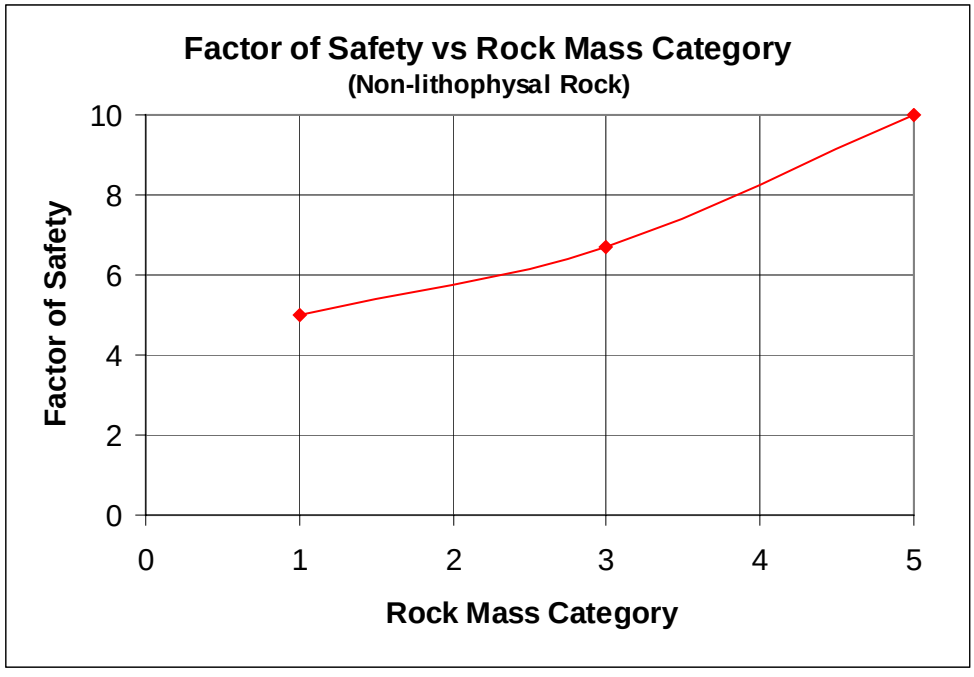

(b)

Figure 6-29. Factor of Safety for Unsupported Emplacement Drifts under Various Rock Conditions: (a) in Lithophysal Rock, (b) in Non-lithophysal Rock

6.1.4 Ground Reaction Curves

Ground reaction curves for emplacement drifts with various rock categories and K_o values were generated using the FLAC models. These curves are shown in Figures 6-30a and 6-30b for the lithophysal and non-lithophysal rocks, respectively. For each point on a curve, a FLAC run was conducted by applying a pressure (or stress) on the drift wall to determine the relation between the applied pressure and the drift wall radial displacements. The applied pressure selected varied from zero to the in situ stress at the drift center, with five equal intervals. This resulted in a total of six points, or six FLAC runs, for each curve. Each point demonstrates the drift state of equilibrium at a specific level of pressure imposed by ground support.

As shown in Figures 6-30a and 6.30b, the ground reaction curves are generally straight lines and all intersect with the displacement axis, indicating that the drifts are anticipated to be stable and self-supporting. The ground support function in these cases is merely retention of occasional loose pieces of rock. The ground reaction curves for the emplacement drifts in category 1 lithophysal rock show stable conditions but the rock displacements are relatively large. To prevent any potential unstable conditions caused by excessive rock displacements, rock reinforcement by installing rock bolts quickly or using lining type support is necessary.

6.1.5 Initial Ground Relaxation

In Section 4.3, it is assumed that 40 percent of the pre-excavation in situ stress be imposed on the final ground support. To evaluate the conservatism of this assumption, three-dimensional analyses using the FLAC3D computer code were conducted. In these analyses, the advance of TBM is simulated. Its effect on rock displacements is examined to assess the value of ground relaxation to be used in the ground support modeling.

In the FLAC3D models (see Figure 6-31), the length of each TBM advance cycle is 5.0 m, which is four times the proposed spacing of rock bolts, and considered as the distance from the excavation face at which ground support is installed. The model dimensions are 81m×100m×50m. The origin of the coordinate system is located at the center of the block, with y-axis along the tunnel axial direction. This gives the coordinates of two tunnel ends of the model at y=-25 m and y=25 m, respectively.

The vertical displacements at the crown of emplacement drifts during the TBM advance are monitored in the models. These displacements are shown in Figures 6-32 and 6-33 for categories 1 and 5 of the lithophysal rock, respectively. It is indicated that though the magnitude of displacements are dependent on the rock mass category or the deformation modulus, the percentage of displacements developed at the time when ground support is installed compared to the total displacements anticipated for a specific rock mass category is nearly independent from the rock mass category. If the ground support is assumed to be installed at a distance of 5.0 m from the tunnel face, or a distance of about one time the drift diameter, about 75 percent (see the –25m curve) of the total anticipated displacements would have already occurred prior to the ground support installation. In other word, only about 25 percent of the total displacements would have an effect on the ground support. An assumption of 60 percent ground relaxation used in the ground support modeling is obviously very conservative, and will result in a

conservative assessment of ground support performance. This conservatism would result in an additional factor of safety of about 20 percent.

Since the percentage of ground relaxation is not very sensitive to the rock mass properties, it can be concluded, without running additional FLAC3D models for the non-lithophysal rock, that use of a ground relaxation of 60 percent for the non-lithophysal rock is also very conservative.

It should be pointed out that the ground support discussed in this calculation is referred to as the final ground support for emplacement drifts. Detailed underground construction plan including timing of the final ground support installation has not been developed. If the final ground support would not be required to act as part of the initial ground support and installed immediately following the excavation, it would probably be put in place after the excavation of an entire emplacement drift is completed. With this construction scenario, the ground relaxation would likely be about 100 percent since creep-induced rock displacements are not expected based on observations from the ESF and the ECRB.

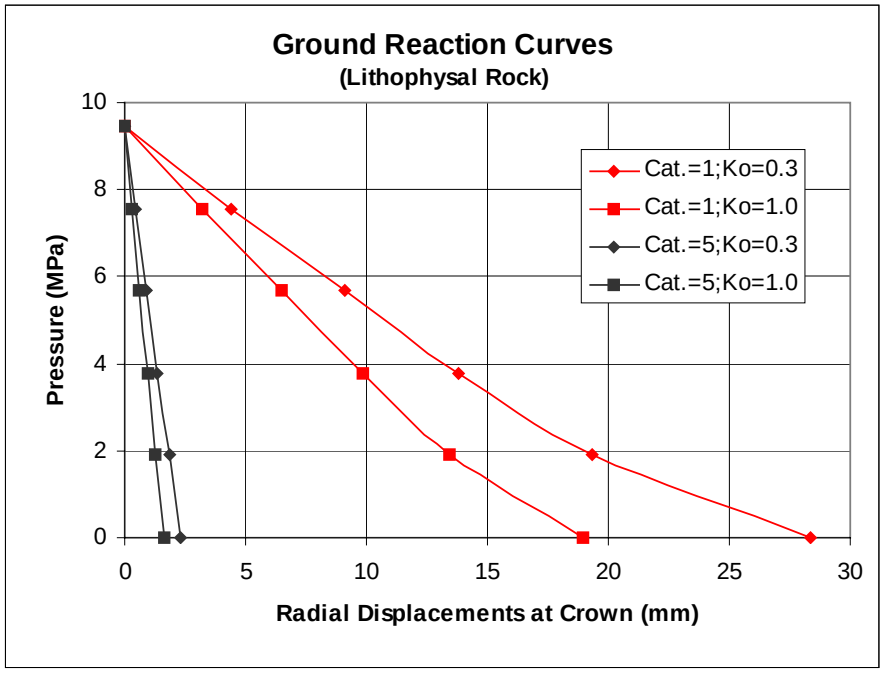

(a)

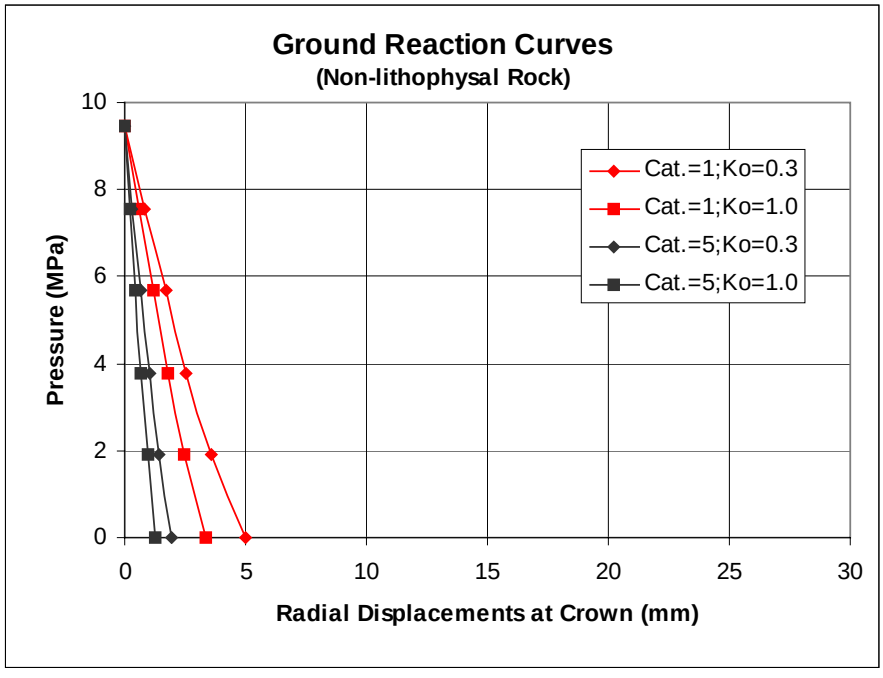

(b)

Figure 6-30. Ground Reaction Curves for Unsupported Emplacement Drifts: (a) Lithophysal Rock; (b) Non-lithophysal Rock.

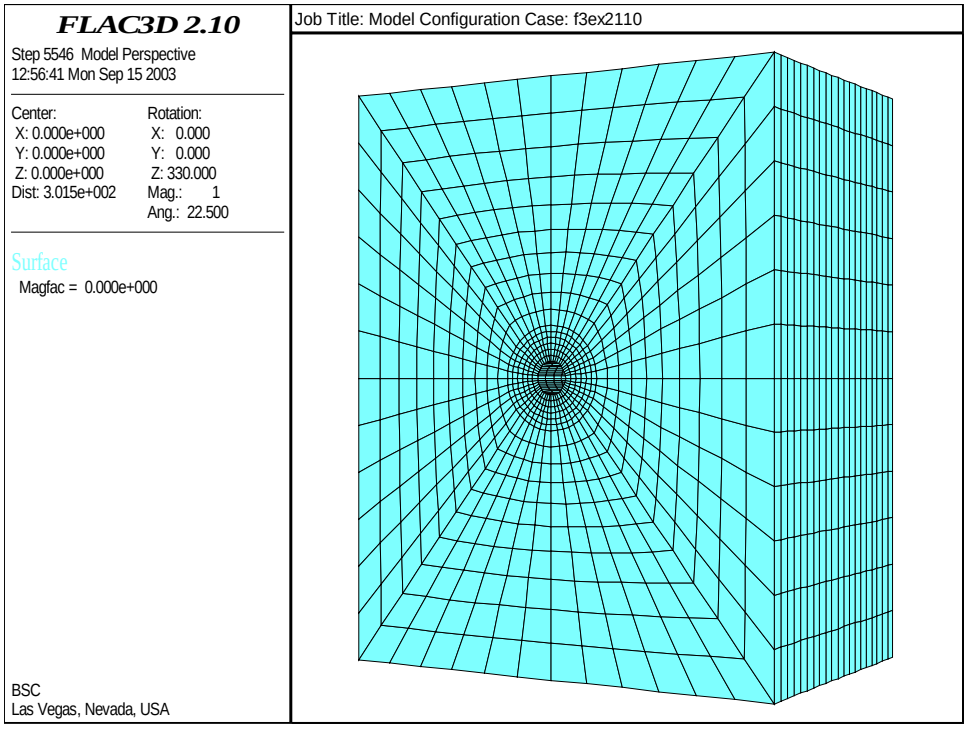

Figure 6-31. Configuration of a FLAC3D Model for Emplacement Drift

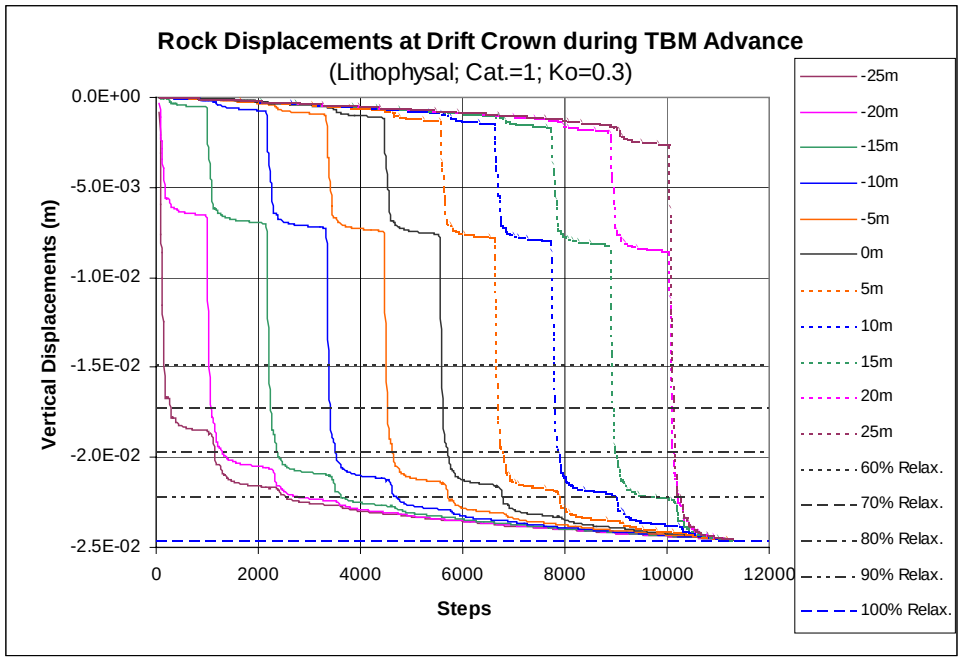

(a)

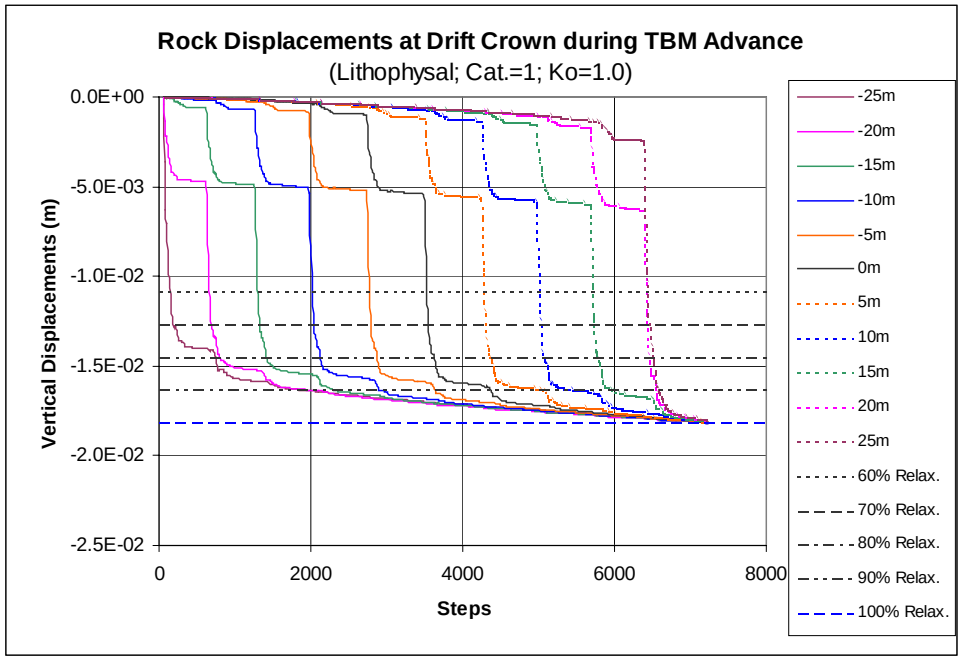

(b)

Figure 6-32. Vertical Displacements at Drift Crown during TBM Advance for Unsupported Emplacement Drifts in Category 1 Lithophysal Rock: (a) K_o=0.3; (b) K_o=1.0.

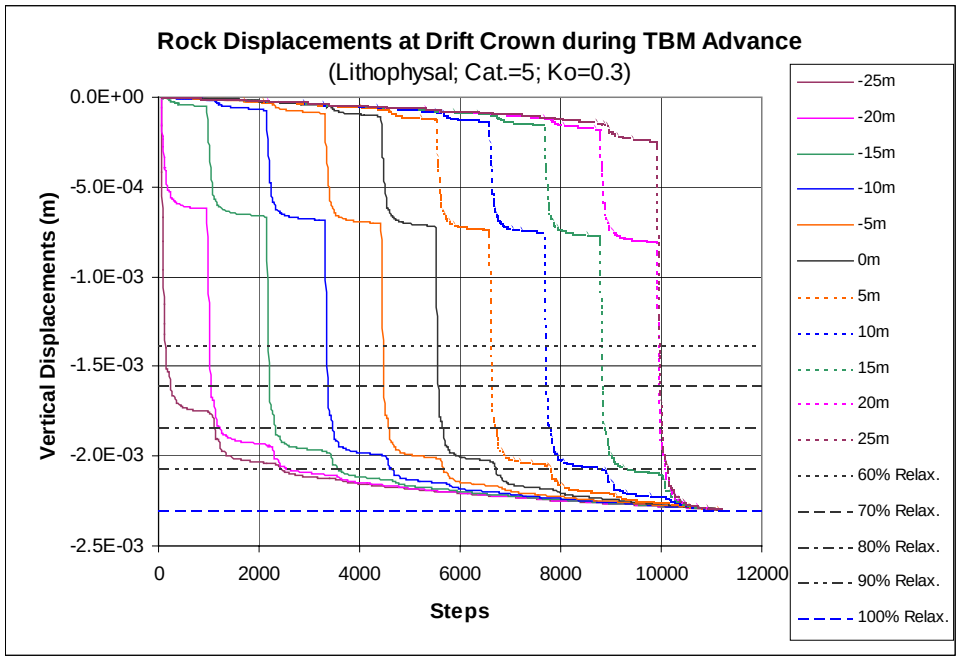

(a)

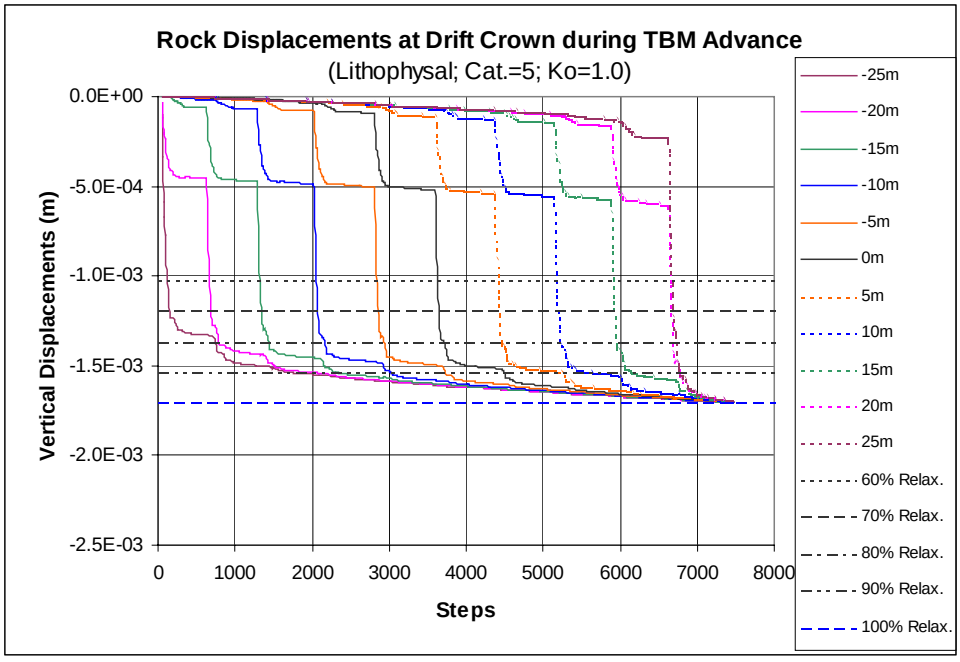

(b)

Figure 6-33. Vertical Displacements at Drift Crown during TBM Advance for Unsupported Emplacement Drifts in Category 5 Lithophysal Rock: (a) K_o=0.3; (b) K_o=1.0.

6.2 EMPIRICAL ANALYSIS OF GROUND SUPPORT NEEDS

Results of the empirical analysis based on the RMR and Q approaches for emplacement drifts in the non-lithophysal rock are presented in the following. The methods used are described in Section 5.4.1. As discussed in Section 5.4.1, these empirical methods are not applicable to emplacement drifts in the lithophysal rock. Assessment of the ground support requirements for these drifts will be based on experiences and observations from the constructions in the ESF and the ECRB tunnels.

The modulus and Q' values for various categories of the non-lithophysal rock are given in Table 3-5. To estimate the Q values from the Q' values, the following information is used:

- Unconfined compressive strength (σ_c) of intact non-lithphysal rock (Tptpmn) is about 207 MPa (BSC 2003a, Table 5-5).

- Major principal stress (σ_1) of rock adjacent to emplacement drifts is expected to be about 28 to 40 MPa (Section 6.1.2.2).

- The ratio σ_c/σ_1 ranges from 5 to 7.

In addition, the joint water reduction factor J_w in Eq. 5-3 is set to 1 for dry rock condition.

According to the *Support of Underground Excavations in Hard Rock* (Hoek et al. 2000, Table 4.6, p. 43), a SRF value ranging from 0.5 to 2 is considered appropriate. The Q values for various categories are then calculated based on Eq. 5-3, and listed in Table 6-1.

The RMR values are estimated using Eq. 5-1 based on the given modulus values for the non-lithophysal rock mass (see Table 3-5), and listed in Table 6-1.

Following the guidance provided from Table 5-1 and Figure 5-5 for the RMR and Q systems, respectively, the needs for ground support in emplacement drifts in the non-lithophysal rock can be estimated. To estimate the requirements of ground support using the Q system, an excavation support ratio (ESR) needs to be selected. The value of ESR is related to the intended use of the excavation and to the degree of security which is demanded of the support system installed to maintain the stability of the excavation. A suggested value for the emplacement drifts is 1.3 (Hoek et al. 2000, p. 40). Hence, the equivalent dimension (D_e), defined as the ratio of span or height to ESR, for the emplacement drifts is determined as 4.2 m (5.5/1.3=4.2 m). With the Q and D_e values determined, the needs for ground support for emplacement drifts in the non-lithophysal rock can be estimated. A recommended ground support system based on both the RMR and Q approaches is presented in Table 6-1 for each category of non-lithophysal rock considered.

As discussed in Section 5.2, typical rock conditions are close to categories 3 and 4. Use of pattern bolting with 3 m long, spaced at 1.25 m, in conjunction with 30 to 50 mm thick shotcrete is adequate, and should also be able to accommodate the category 1 rock conditions. Note that since shotcrete cannot be installed in emplacement drifts in order to meet the material requirement for long-term waste isolation, any recommended use of shotcrete is replaced by the Bernold-type steel sheet.

Table 6-1. Estimate of Ground Support Needs for Emplacement Drifts in Non-lithophysal Rock Based on RMR and Q Systems

Category	E_m (GPa)	RMR	SRF	Q	Ground Support Needs
1	10.25	50	0.5 – 2.0	0.97 – 3.90	Bolts: 3 m long, spaced 1.7-2.1 m in crown and walls, with Bernold-type sheet, or wire mesh and 40-60 mm shotcrete
2	13.66	55	0.5 – 2.0	1.70 – 6.79	Bolts: 3 m long, spaced 1.8-2.2 m in crown and walls, with Bernold-type sheet, or wire mesh and 30-50 mm shotcrete
3	16.74	59	0.5 – 2.0	2.65 – 10.59	Bolts: 3 m long, spaced 2.0-2.3 m in crown and walls, with Bernold-type sheet, or wire mesh and 30-50 mm shotcrete
4	20.23	62	0.5 – 2.0	3.69 – 14.78	Bolts: 3 m long, spaced 2.1-2.4 m in crown and walls, with Bernold-type sheet, or wire mesh and 30-50 mm shotcrete
5	26.18	67	0.5 – 2.0	6.44 – 25.76	Bolts: 3 m long, spaced 2.2-2.5 m in crown and walls, with Bernold-type sheet, or wire mesh and 30-40 mm shotcrete

6.3 SELECTION OF GROUND SUPPORT METHODS

The ground support methods for emplacement drifts are selected based on the requirements of functions, performance, and service life of ground support system. As stated in Sections 3.2.1 and 5.3, ground support installed in emplacement drifts must ensure stable conditions required for operational worker safety, limit the potential rockfall which might damage waste packages, and be functional with little or no planned maintenance throughout the preclosure period of 50 years. For a preclosure period of up to 300 years, an appropriate maintenance and monitoring program needs to be developed. In addition, the ground support materials selected should have acceptable long-term effect on waste isolation.

6.3.1 Candidate Ground Support Components and Materials

Cementious materials are ruled out for use in emplacement drifts due to their potential adverse impact on the long-term waste isolation. As a result, all ground support components installed in emplacement drifts will made of steel based, either carbon steel or stainless steel. Candidate ground support components that meet these criteria are friction-type rock bolts and perforated steel sheets (BSC 2003c, Section 6.3).

6.3.1.1 Friction-type Rock Bolts

There are two kinds of widely used friction-type, or friction-anchored, rock bolts: the Split Sets and the Swellex. Both types of rock bolting system rely on frictional resistance along the whole length of a bolt to prevent potential loosening rock blocks from becoming detached from the

rock mass. The frictional resistance is generated by a radial force against the borehole wall during installation of the bolts.

Split Sets The Split Set system, as shown in Figure 6-34, has two parts, a tube and a bearing plate. The steel tube has a slot along its length; one end is tapered for easy insertion, and the other has a welded ring flange to hold the plate. With the bearing plate in place, the tube is driven into a slightly smaller hole. As the tube slides into place, its full-length slot narrows; the tube exerts radial pressure against the rock over its full contact length. Plate loading is generated immediately. The result is a tight grip which actually grows stronger with time and ground movement. The anchorage capacity of a Split Set rock bolt depends on the borehole diameter and the tube length. It typically ranges from 6 to 10 tons for upper range (i.e., for SS-46 Split Set) (International Rollforms, p. 9).

Swellex The Swellex system, as illustrated in Figure 6-35, consists of rock bolts made from circular steel tube, which has been folded to reduce its diameter, and a high pressure water pump. The Swellex rock bolts are placed in a drilled hole and expanded by high pressure water. During the expansion process, the Swellex bolt compacts the material surrounding the hole and adapts its shape to fit the irregularities of the borehole. A combination of frictional and mechanical interlock is generated throughout the entire bolt length, reinforcing and increasing the load-bearing strength of the rock surrounding the drilled hole. The anchorage capacity of a Swellex bolt relies on the original tube diameter and material thickness and the tube length. It varies from 10 metric tons for standard Swellex bolts to 20 metric tons for Super Swellex bolts (Atlas Copco 2003, p. 10). The advantages of a Swellx bolt over a Split Set bolt are: a) it can adapts to irregularities of the borehole, which may increase its anchorage capacity, especially for the lithophysal rock with various cavities; and b) it has a higher anchorage capacity than Split Set.

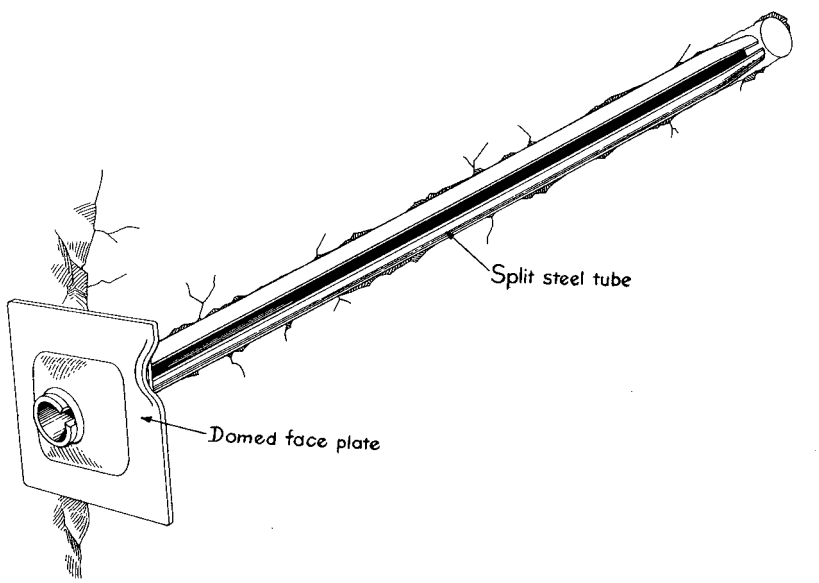

Source: Stillborg 1994, p. 13.

Figure 6-34. A Typical Split Set Rock Bolt

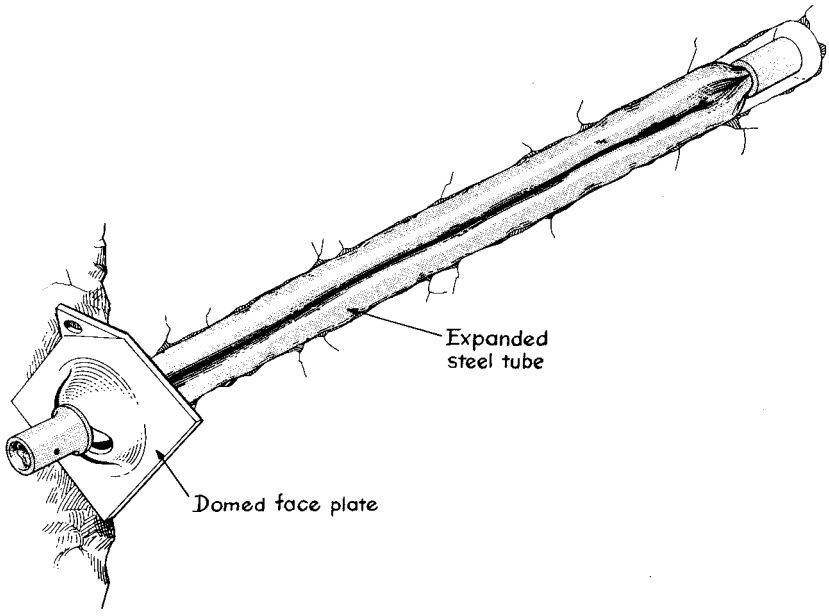

Source: Stillborg 1994, p. 14.

Figure 6-35. A Typical Swellex Rock Bolt

6.3.1.2 Perforated Steel Sheets

The perforated steel sheets, often called Bernold sheets (Michel 1999, p. 10), as shown in Figure 6-36, consists of thin (2 to 3 mm thick), slotted and slightly corrugated steel sheets bolted tight to the drift surface using friction-type rock bolts. The close contact of the sheets to the drift wall, combined with the holding action of the rock bolts and the extensional strain resistance of the sheets, provides a confinement to potential surface loosening and raveling. The holes stamped in sheets also allow air circulation for rock dry-out and reduce the relative humidity between the sheets and the rock (BSC 2003c, Section 6.3.2).

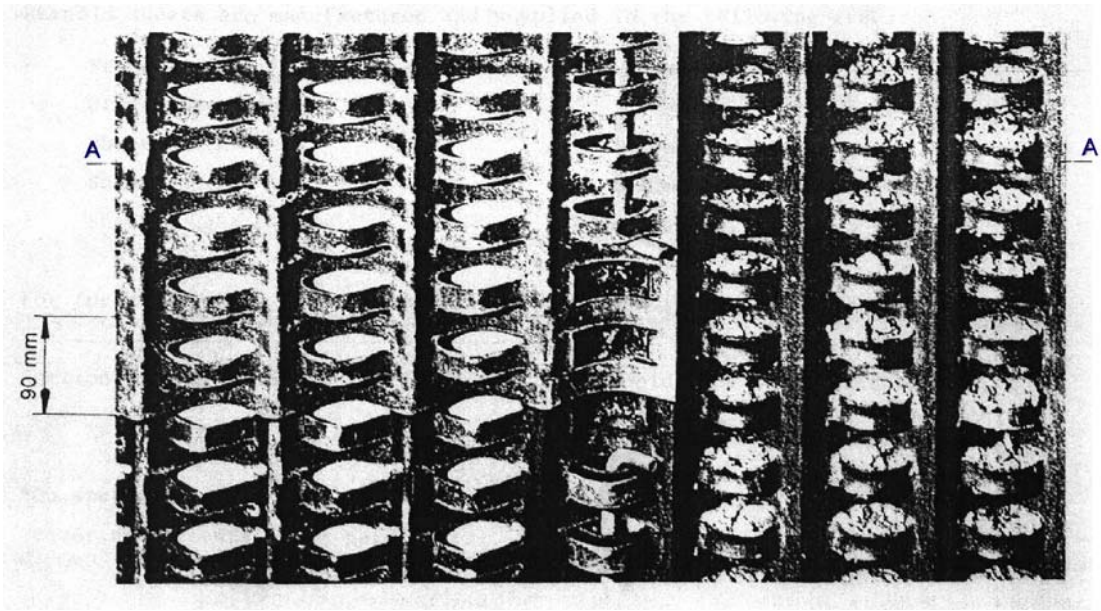

Source: Michel 1999, p. 10.

Figure 6-36. Bernold-type Perforated Steel Sheet

6.3.1.3 Candidate Ground Support Materials

According to the *Longevity of Emplacement Drift Ground Support Materials for LA* (BSC 2003c, Section 7.4), candidate materials for both friction-type rock bolts and Bernold-type perforated sheets need to be made of stainless steel, such as 316 equivalent or better, in order to prevent ground support failure prematurely due to corrosion and achieve its longevity during the preclosure period (BSC 2003c, Section 7.4).

6.3.2 Candidate Ground Support Methods

6.3.2.1 Lithophysal Rock

Observations made in the ESF and the ECRB (Board 2003, Section 7.3.1.3) indicate that the *lithophysal rock* contains intense small-scale fractures together with voids of various sizes. Ground support in this type rock should primarily play a role of retention to hold small pieces of loosening rock in place. Swellex bolts and wire mesh installed in the crown and springline of these tunnels appear to provide adequate support and stability. It is noted that ground support required in the ECRB drift is considered to be very minimal.

Numerical analyses of the unsupported emplacement drifts in the lithophysal rock, discussed in Sections 6.1.2 and 6.1.3, indicate that the drifts are generally stable under combined in situ, thermal, and seismic loading conditions, with small anticipated rock deformation and potential yield zone. The overall condition of the drifts is stable without ground support, with an estimated minimum factor of safety of 2.2.

By considering observations from the ESF and the ECRB and results from numerical analyses, the final ground support consisting of Super Swellex bolts of 3 m long, spaced at 1.25 m, and

thin-walled (3 mm thick), perforated Bernold-type sheets, all installed in a 240° arc around the drift periphery, is recommended for use in emplacement drifts in various rock conditions. As recommended by the *Longevity of Emplacement Drift Ground Support Materials for LA* (BSC 2003c, Section 7.4), the materials of these bolts and Bernold-type perforated sheets need to be made of stainless steel in order to prevent ground support failure prematurely due to corrosion and achieve its longevity during the preclosure period.

Swellex rock bolts are preferred over Split Sets because the former generally has higher holding capacity, and will deform, to a certain degree, to accommodate lithophysal cavities along the borehole, which will further increase the holding capacity.

6.3.2.2 Non-lithophysal Rock

Observations made in the ESF and the ECRB (Board 2003, Section 7.3.1.2) that the non-lithophysal rock (Tptpmn) contains multiple joint sets, dominated by three major subsets, two horizontal and one vertical. This ground condition will most likely result in gravity-induced wedge-type failures, which have occurred in both the ESF and the ECRB. Primary function of the ground support for the non-lithophysal rock is to prevent wedge-type rockfall. Rock bolts with appropriate length and spacing supplemented by wire mesh perform adequately under these ground conditions.

Numerical analyses of the unsupported emplacement drifts using the non-lithophysal rock properties, presented in Sections 6.1.2 and 6.1.3, show that the drifts are expected to be stable under combined in situ, thermal, and seismic loading conditions, with very small rock deformation and little yield zone for various rock categories. An estimated minimum factor of safety is 5 for this rock type. In general, no ground support is needed for the drifts to maintain a stable condition.

Empirical analyses discussed in Section 6.2 suggest that the ground support for emplacement drifts in the non-lithophysal rock consist of rock bolts of 3 m long, spaced at 1.25 m, with wire mesh and 30 to 50 mm thick shotcrete in crown and springline for the ground conditions anticipated. Bernold-type perforated steel sheets should be in place of shotcrete.

Figure 6-37 illustrates the recommended ground support methods for emplacement drifts in both lithophysal and non-lithophysal rocks.

6.3.3 Initial Ground Support Methods

The initial ground support will be installed as necessary for worker safety during excavation of the emplacement drifts if a two-pass construction scheme is used. The initial ground support consists of friction-type rock bolts, such as Split Sets, and wire mesh based on industry standard materials (carbon steel). Rock bolts with a length of 1.5 m and a spacing of 1.5 m, installed in the crown (four bolts in each row), are considered adequate for the rock conditions anticipated. Wire mesh will be removed prior to the installation of the final ground support, while rock bolts will remain in place. During the preclosure period, these carbon steel rock bolts may corrode, however, they are very unlikely to fall out because they are friction-type bolts (anchored over

their entire length). In addition, all of these bolts will be covered by the Bernold sheets (see Section 6.3.2).

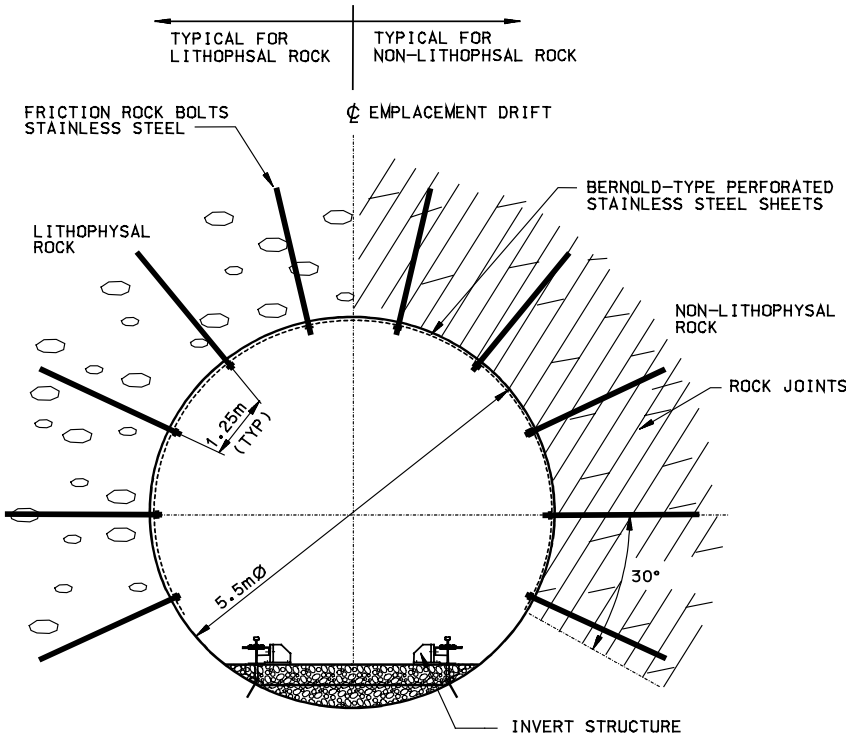

Source: Modified from BSC 2004a, Fig. 2.

Figure 6-37. Final Ground Support Methods Recommended for Emplacement Drifts.

6.4 EVALUATION OF GROUND SUPPORT PERFORMANCE

To evaluate the performance of proposed final ground support system under in situ, thermal, and seismic loading conditions, numerical analyses were conducted. These analyses were based on two-dimensional FLAC models.

6.4.1 Numerical Calibration of Swellex Bolt Pull Test

As discussed in Section 6.3.1.1, reinforcing mechanism of Swellex bolts is frictional and mechanical interlock over the entire bolt length. This kind of mechanism can be simulated using the approach similar to what is used for fully-grouted bolts. Two key input parameters in this approach are the bond stiffness (K_{bond}) and the shear strength (S_{bond}), which reflect the interaction between bolt and rock and control the bolt behavior. These parameter values depend on the frictional resistance at the interface, stiffness of the rock mass, and any near-field stress changes. Values of these two parameters can be estimated either based on empirical correlations developed from pull test data or using numerical calibrations of pull test results. Since there is no empirical correlation currently available, the latter is the only approach that can be used for this calculation. The numerical calibration was performed using the FLAC code. The pull test data used was for a Super Swellex bolt, and obtained from the Atlas Copco (Charette 2003, Bolt 12, p. 16).

In numerical calibration, a pull test of rock bolts was simulated. A model configuration and the final failure state of the simulation are shown in Figure 6-38. During the simulation, an initial value of K_{bond} was chosen to be the same order of magnitude as the stiffness of rock. The stiffness is then decreased until the slope on the load-versus-displacement curve matches the measured from the pull test (Charette 2003, Bolt 12, p. 16). The value of S_{bond} was then adjusted until the model approximated the pull-out load determined from the test. Figure 6-39 shows the results of numerical calibration of the Super Swellex bolt pull test. The values of K_{bond} and S_{bond} estimated from this calibration are 3×10^{8} N/m/m and 2.75×10^{5} N/m, respectively.

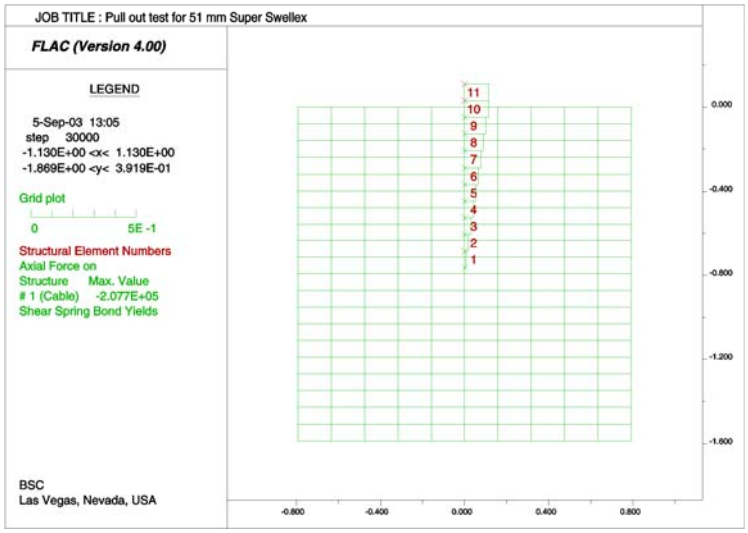

Figure 6-38. Configuration and Failure State of FLAC Model Simulation of a Pull Test of Swellex Bolts

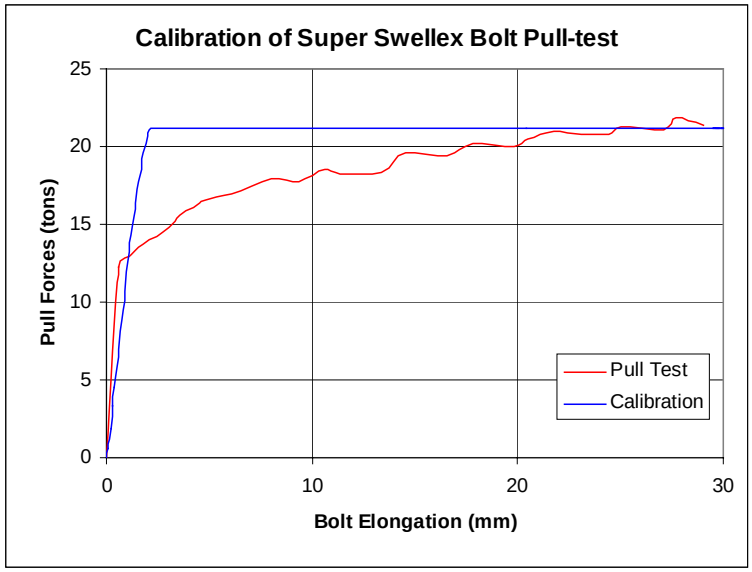

Source: Charette 2003, Bolt 12, p. 16.

Figure 6-39. Numerical Calibration of Super Swellex Bolt Pull Test

6.4.2 Performance of Swellex Bolts in Emplacement Drifts

Performance of Swellex bolts is evaluated using the two-dimensional FLAC models. In these models, the bolts are simulated by one-dimensional cable elements. Each cable element is divided by two nodes, together with the cross-sectional area and the material properties. The cable element is an axial member, meaning that only the uniaxial resistance, compression or tension, is taken into account. Since two-dimensional modeling the bolts with regular spacing in the drift axial direction involves averaging the three-dimensional effect over the distance between the adjacent rows of bolts, linear scaling of material properties of bolt is required in the FLAC models. This scaling is achieved by divided the actual property by the bolt spacing along the drift. The material properties that need to be scaled include the modulus of elasticity, the strength, K_{bond}, and S_{bond}. Axial force outputs from the models are then multiplied by the bolt spacing to obtain the actual loads. The sign convention in the FLAC models is that axial forces in bolts are positive in compression and negative in tension.

In calculating the effect of excavation-induced rock displacements on rock bolts, it is assumed that 60 percent of rock displacements has occurred prior to the installation of rock bolts, meaning that only 40 percent of excavation-induced rock displacements will affect the bolt behavior (Assumption 4.3). As indicated in Section 6.1.4, the displacements developed before the installation of ground support are predicted to be as much as 75 percent of the total displacements anticipated if a stand-off distance between the bolts and the tunnel face is 5 m. A ground relaxation of 60 percent used in this calculation is very conservative and is expected to give an additional factor of safety of about 20 percent ((75-60)/75=0.2 or 20 percent) as far as the in situ load is concerned.

It is noted that the ground relaxation will depend on the construction sequence, or the time when ground support is installed. If the final ground support is installed after the excavation of an entire emplacement drift is completed, the ground relaxation will likely be about 100 percent. Any loads induced in ground support will be subsequently cased by nearby mining activities or thermal and seismic loading conditions.

It is also noted that in analyzing the behavior of Swellex rock bolts the effect of Bernold-type steel sheet is not accounted for. This will result in a slightly higher stress or load in rock bolts than anticipated, and is therefore conservative for the purpose of this calculation.

6.4.2.1 Swellex Bolts in Lithophysal Rock

Time histories of axial forces in Swellex bolts installed in emplacement drifts in the lithophysal rock are shown in Figure 6-40 for in situ and thermal loading conditions. The results indicate that axial forces in the bolts are very sensitive to the rock mass modulus or the rock deformation induced by excavation. In weak ground conditions (category 1), the bolts will be in tension throughout the operational time of 50 years considered. In strong ground conditions (category 5), the bolts will be in tension when subjected to in situ load, and become in compression when the rock is heated up. In general, heating in rock is expected to reduce the tensile forces in bolts.

The maximum axial forces in the Swellex bolts are predicted to be about 100 kN (10 tonnes) in tension for category 1 lithophysal rock and from about 10 kN (1 tonne) in tension to about 21 kN

(2 tonnes) in compression for category 5 rock. These give a minimum factor of safety of approximately 3 (298/100=3) (see Table 3-6), which is greater than the required upper bound of factor of safety of 1.8, as specified in Section 3.2.1.5.

Distributions of axial forces in Swellex bolts are presented in Figures 6-41 to 6-44 for various rock and initial stress conditions. These forces are not uniformly distributed, and higher near the crown than near the springline. Under heating, some bolts, especially near the springline, experience tension close to the drift surface and compression away from the surface. Comparing the axial forces under in situ loading condition (year=0) to those under combined in situ and thermal conditions (year=50), the maximum values in bolts are reduced for the category 1 rock, and change from negative (in tension) to positive (in compression) for the category 5 rock. It should be noted that the actual loads in bolts illustrated in Figures 6-41 to 6-44 are equal to those shown in the figures times the bolt spacing of 1.25 m.

Time histories of axial forces in the bolts during seismic motions are presented in Figures 6-45 to 6-46 for earthquakes occurred at 0 year and 50 years after waste emplacement, respectively. It is seen that the seismic motions are expected to induce additional forces in the bolts installed in the weakest rock, and these additional forces vary with location, rock quality, and loading condition prior to earthquake motions. For a bolt installed near the crown, a total axial force of about 110 kN (11 tonnes) is predicted for combined in situ and seismic loading conditions (see Figure 6-45a). As mentioned above, heating will result in a reduction in tensile forces (compared the axial forces shown in Figure 6-46 with those in Figure 6-45). So the total tensile force predicted in the same bolt near the crown is about 103 kN (10 tonnes), when subjected to combined in situ, thermal, and seismic loading conditions (see Figure 6-46a). The factor of safety under the worst loading combinations is about 2.7 (298/110=2.7), greater than the required upper bound factor of safety of 1.5, as specified in Section 3.2.1.5.

In summary, the recommended Swellex bolts for emplacement drifts in the lithophysal rock are expected to behave satisfactorily under in situ, thermal and seismic loading conditions, with a factor of safety exceeding 2.

6.4.2.2 Swellex Bolts in Non-lithophysal Rock

Time histories of predicted axial forces in the Swellex bolts installed in emplacement drifts in the non-lithophysal rock are shown in Figure 6-47 for in situ and thermal loading conditions. The behavior of the bolts is also dependent on the rock mass modulus. The bolts are in tension under in situ loading condition, and turn to compression when the rock is heated up following waste emplacement. The axial forces induced are generally very low. The maximum axial forces predicted vary from -20 kN (-2 tonnes) to 22 kN (2 tonnes) in the category 1 non-lithohysal rock and from -8 kN (-1 tonne) to 23 kN (2 tonnes) in the category 5 rock. The expected factor of safety based on these values exceeds 10, which is well greater than 1.8.

Variations of axial forces in the Swellex bolts during seismic motions are shown in Figures 6-48 and 6-49. It is indicated that additional forces induced by the seismic motions are very small, only about 6 kN (0.6 tonnes). Therefore, the proposed Swellex bolts for emplacement drifts in the non-lithophysal rock are anticipated to perform satisfactorily under combined in situ, thermal, and seismic loading conditions, with a factor of safety exceeding 10.

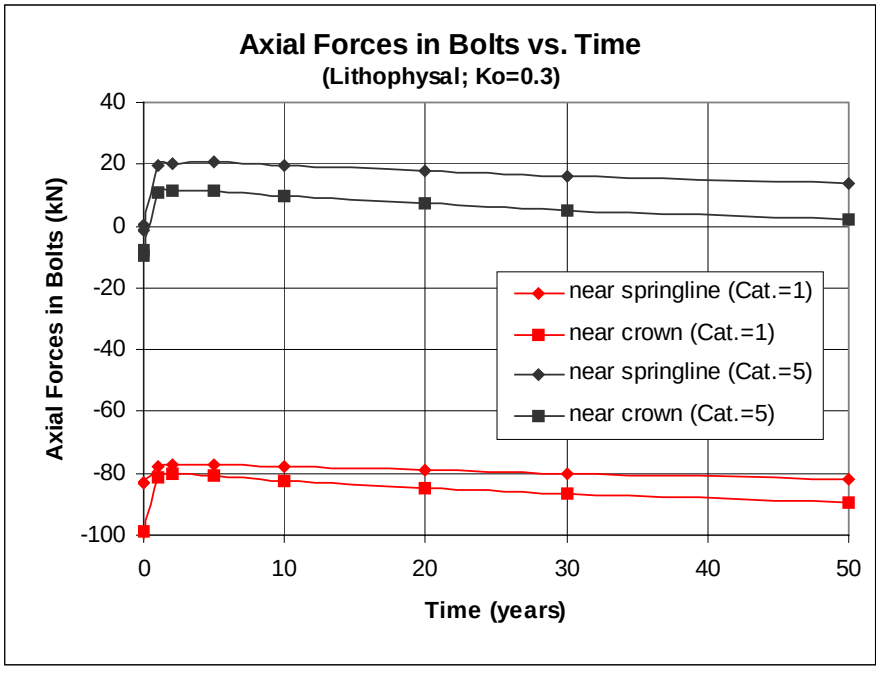

(a)

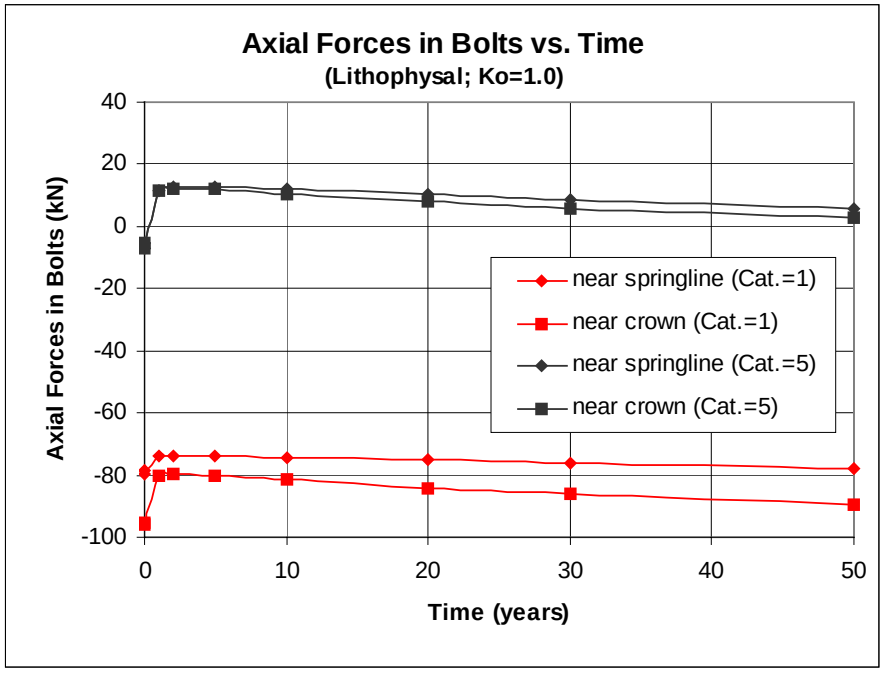

(b)

Figure 6-40. Axial Forces in Bolts Installed in Emplacement Drifts in Lithophysal Rock under In Situ and Thermal Loads: (a) K_o=0.3; (b) K_o=1.0

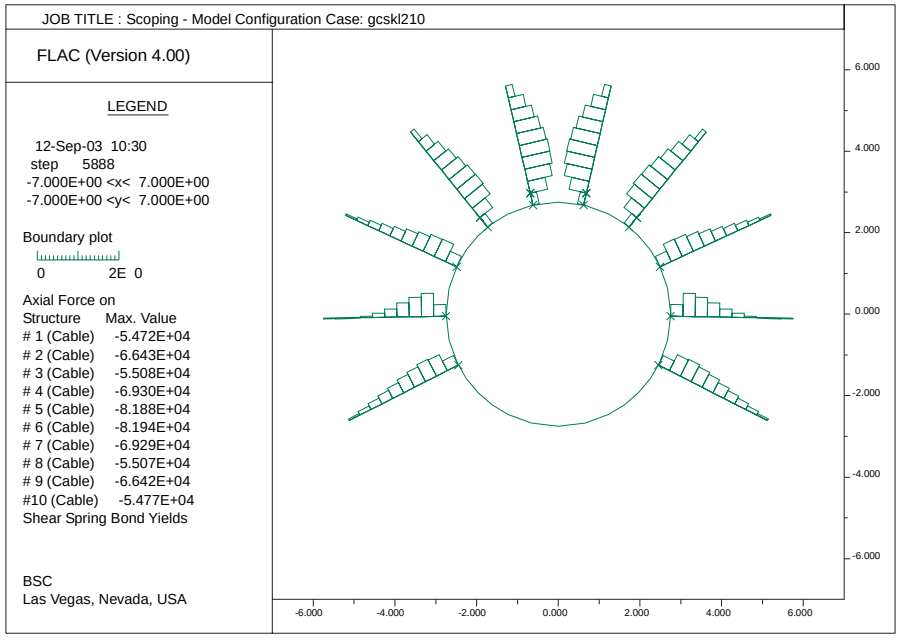

(a)

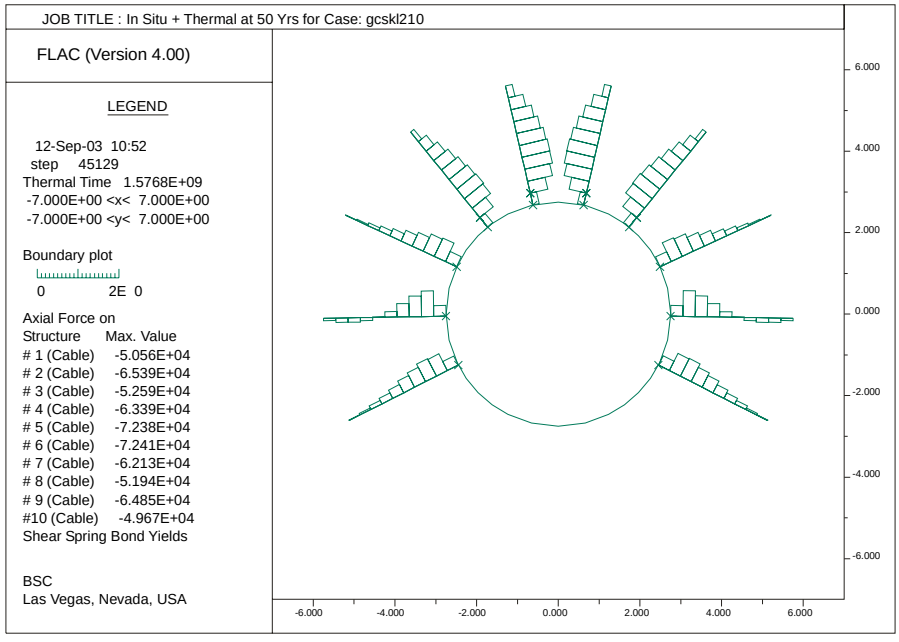

(b)

Note: Actual forces (N) in bolts are equal to those shown times the bolt spacing of 1.25 m.

Figure 6-41. Axial Forces in Bolts Installed in Emplacement Drifts in Lithophysal Rock under In Situ and Thermal Loads for Cat.=1 and K_o=0.3: (a) at 0 years (b) at 50 years

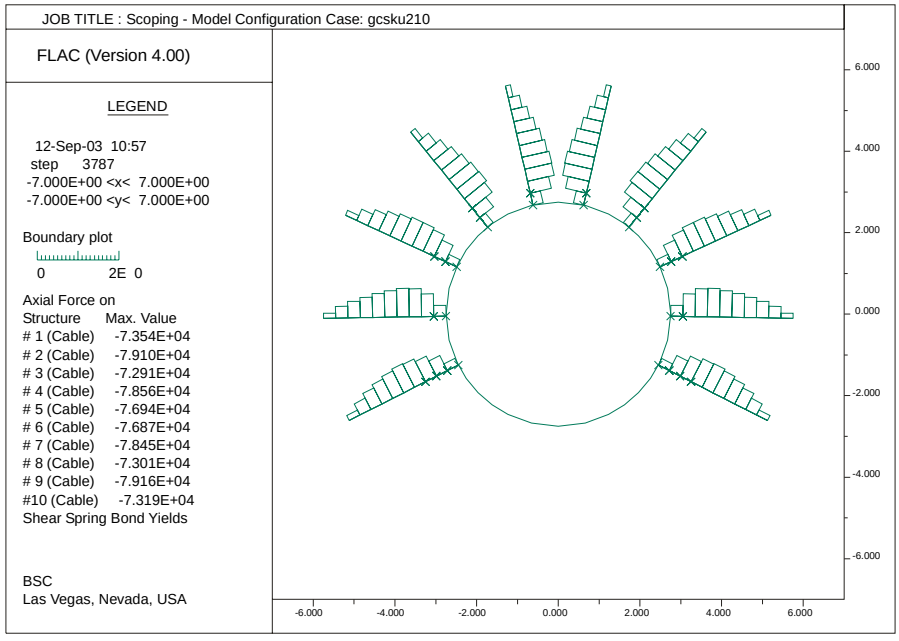

(a)

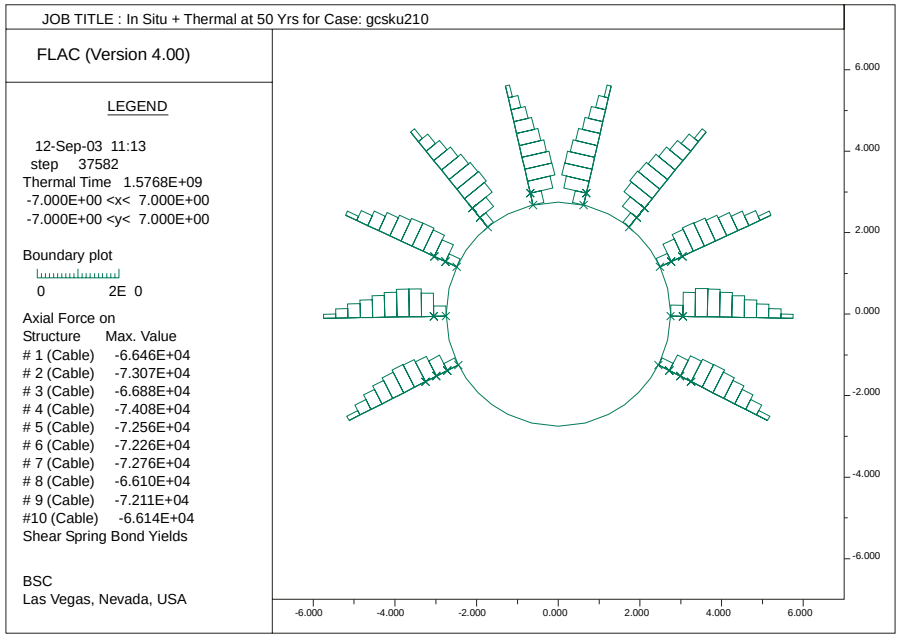

(b)

Note: Actual forces (N) in bolts are equal to those shown times the bolt spacing of 1.25 m.

Figure 6-42. Axial Forces in Bolts Installed in Emplacement Drifts in Lithophysal Rock under In Situ and Thermal Loads for Cat.=1 and K_o=1.0: (a) at 0 years (b) at 50 years

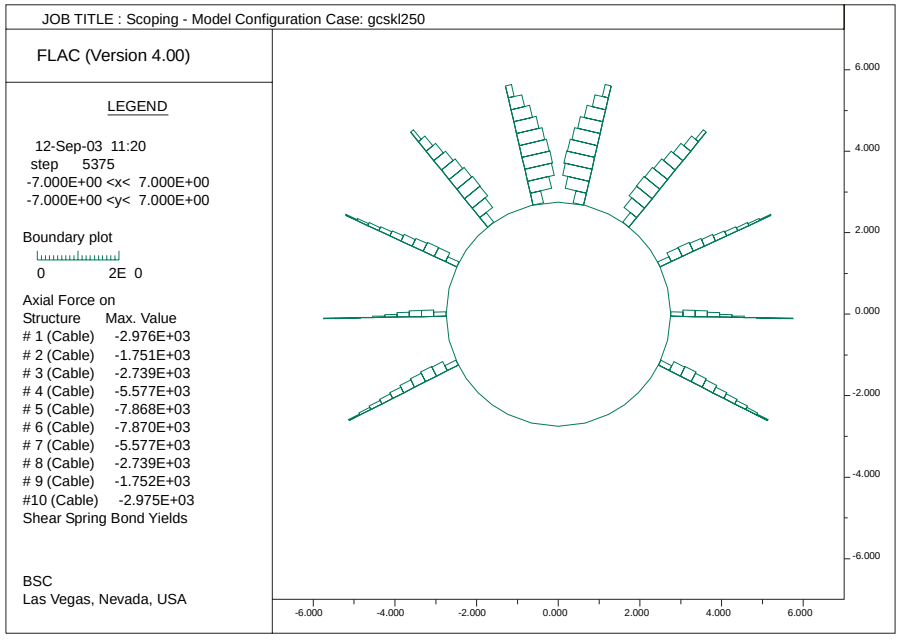

(a)

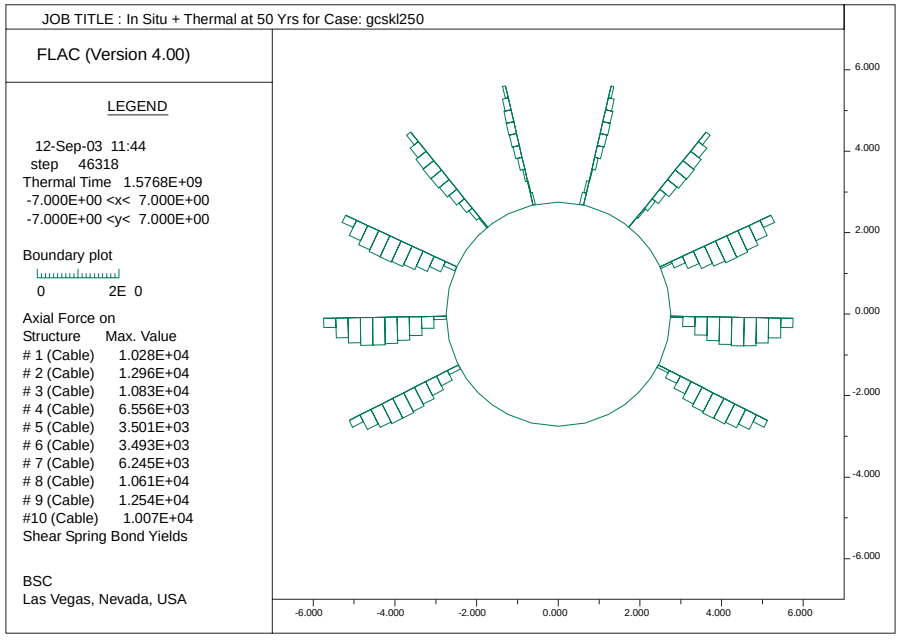

(b)

Note: Actual forces (N) in bolts are equal to those shown times the bolt spacing of 1.25 m.

Figure 6-43. Axial Forces in Bolts Installed in Emplacement Drifts in Lithophysal Rock under In Situ and Thermal Loads for Cat.=5 and K_o=0.3: (a) at 0 years (b) at 50 years

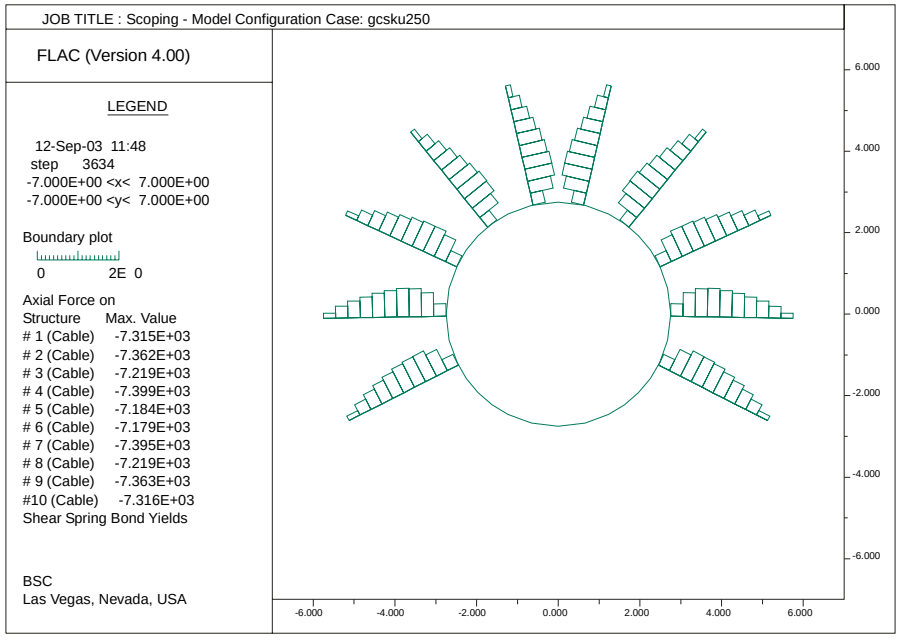

(a)

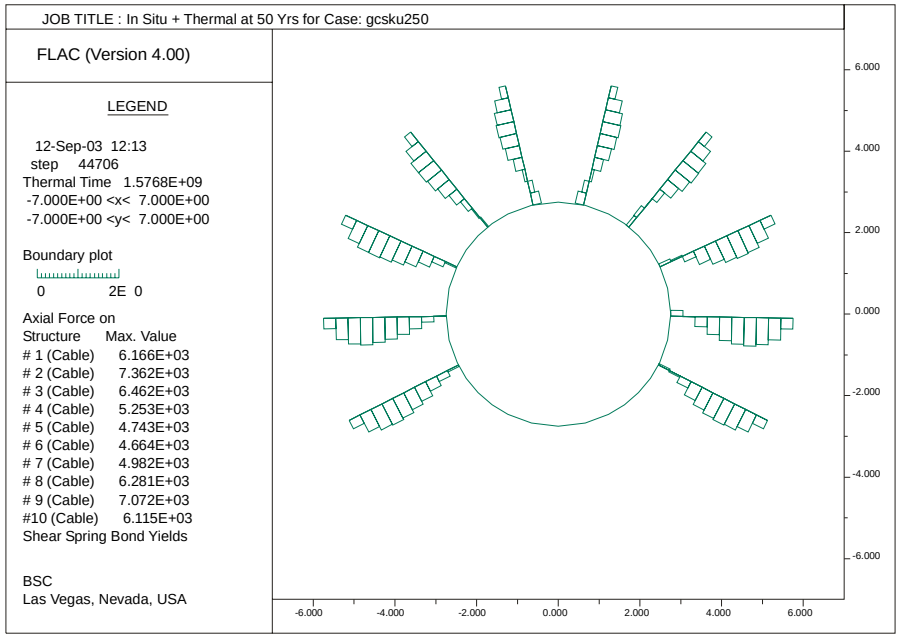

(b)

Note: Actual forces (N) in bolts are equal to those shown times the bolt spacing of 1.25 m.

Figure 6-44. Axial Forces in Bolts Installed in Emplacement Drifts in Lithophysal Rock under In Situ and Thermal Loads for Cat.=5 and K_o=1.0: (a) at 0 years (b) at 50 years

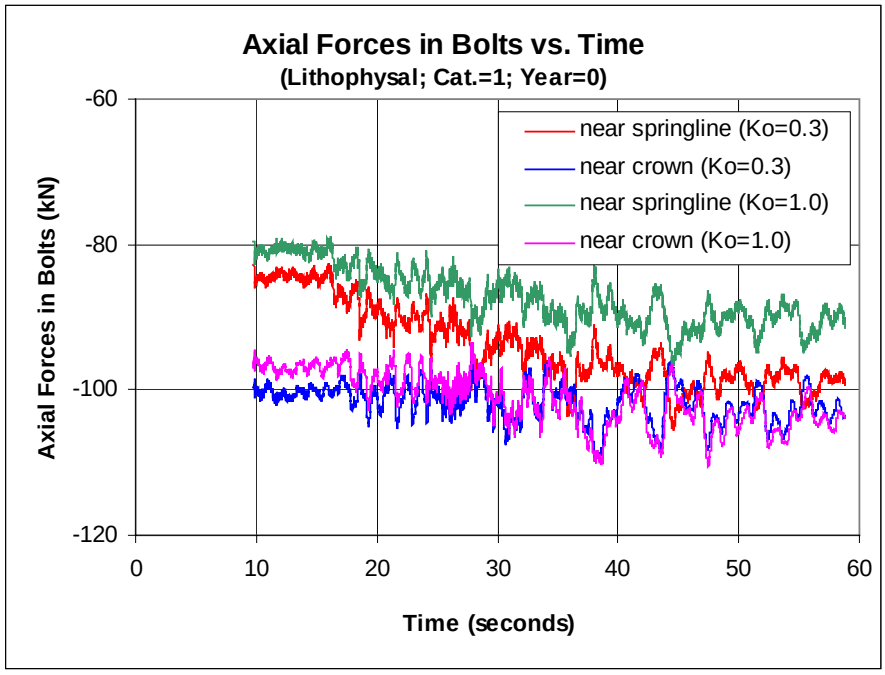

(a)

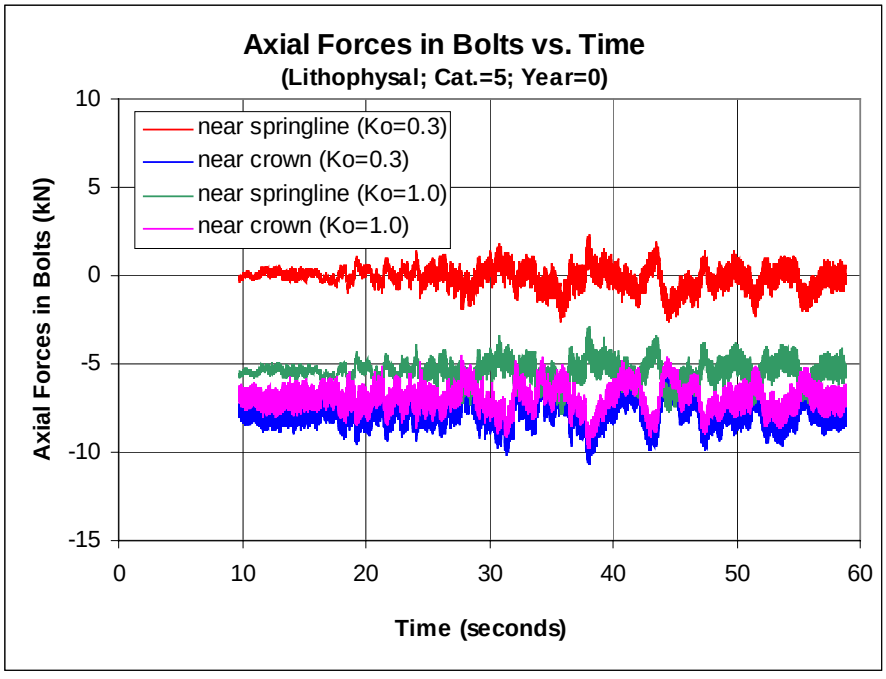

(b)

Figure 6-45. Axial Forces in Bolts Installed in Emplacement Drifts in Lithophysal Rock under In Situ and Seismic Loads: (a) Cat.=1; (b) Cat.=5.

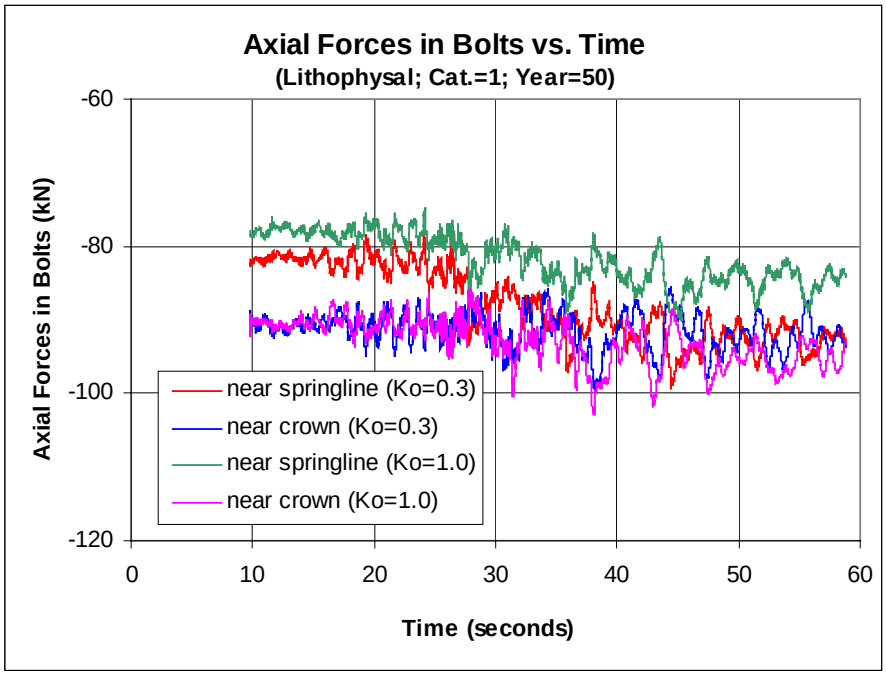

(a)

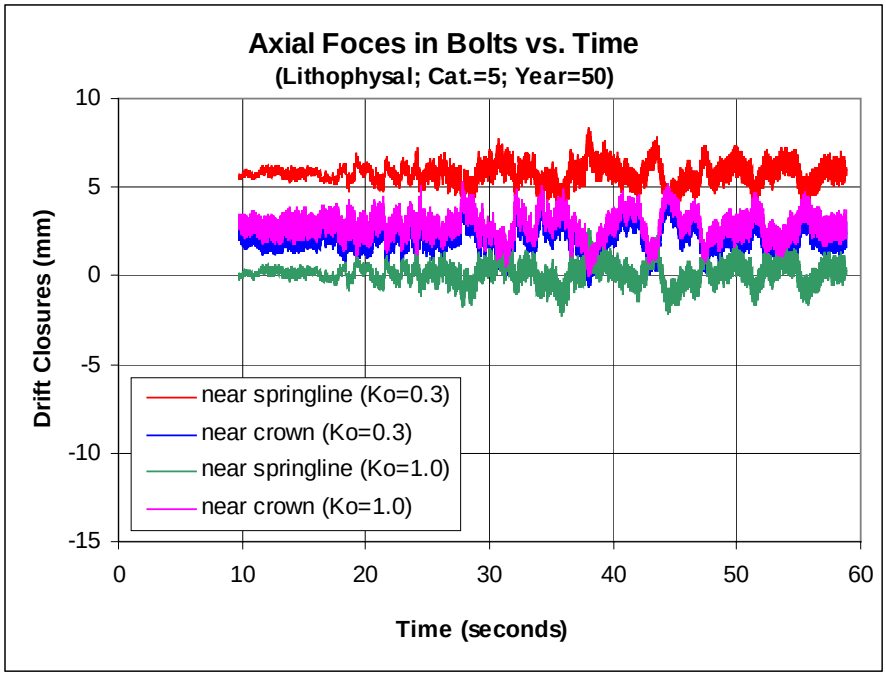

(b)

Figure 6-46. Axial Forces in Bolts Installed in Emplacement Drifts in Lithophysal Rock under In Situ, Thermal, and Seismic Loads: (a) Cat.=1; (b) Cat.=5.

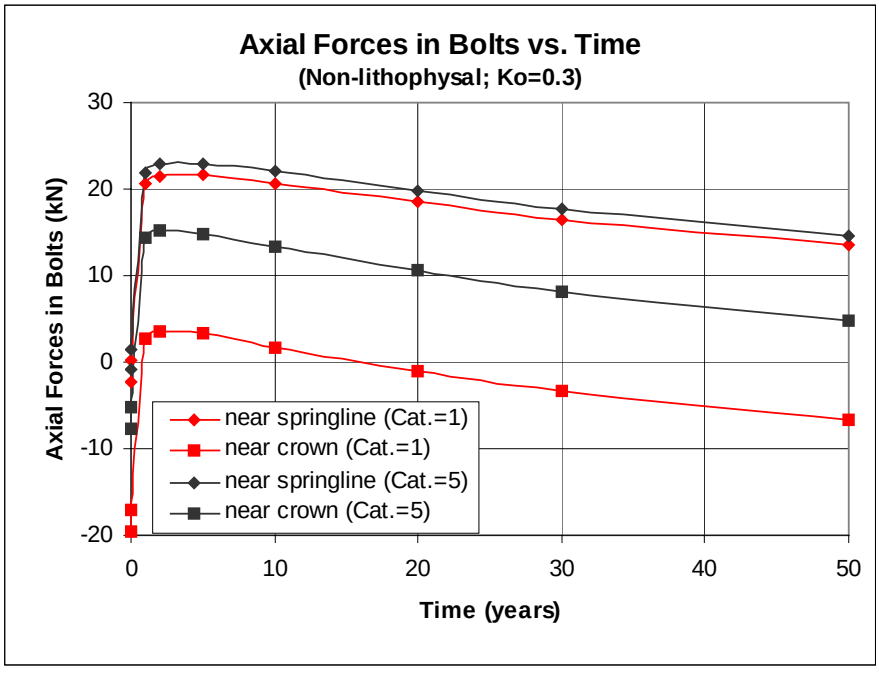

(a)

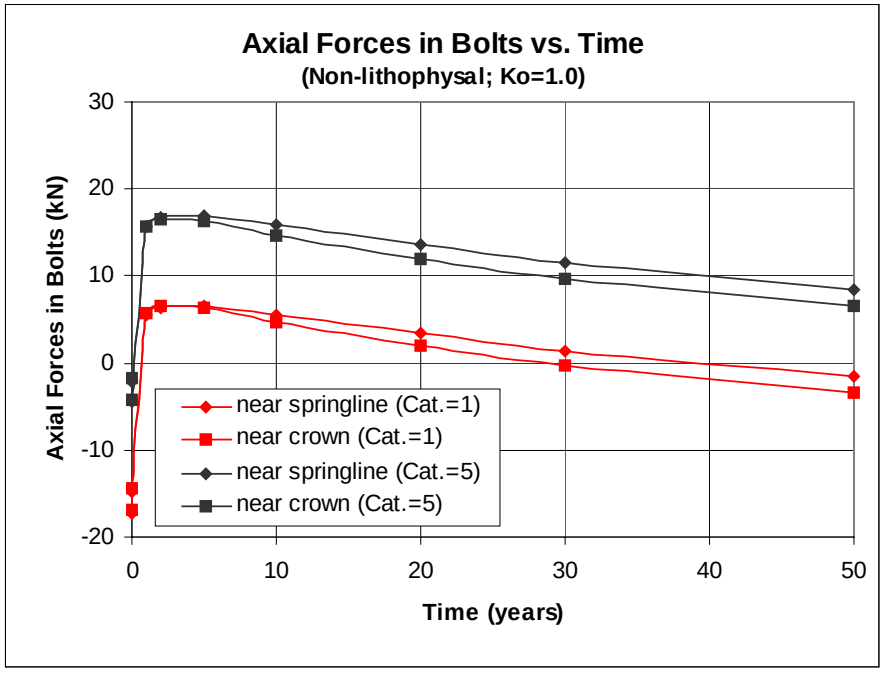

(b)

Figure 6-47. Axial Forces in Bolts Installed in Emplacement Drifts in Non-lithophysal Rock under In Situ and Thermal Loads: (a) K_o=0.3; (b) K_o=1.0.

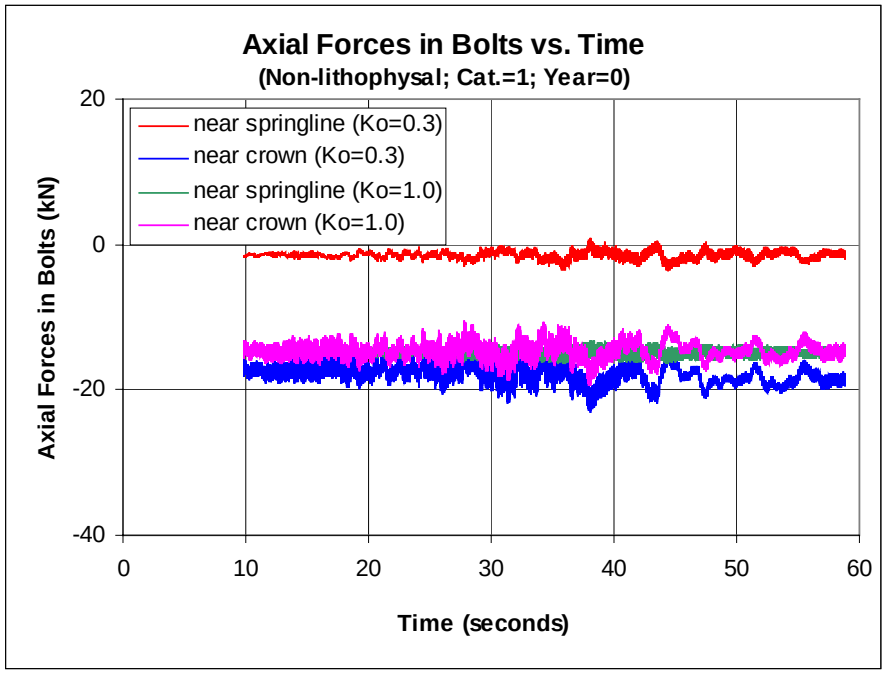

(a)

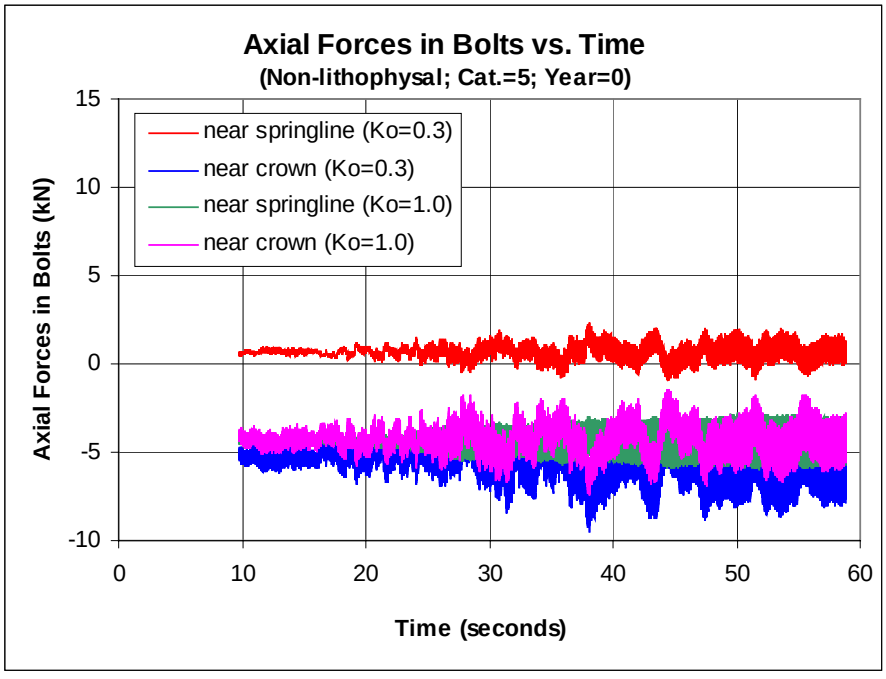

(b)

Figure 6-48. Axial Forces in Bolts Installed in Emplacement Drifts in Non-lithophysal Rock under In Situ and Seismic Loads: (a) Cat.=1; (b) Cat.=5.

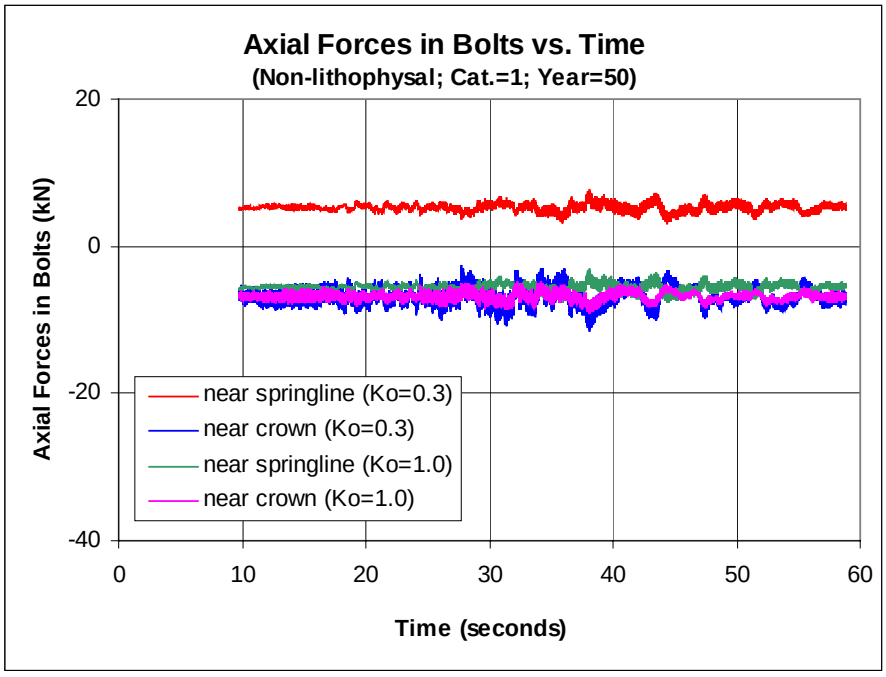

(a)

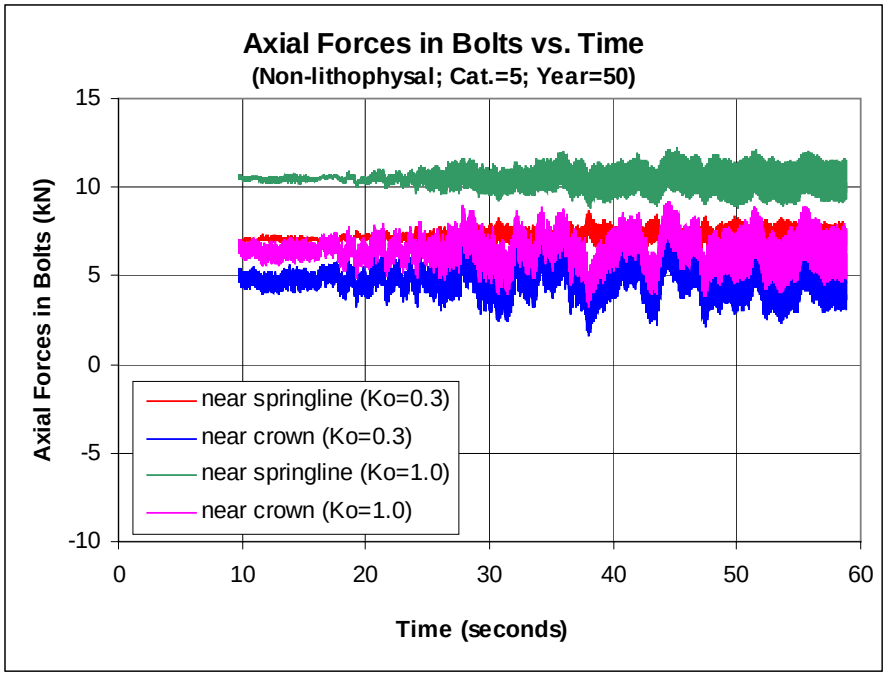

(b)

Figure 6-49. Axial Forces in Bolts Installed in Emplacement Drifts in Non-lithophysal Rock under In Situ, Thermal, and Seismic Loads: (a) Cat.=1; (b) Cat.=5.

6.4.3 Performance of Bernold-type Steel Sheets

Performance of the Bernold-type stainless steel sheets is evaluated using a simple hand calculation based on the plate theory. The approach and results are presented below.

6.4.3.1 Estimate of Support Load

- Estimate of In Situ Stress Induced Load

Bernold-type sheets with a thickness of 3 mm are assumed to be pinned to the rock surface by the permanent 3-m long Swellex rock bolts, spaced at of 1.25 m. The rock bolts provide reinforcement for the sheets and may greatly improve their load-bearing capacity. The sheets act more like an assembly of arched plates with each of them supported at its four corners, subjected to a dead load shaped like a pyramid between bolts, as illustrated in Figure 6-50. For simplicity, the sheets are assumed to be flat with a span (l) of 1.25 m in both sides (see Figure 6-50). So, the load pyramid has a height of 0.625 m, and a volume of

$$V = \frac{1}{3} \times 1.25^2 \times 0.625 = 0.33 \quad m^3$$

The total dead load over the plate can be estimated as

$$W = V\gamma = 0.33 \times 2410 \times 9.81 = 0.0078 \quad MN$$

where γ = rock mass density, kg/m^3

If this dead load is smeared uniformly over the entire area of plate (sheet), the unit load is

$$w_s = \frac{W}{A} = \frac{0.0078}{1.25^2} = 0.005 \quad MN/m^2$$

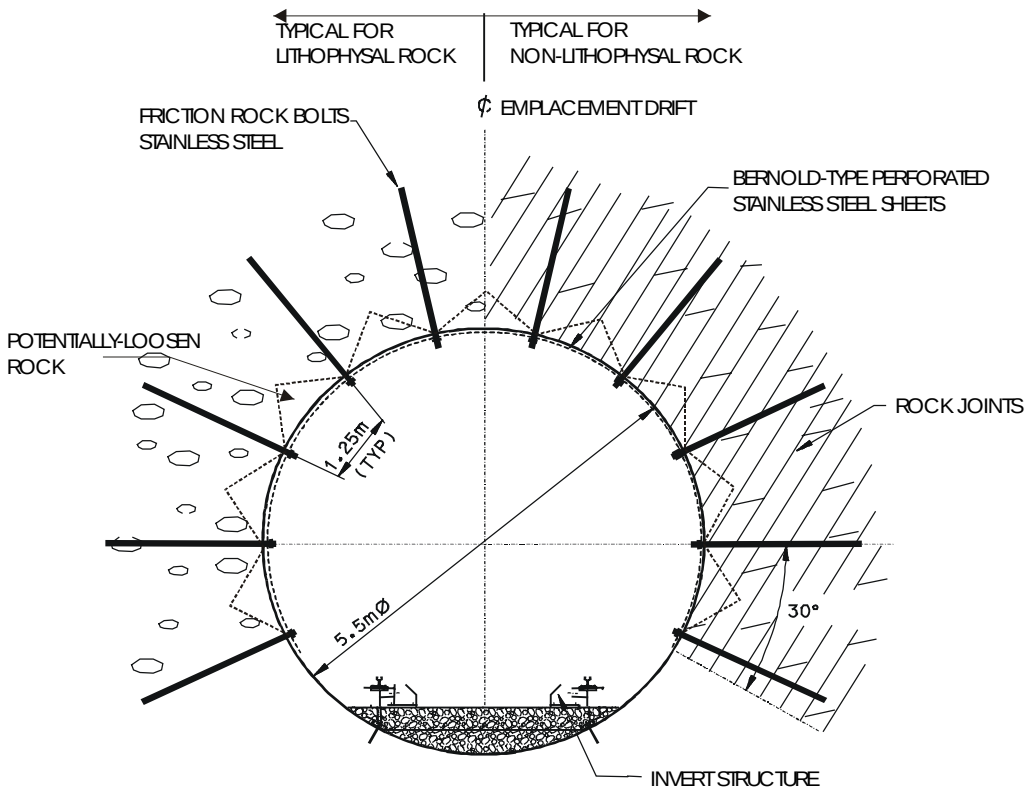

Note: Only the final ground support is shown.

Figure 6-50. Illustration of Potentially-loosen Rock on Periphery of an Emplacement Drift

- Estimate of Seismically-induced Load

Seismically-induced load on the Bernold-type sheets is treated similarly to that of in situ stress, as discussed above. This is a reasonable assumption since the wavelength of the ground motion is much larger than the dimension of the rock wedge. The increased dynamic load component can then be treated as a quasi-static problem in which the peak ground acceleration is added to the gravitational acceleration. The dynamic effect is reflected in an increased value of gravitational acceleration as

$$g_d = g + PGA \qquad \text{(Eq. 6-1)}$$

where g_d = effective gravitational acceleration during seismic motions, m/s^2
g = gravitational acceleration, equal to 9.81 m/s^2
PGA = peak ground acceleration during seismic motions, m/s^2

According to DTN: MO0306SDSAVDTH.000 (MatH1.ath, MatH2.ath, and MatV.ath), the maximum value of PGA associated with a seismic event of the mean annual exceedance probability of 1×10^{-4} is about 0.47g. With this PGA value, the equivalent uniform load on the sheets induced during seismic shaking can be estimated as

$$w_{s+d} = w_s + w_d = (g + 0.47g)\frac{w_s}{g} = 1.47 w_s = 1.47 \times 0.005 = 0.0074 \quad MN/m^2$$

This is the total load under combined in situ and seismic effects.

- Estimate of Thermally-induced Load

Thermally-induced load on Bernold-type sheets is mainly due to thermal expansion of rock mass and sheets themselves. This load depends on the nature of contact between the sheets and the rock surface. In general, the corrugated Bernold sheets are not in perfect contact with the rock. Any gap present between the sheets and the rock surface will allow a relief in thermally-induced load. In this calculation, it is conservatively assumed that the sheets are in perfect contact with the rock, and thermally-induced rock displacements will result in additional load on the sheets. This load can be estimated by using the plate theory.

For a square flat plate with all four edges rigidly fixed, the equivalent uniform load (w_T) over the entire plat, which causes a maximum deflection (δ_T), can be calculated as (Young 1989, p. 464, Case No. 8, Loading Case No. 8a):

$$w_T = \frac{Et^3}{\alpha l^4}\delta_T \qquad \text{(Eq. 6-2)}$$

where E = Young's modulus of sheet material, Pa
t = thickness of sheet, m
α = a constant, equal to 0.0138 for a square plate with uniform load.

According to Section 6.1.2.1, the maximum thermally-induced drift closure is about 2 mm for all rock conditions considered. So the actual maximum deflection of a sheet between bolts is approximately 1 mm, or half of the maximum drift closure. For conservatism, a deflection of 2 mm is used. With this deflection, the equivalent uniform load induced by increase in rock temperature can be estimated based on Eq. 6-2 as

$$w_T = \frac{193 \times 10^9 \times 0.003^3}{0.0138 \times 1.25^4 \times 10^6} \times 0.002 = 3.1 \times 10^{-4} \quad MN/m^2$$

It should be noted that the calculation presented here is ultra-conservative. In reality, the opening closes more or less uniformly under thermal load. The heads of the rock bolts will move inward with the tunnel surface, which will put some differential strain on the bolt, over its length, and load it. However, the Bernold sheets and the heads of rock bolts will likely move together, as the circular opening is closing more or less uniformly and becoming smaller. At the same time, the Bernold sheets themselves will thermally expand more than the drift closure. The end result is that the sheets will probably be compressed rather than tensioned since the sheet thermal expansion is greater than the rock thermal expansion. The thermally-induced stress will likely offset the tensile stress caused by the load from dead weight of potentially loosen rock. In other words, all of these things would indicate that the sheets will be under little additional strain from thermal loading.

- Combined In Situ, Thermal, and Seismic Loads

The total combined in situ, thermal, and seismic load over the square flat sheet is determined as

$$w = w_s + w_d + w_T = 0.0074 + 0.00031 = 0.0077 \quad MN/m^2$$

It is seen that major contributor of the load is the dead weight of a potentially-loosened rock wedge.

6.4.3.2 Estimate of Stress and Factor of Safety

As mentioned above, thin-walled, corrugated Bernold-type stainless steel sheets installed in emplacement drifts may be very conservatively assumed to behave like a flat plate, rigidly fixed on all edges, subjected to a uniform load over its entire area. The maximum stress at the center of the plate under a uniform load can be estimated using the following expression (Young 1989, p. 464, Case No. 8, Loading Case No. 8a):

$$\sigma = \frac{\beta w l^2}{t^2} \qquad \text{(Eq. 6-3)}$$

where β = a constant, equal to 0.1386 for the case considered.

Using this expression and the loads estimated for different loading conditions, stresses in Bernold-type sheets can be estimated. Their values and corresponding safety factors are presented in Table 6-2. The factor of safety is calculated based on a tensile strength of 620 MPa for stainless steel (see Table 3-6). Note that the factor of safety calculated is against the stress associated with peak elastic strain in the steel – i.e., the stress state at onset of inelastic hardening. However, it is not the rupture condition since this sheet will have considerable inelastic strain prior to rupture.

Table 6-2. Estimated Stresses and Factors of Safety in Bernold-type Stainless Steel Sheets for Various Loading Conditions

Loading Conditions	Load (MN/m^2)	Stress (MPa)	Factor of Safety
In Situ	0.005	120	5.2
In Situ + Seismic	0.0074	178	3.5
In Situ + Thermal	0.0053	128	4.8
In Situ + Thermal + Seismic	0.0077	185	3.4

In summary, Bernold-type stainless steel sheets are expected to perform satisfactorily under combined in situ, thermal, and seismic loading conditions. The key factor that controls the stresses in the sheets is the in situ load, or dead load of potentially loosen rock formed between rock bolts. The thermal load has minimal effect. The results are based on a simple hand calculation. Further analyses based on more comprehensive numerical methods may be desirable in the detail design stage since numerical analyses can simulate the interaction between

the Bernold sheets and the rock as well as the loading history during heating and seismic motions.

6.4.4 Prevention of Rockfall by Ground Support

The key function of Swellex bolts installed in emplacement drifts is to reinforce rock mass and to prevent any potential rockfall. A comprehensive analysis of potential rockfall in emplacement drifts in both lithophysal and non-lithophysal rocks was preformed in the *Drift Degradation Analysis* (BSC 2004b).

According to the *Drift Degradation Analysis*, the probability of wedge-type failure in the lithophysal rock during the preclosure period is vary low, with a volume of rockfall per linear kilometer drift of 0.16 m^3 (BSC 2004b, Table 41). Any potential rockfall will be associated with small loosening and unravelling rock pieces, which can be prevented by installed Bernold-type steel sheets.

In the non-lithophysal rock, the predicted heaviest key block is 2.89 tonnes (BSC 2004b, Table 19). Assume that the rock has a density of 2410 kg/m^3 (see Section 3.1.6) and the shape of the key block is a cube. So the dimension of the cube is 1.1 m. Also assume that the key block is fully mobilized and its total weight is carried by a single Swellex bolt, meaning that frictional resistance or confinement along discontinuities is neglected. The holding capacity of the bolt may be estimated based on the smaller of the anchorage force and the shear resistance force along the interface between the bolt and the key block. The effective anchorage force of the bolt is about 13 tonnes ($20/3\times(3-1.1)=13$), while the shear resistance force is about 5.2 tonnes ($2.75\times10^5\times\pi\times0.054\times1.1/1000/9.81=5.2$), both exceeding the weight of 2.89 tonnes with factors of safety of about 4.5 and 1.8, respectively.

The calculation presented here is very simple. More detailed analysis is needed to further evaluate the bolt function for preventing rockfall. It is also noted that the predicted sizes of rockfall provided by the *Drift Degradation Analysis* (BSC 2004b) are based a seismic event with the mean annual exceedance probability of 5×10^{-4} (2,000 years), while the design basis seismic event for the emplacement drift ground support design is associated with the mean annual exceedance probability of 1×10^{-4} (10,000 years) (see Section 3.1.7). The maximum sizes of rockfall under the design basis seismic event might be different from what were used in the above calculation. These data are currently under development through a revision of the *Drift Degradation Analysis*. Judging by the relatively small sizes of key blocks predicted for the seismic event with the mean annual exceedance probability of 5×10^{-4}, it may be reasonably expected that the sizes of key blocks induced by a seismic event with the mean annual exceedance probability of 1×10^{-4} would be comparable with what was used. This should be further confirmed by results of the revised *Drift Degradation Analysis*.

Therefore, with proposed ground support system installed, any potential rockfall in emplacement drifts is expected to be prevented as long as the ground support is functional during the anticipated service life.

6.5 UNCERTAINTY ANALYSIS

There are uncertainties in the calculation. These uncertainties are primarily associated with the design inputs and calculation methods used. To minimize the effect of uncertainties on the design solution, it is necessary to understand the key factors that contribute to the uncertainties.

6.5.1 Uncertainty Associated with Design Inputs

Virtually all design inputs have uncertainties since a "true value" of any input parameter is hard or impossible to obtain. However, not all uncertainties need to be addressed and uncertainties of some input values, such as Poisson's ratio of steel, have little or no effect on the design solution. The discussions provided below are focused on uncertainties of some key input parameters and how to cover these uncertainties in selection of input values and calculation methods.

6.5.1.1 Variations in Material Properties

Input parameters that have large uncertainties are rock mass properties. These large uncertainties are mainly associated with large spatial variations in rock mass quality. For examples, discontinuities in rock mass due to the presence of joints and voids are location dependent, and have significant impact on the behavior of rock mass. To account for these variations, the rock mass important to the repository design has been divided into five categories based on its quality and probability of occurrence. The category 1 represents the weakest rock, while the category 5 is for the strongest rock. Statistically, these five categories cover about 90 percent of the rock mass conditions anticipated (BSC 2003b, Section 8.5).

In this calculation, the mechanical properties corresponding to the categories 1 and 5 of both the lithophysal and non-lithophysal rocks are selected. Since typical rock mass quality may be represented by the category 3 rock, use of these lower and upper bounds of the rock mass properties is not only conservative but can also serve to reduce uncertainties in the design solutions.

Rock mass thermal properties, such as thermal conductivity, specific heat, and coefficient of thermal expansion, have uncertainties due largely to spatial variations in distributions of fractures and cavities. Most of the values used in the design calculations are obtained based on tests conducted in a laboratory using small-scale specimens that contain few fractures or voids. From a thermal analysis perspective, use of thermal conductivity values from laboratory tests may underestimate the increase in temperature, because these values are generally higher than the actual ones that represent for the rock mass. On the other hand, use of the higher coefficients of thermal expansion from laboratory tests in a thermomechanical analysis may result in overestimate of thermally-induced rock deformations and stresses. In this calculation, all thermal properties are selected based on the mean values.

There are uncertainties associated with ground support materials. Bonding stiffness and shear strength values for Swellex bolts are derived from numerical calibration based on the results of a single pull test. These values may vary since the performance of Swellex bolts may depend on rock conditions, in which the bolts are installed, and near-field stress variations. There are few data published on the Swellex capacities for different rock types and loading conditions. In

addition, changes in material properties due to temperature-induced degradation, though insignificant (BSC 2003c, Section 7.3), may also contribute to these uncertainties.

A comprehensive sensitivity study on the effect of uncertainties associated with variations in rock mass properties is being conducted in an ongoing scoping analysis, and details will be presented in the related document.

6.5.1.2 Variations in Loading Conditions

Loads considered in the ground support design include, but not limited to, in situ, thermal, and seismic. The loading conditions that emplacement drifts are subjected to may vary. For example, overburden of emplacement drifts changes from one drift to another. Temperatures in different drifts also vary dependent on the timing and sequence of waste emplacement. These variations in loading conditions will contribute to uncertainties in the results of design calculations.

To minimize the uncertainties associated with the load variations, the bounding conditions are considered in this calculation. In determining the overburden, a depth of 400 m is used, while the depths of most emplacement drifts vary from about 260 to 370 m (see Section 4.1). This results in a higher in situ load. In addition, the horizontal-to-vertical stress ratios (K_o) selected are 0.3 and 1.0, while the actual value may range from 0.36 to 0.82 based on the field measurements in the ESF (DTN: MO0007RIB00077.000, Tables 4 and 5). The K_o values used are considered bounding and may cover most of the uncertainties associated with in situ stress conditions anticipated.

The thermal load considered corresponds to a scenario that all waste packages will be emplaced simultaneously and for an emplacement drift located in the central area of the repository block. The effect of waste emplacement sequence and heat absorption near the edge of repository area is ignored, resulting in a higher rock temperature. The dealing of thermal conditions this way may reduce the effect of associated uncertainties on results. Impact of other uncertainties related to abnormal events such as earthquakes which may damage and disrupt ventilation in emplacement drifts, causing a temporary surge in rock temperature, will be addressed in the ongoing scoping analysis.

The seismic load used in the calculation is related to a mean annual exceedance probability of 1×10^{-4} earthquake event. For the ground support system with a design service life of 50 years, use of this seismic load is very conservative, and the impact of uncertainties related to seismic loads on the design solutions is not considered significant. Nevertheless, some issues associated with the variations in seismic motions and their impact on the ground support system will be discussed in the scoping analysis.

6.5.1.3 Variations in Duration of Design Service Life

In this calculation, all analyses are based on a thermal condition with a forced ventilation lasting for 50 years following waste emplacement. It is likely, however, that the preclosure period will be as long as 100 years, which means that an additional 50-year heating in rock may need to be considered in assessment of stability of emplacement drifts and performance of ground support.

Whether the performance predicted based on a preclosure period of 50 years is still applicable to a longer service life depends on what thermal environments are expected beyond 50 years. If the forced ventilation with a constant air flow quantity would last for an entire preclosure period, it is expected that near-field rock temperatures would continuously decrease beyond 50 years based on the trend of predicted rock temperatures shown in Figure 5-6. Behavior of emplacement drifts and installed ground support are not anticipated to change substantially with this scenario, as long as corrosion of ground support materials does not undermine the functionality of ground support.

Details on the analyses of stability of emplacement drifts for a period of 100 years will be addressed in the ongoing scoping analysis.

6.5.2 Uncertainty Associated with Calculation Methods

Design calculations usually involve idealization to simplify the system simulated and to reduce computational efforts. Without the idealization or simplification, the calculations are sometimes impractical or even impossible based on the tools currently available. The greater the difference between the actual system to the idealized, the greater the uncertainties will be.

6.5.2.1 Continuum versus Discontinuum

The rock mass which is dealt with in this calculation contains many joints and voids. These discontinuities affect the behavior of emplacement drifts excavated in the discontinuous rock mass. Ideally, a discontinuum approach which explicitly simulates these discontinuities is preferred. In conventional mining or tunnel design, however, an equivalent continuum approach is most popular due to its simplicity and easy understanding of the results. In the continuum approach, the values of rock mass properties used are equivalent, meaning that the effect of discontinuities can be accounted for by choosing these property values. The continuum approach has been approved useful and reasonable through many years of industry practice.

The ground support designs for the ESF and the ECRB tunnels were based primarily on the conventional continuum approach. The experiences from these tunnel designs and excavations indicate that the continuum approach is still applicable to the ground support design for emplacement drifts as long as the values of rock mass properties are able to reflect the effect of discontinuities present in the rock. Results from the continuum approach, such as rock deformation and stress, are considered equivalent to those which would be generated otherwise by using a discontinuum approach.

Some information, such as size of potential rockfall, may not be obtained from a continuum approach. A discontinum approach should be supplemented to address some specific design issues. Since the *Drift Degradation Analysis* (BSC 2004b) uses the discontinuum approach to quantify the effect of joints on potential wedge failure and the results are available, it is not necessary for this calculation to conduct similar analyses in order to obtain the information about rockfall.

To further examine the uncertainties associated with the use of continuum approach, sensitivity study is being conducted in the ongoing scoping analysis. The results of this analysis will

hopefully provide additional information on how to quantify the uncertainties and further guidance on the selection of calculation approaches.

6.5.2.2 Model Dimensions

Most of calculations on ground support design are performed using numerical modeling. In developing a numerical model, a model dimension needs to be decided first. The model dimension covers two aspects, one is related to the choice of either two dimensions or three dimensions, and the other is the selection of a model size.

Factors that are considered in the choice of model dimensions include the location where an opening of interest is excavated, the loading conditions which the excavation is subjected to, and the size of the opening. For emplacement drifts, the average length is about 600 m, and the loads are generally perpendicular to the drift axis. Use of two-dimensional models is appropriate to assess the behavior of emplacement drifts if a continuum approach is employed. Uncertainties associated are primarily with evaluating the performance of the drifts located near intersections, where the loading and stress conditions are predominately three-dimensional. Generally, two-dimensional models give more conservative results than three-dimensional ones, which will in part offset some related uncertainties.

The size of a model usually affects the accuracy of results and the computational time. However, the accuracy will not necessarily be improved by increasing the model size. For the ground support design, a model size which is equal to about 5 to 10 times the drift diameter is adequate. Any uncertainties associated with the variations of model size are considered to have insignificant effect on the results. Details on the evaluation of this effect will be presented in the scoping analysis.

7. SUMMARY AND CONCLUSION

This calculation analyzes the stability of emplacement drifts excavated in both the lithophysal and the non-lithophysal rocks and the performance of ground support system installed in these drifts during the repository preclosure period. The loading conditions considered include in situ, thermal, and seismic. Both empirical and numerical methods are employed. The empirical methods used are the RMR and the Q systems. The numerical methods are based on the continuum approach using the FLAC and the FLAC3D computer codes.

Findings from this calculation can be summarized as follows:

Thermomechanical Response and Stability of Unsupported Emplacement Drifts

- Unsupported emplacement drifts are expected to be stable with relatively small rock displacements and yield zones induced by excavation. Rock displacements and stresses are very sensitive to the rock mass modulus and the initial horizontal-to-vertical stress ratio.

- The maximum drift closures anticipated for in situ and thermal loading conditions vary from 3 to 55 mm in the vertical direction and from less than 1 to 39 mm in the horizontal direction. With these displacements, the drift operating envelopes can be maintained.

- The major principal stresses subjected to in situ and thermal loading conditions vary from 17 to 31 MPa near the springline and from 1 to 31 MPa near the crown. Potential yield zones developed around the openings are about 1 m deep or less.

- Heating after waste emplacement does not show a profound effect on rock displacements and stresses. This is because that increase in temperature is insignificant (about 50°C above the ambient temperature) owing to the thermal management measures of continuous ventilation during the preclosure period.

- Seismic motions associated with a mean annual exceedance probability of 1×10^{-4} earthquake event are not anticipated to significantly change the stable conditions of emplacement drifts.

- Factors of safety for emplacement drifts are expected to vary from 2.2 to 10 for various rock conditions.

Performance of Ground Support

- The initial ground support will be installed as necessary to provide worker safety until the final ground support is installed. Recommended initial ground support consists of 1.5 m long friction-type rock bolts, such as Split Sets, spaced at 1.5 m, and wire mesh, all installed in the drift crown (four bolts in each row), using industry standard materials (carbon steel). Wire mesh will be removed prior to the installation of the final ground support, while rock bolts will remain in place.

- Recommended final ground support system consists of 3 m long Super Swellex rock bolts, spaced at 1.25 m, and 3 mm thick Bernold-type perforated sheets, all installed in a 240° arc around the drift periphery. The materials for the final ground support should be made of stainless steel of 316 or better in order to ensure their longevity. This ground support system is considered suitable for various ground conditions anticipated during the preclosure period.

- Recommended ground support methods are flexible to accommodate geologic mapping. They are based on industry experience, and considered to be conventional.

- Swellex rock bolts are expected to perform satisfactorily under in situ, thermal, and seismic loads, with a minimum factor of safety of 2.7, exceeding required safety margins.

- Swellex rock bolts are capable of preventing rockfall with a maximum size of about 3 tonnes during the preclosure period.

- Bernold-type stainless steel sheets are expected to perform satisfactorily under in situ, thermal, and seismic loads, with a minimum factor of safety of 3.4, exceeding required safety margins.

Uncertainties in Calculation

- Factors that contribute to uncertainties in design inputs and calculation methods are discussed. Detailed evaluation of the effect of uncertainties is not covered since an ongoing scoping analysis will address related issues.

- Effect of fault displacement hazard on stability of emplacement drifts is not discussed in this calculation because an ongoing calculation will address this issue in detail.

The outputs of this calculation are reasonable compared to the inputs, and the results are suitable for the intended use.

8. REFERENCES

8.1 DOCUMENTS CITED

ASM International 1990. *Properties and Selection: Irons, Steels, and High-Performance Alloys*. Volume 1 of *Metals Handbook*. 10th Edition. Materials Park, Ohio: ASM International. TIC: 245666.

Atlas Copco. 2003. *Swellex® – The Engineered Rock Reinforcement System, Extending the Traditional Role of Rock Bolts*. [Commerce City, Colorado]: Atlas Copco. TIC: 254198.

Barton, N.; Lien, R.; and Lunde, J. 1974. "Engineering Classification of Rock Masses for the Design of Tunnel Support." *Rock Mechanics*, 6, (4), 189-236. New York, New York: Springer-Verlag. TIC: 219995.

Barton, N. 2002. "Some New Q-Value Correlations to Assist in Site Characterisation and Tunnel Design." *International Journal of Rock Mechanics & Mining Sciences*, 39, (2), 185-216. New York, New York: Elsevier. TIC: 252648.

Bieniawski, Z.T. 1989. *Engineering Rock Mass Classifications*. New York, New York: John Wiley & Sons. TIC: 226350.

Board, M. 2003. *Resolution Strategy for Geomechanically-Related Repository Design and Thermal-Mechanical Effects (RDTME)*. REV 00. Las Vegas, Nevada: Bechtel SAIC Company. ACC: MOL.20030708.0153.

BSC (Bechtel SAIC Company) 2001. *Ground Control for Emplacement Drifts for SR*. ANL-EBS-GE-000002 REV 00 ICN 01. Las Vegas, Nevada: Bechtel SAIC Company. ACC: MOL.20010627.0028.

BSC 2002a. *Software Implementation Report for FLAC Version 4.0*. Document Number: 10167-SIR-4.0-00. Las Vegas, Nevada: Bechtel SAIC Company. ACC: MOL.20020925.0376.

BSC 2002b. *Software Implementation Report for FLAC3D Version 2.1*. Document Number: 10502-SIR-2.1-00. Las Vegas, Nevada: Bechtel SAIC Company. ACC: MOL.20020730.0346.

BSC 2003a. *Input Parameters for Ground Support Design*. 800-K0C-TEG0-00500-000-00A. Las Vegas, Nevada: BSC. ACC: ENG.20030515.0002.

BSC 2003b. *Subsurface Geotechnical Parameters Report*. 800-K0C-WIS0-00400-000-00A. Las Vegas, Nevada: Bechtel SAIC Company. ACC: ENG.20040108.0001.

BSC 2003c. *Longevity of Emplacement Drift Ground Support Materials for LA*. 800-K0C-TEG0-01200-000-00A. Las Vegas, Nevada: Bechtel SAIC Company. ACC: ENG.20030922.0004.

BSC 2003d. *Underground Layout Configuration*. 800-P0C-MGR0-00100-000-00E. Las Vegas, Nevada: Bechtel SAIC Company. ACC: ENG.20031002.0007.

BSC 2003e. *Q-List*. TDR-MGR-RL-000005 REV 00. Las Vegas, Nevada: Bechtel SAIC Company. ACC: DOC.20030930.0002.

BSC 2004a. *Committed Ground Support Materials for LA Design*. 800-K0C-WIS0-00100-000-00C. Las Vegas, Nevada: Bechtel SAIC Company. ACC: ENG.20040119.0011.

BSC 2004b. *Drift Degradation Analysis*. ANL-EBS-MD-000027 REV 02, Errata 1. Las Vegas, Nevada: Bechtel SAIC Company. ACC: DOC.20040325.0002; DOC.20030709.0003.

BSC 2004c. *Ground Control for Non-Emplacement Drifts for LA*. 800-KMC-SSD0-00700-000-00A. Las Vegas, Nevada: Bechtel SAIC Company. ACC: ENG.20040302.0022.

Charette, F. 2003. "Pull Out Curves." E-mail from F. Charette (Atlas Copco) to D. Tang, July 15, 2003, with attachments. ACC: MOL.20030825.0307.

DOE (U.S. Department of Energy) 2004. *Quality Assurance Requirements and Description*. DOE/RW-0333P, Rev. 14. Washington, D.C.: U.S. Department of Energy, Office of Civilian Radioactive Waste Management. ACC: DOC.20040331.0004.

Goodman, R.E. 1980. *Introduction to Rock Mechanics*. New York, New York: John Wiley & Sons. TIC: 218828.

Hardy, M.P. and Bauer, S.J. 1991. *Drift Design Methodology and Preliminary Application for the Yucca Mountain Site Characterization Project*. SAND89-0837. Albuquerque, New Mexico: Sandia National Laboratories. ACC: NNA.19910808.0105.

Hoek, E.; Kaiser, P.K.; and Bawden, W.F. 2000. *Support of Underground Excavations in Hard Rock*. Rotterdam, The Netherlands: A.A. Balkema. TIC: 252991.

International Rollforms. [n.d.]. *Split Set® Friction Rock Stabilizers*. Deptford, New Jersey: International Rollforms. TIC: 254808.

Itasca Consulting Group. [2002]. *Itasca Software–Cutting Edge Tools for Computational Mechanics*. Minneapolis, Minnesota: Itasca Consulting Group. TIC: 252592.

Michel, H. 1999. "Bernold Sheets." Letter from H. Michel (Bernold AG) to M. Grigore (MK), July 2, 1999, with enclosures. ACC: MOL.20030506.0321.

Minwalla, H.J. 2003. *Project Design Criteria Document*. 000-3DR-MGR0-00100-000-001. Las Vegas, Nevada: Bechtel SAIC Company. ACC: ENG.20030402.0001.

Stillborg, B. 1994. *Professional Users Handbook for Rock Bolting*. Series on Rock and Soil Mechanics Volume 18. 2nd Edition. Clausthal-Zellerfield, Germany: Trans Tech Publications. TIC: 253370.

Sun, Y. 2002. *Ground Control Methodology for Emplacement Drifts*. TDR-GCS-GE-000002 REV 00. Las Vegas, Nevada: Bechtel SAIC Company. ACC: MOL.20021118.0097.

Young, W.C. 1989. *Roark's Formulas for Stress and Strain.* 6th Edition. New York, New York: McGraw-Hill. TIC: 10191.

8.2 CODES, STANDARDS, REGULATIONS, AND PROCEDURES

10 CFR 63. 2002. *Energy: Disposal of High-Level Radioactive Wastes in a Geologic Repository at Yucca Mountain, Nevada*. Readily available.

AP-3.12Q, Rev. 2, ICN 2. *Design Calculations and Analyses.* Washington, D.C.: U.S. Department of Energy, Office of Civilian Radioactive Waste Management. ACC: DOC.20040318.0002.

AP-3.15Q, Rev. 4, ICN 4. *Managing Technical Product Inputs.* Washington, D.C.: U.S. Department of Energy, Office of Civilian Radioactive Waste Management. ACC: DOC.20040510.0004.

ASTM A 240/A 240M-03b. 2003. *Standard Specification for Chromium and Chromium-Nickel Stainless Steel Plate, Sheet, and Strip for Pressure Vessels and for General Applications*. West Conshohocken, Pennsylvania: American Society for Testing and Materials. TIC: 254845.

ASTM A 276-03. 2003. *Standard Specification for Stainless Steel Bars and Shapes*. West Conshohocken, Pennsylvania: American Society for Testing and Materials. TIC: 254842.

ASTM F 432-95 (Reapproved 2001). 1995. Standard Specification for Roof and Rock Bolts and Accessories. West Conshohocken, Pennsylvania: American Society for Testing and Materials. TIC: 253986.

BSC 2002c. Software Code: FLAC. V4.0. PC WINDOWS 2000/NT 4.0. 10167-4.0-00.

BSC 2002d. Software Code: FLAC3D. V2.1. PC WINDOWS 2000/NT 4.0. 10502-2.1-00.

LP-SI.11Q-BSC, Rev. 0, ICN 0. *Software Management.* Washington, D.C.: U.S. Department of Energy, Office of Civilian Radioactive Waste Management. ACC: DOC.20040225.0007.

8.3 SOURCE DTNS CITED

MO0007RIB00077.000. In Situ Rock Conditions. Submittal date: 07/18/2000.
MO0306MWDALAFV.000. ANSYS-LA-Fine Ventilation. Submittal date: 06/23/2003.

MO0306SDSAVDTH.000. Seismic Design Spectra and Acceleration, Velocity, and Displacement Time Histories for the Emplacement Level at 10-4 Annual Exceedance Frequency. Submittal date: 06/26/2003.

SN0307T0510902.003. Updated Heat Capacity of Yucca Mountain Stratigraphic Units. Submittal date: 07/15/2003.

8.4 OUTPUT DTN

MO0310MWDGCCED.001. Results of Numerical Analyses for Ground Support of Emplacement Drifts for LA. Submittal date: 10/7/2003.